NAYARA TAMIRES DA SILVA CARVALHO

OTIMIZAÇÃO DOS PARÂMETROS DO PROCESSO DE TRATAMENTO HIDROTÉRMICO PARA OBTENÇÃO DE *HYDROCHAR* COMO FONTE DE BIOCOMBUSTÍVEL SÓLIDO

LAVRAS – MG

2024

NAYARA TAMIRES DA SILVA CARVALHO

OTIMIZAÇÃO DOS PARÂMETROS DO PROCESSO DE TRATAMENTO HIDROTÉRMICO PARA OBTENÇÃO DE *HYDROCHAR* COMO FONTE DE BIOCOMBUSTÍVEL SÓLIDO

Tese apresentada à Universidade Federal de Lavras, como parte das exigências do Programa de Pós-graduação em Ciência e Tecnologia da Madeira, área de concentração Bioenergia e Resíduos Lignocelulósicos, para a obtenção do título de Doutora.

Profª. Drª. Maria Lúcia Bianchi

Orientadora

Prof. Dr. Paulo Fernando Trugilho

Coorientador

LAVRAS – MG

2024

Ficha catalográfica elaborada pelo Sistema de Geração de Ficha Catalográfica da Biblioteca Universitária da UFLA, com dados informados pelo(a) próprio(a) autor(a).

Carvalho, Nayara Tamires da Silva.
Otimização dos parâmetros do processo de tratamento hidrotérmico para obtenção de *hydrochar* como fonte de biocombustível sólido / Nayara Tamires da Silva Carvalho. - 2023.
121 p. : il.

Orientador(a): Maria Lúcia Bianchi.
Coorientador(a): Paulo Fernando Trugilho.
Tese (doutorado) - Universidade Federal de Lavras, 2023.
Bibliografia.

1. Bioenergia. 2. Hidrotratamento térmico. 3. Otimização. I. Bianchi, Maria Lúcia. II. Trugilho, Paulo Fernando. III. Título.

NAYARA TAMIRES DA SILVA CARVALHO

OTIMIZAÇÃO DOS PARÂMETROS DO PROCESSO DE TRATAMENTO HIDROTÉRMICO PARA OBTENÇÃO DE *HYDROCHAR* COMO FONTE DE BIOCOMBUSTÍVEL SÓLIDO

OPTIMIZATION OF PARAMETERS OF THE HYDROTHERMAL TREATMENT PROCESS TO OBTAIN HYDROCHAR AS A SOURCE OF SOLID BIOFUEL

Tese apresentada à Universidade Federal de Lavras, como parte das exigências do Programa de Pós-graduação em Ciência e Tecnologia da Madeira, área de concentração Bioenergia e Resíduos Lignocelulósicos, para a obtenção do título de Doutora.

APROVADO em 29 de novembro de 2023.
Dra. Maria Lúcia Bianchi / UFLA
Dr. Paulo Fernando Trugilho / UFLA
Dr. Edgar Amaral Silveira / UnB
Dr. Thiago de Paula Protásio / UFRA
Dra. Clara Lisseth Mendoza Martinez / LUT

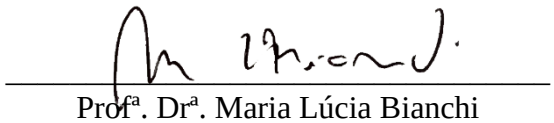

Profª. Drª. Maria Lúcia Bianchi
Orientadora

Prof. Dr. Paulo Fernando Trugilho
Coorientador

LAVRAS – MG
2024

À minha tia, Maria Helena de Carvalho e Lima (in memoriam), minha eterna tia Lelena, que nunca mediu esforços para me apoiar, que sempre se fez presente em minha vida e da qual eu me lembro todos os dias, dedico este trabalho.

AGRADECIMENTOS

A Deus pelo dom da vida, por me conceder saúde, força e coragem para seguir em frente.

À Universidade Federal de Lavras, em especial ao Departamento de Engenharia Florestal e ao Programa de Pós-graduação em Ciência e Tecnologia da Madeira, pela oportunidade concedida.

À FAPEMIG, pela concessão da bolsa de estudos de Doutorado, ao CNPq e à CAPES.

Aos meus orientadores, Maria Lúcia Bianchi e Paulo Fernando Trugilho agradeço imensamente por todos os ensinamentos durante o Doutorado (e Mestrado), toda paciência, disponibilidade e colaboração. Vocês são os melhores orientadores que eu poderia ter!

Aos membros da banca, Clara Mendoza Martinez, Edgar Silveira, Thiago Protásio e meus orientadores, pela disponibilidade e generosidade nas valiosas contribuições para este trabalho. Reitero meus agradecimentos, ao Edgar e ao Thiago, pelas ricas orientações e contribuições nos artigos oriundos da tese.

Ao Antônio Luís Maciel, por todo suporte com o equipamento fundamental para a realização dos experimentos.

A todos que eu tive a honra de conviver no Laboratório Multiusuário de Biomateriais e Energia da Biomassa, pelos aprendizados e momentos de descontração.

Às amizades que eu conquistei ao longo destes anos de UFLA/Lavras e que levarei para a vida. Vocês foram essenciais para que eu caminhasse até aqui! Obrigada pela amizade, suporte nos momentos difíceis e por tornarem meus dias mais leves e felizes.

À toda minha família, em especial a minha mãe, Vandinha, razão da minha vida. Obrigada pelo apoio incondicional, por todo amor e orações.

A todos vocês, tudo o que eu dizer é pouco perto do que representam para mim. MUITO OBRIGADA, de coração!

RESUMO GERAL

A iniciativa de se utilizar fontes renováveis de energia tem sido estimulada em todo o mundo, alinhada à política de Carbono Zero. Por isso, há interesse crescente no desenvolvimento de fontes alternativas para a produção de energia renovável, como a biomassa. Neste contexto, a carbonização hidrotérmica (HTC) é um método de conversão promissor para valorizar os constituintes da biomassa. Assim, o objetivo principal do estudo foi verificar o desempenho da serragem de *Eucalyptus grandis* na produção de *hydrochar* por meio da HTC em reatores simplificados, visando otimizar os efeitos dos parâmetros de produção para maximizar os rendimentos sólido e energético. O processo de HTC foi realizado em reatores de aço inox laboratorial, onde a biomassa foi inserida juntamente com diferentes soluções em proporção de 1:10 (sólido/líquido). Assim, foram conduzidas a HTC de todas as combinações possíveis entre temperaturas de 150, 170, 190 e 220 °C, tempos de reação de 30, 60 e 90 minutos e soluções de água e concentrações de 0,1 e 0,2 mol L^{-1} de ácido sulfúrico (H_2SO_4). Os diferentes *hydrochars* produzidos foram caracterizados minuciosamente, por meio de análises químicas imediata, elementar e estrutural, além de investigações sobre o comportamento de combustão e emissões potenciais. A otimização das condições do processo foi realizada por meio da metodologia de superfície de respostas (RSM). A presente tese foi dividida em dois capítulos. O primeiro apresenta o potencial da metodologia utilizada e investiga as propriedades dos *hydrochars* em três experimentos distintos, em que a concentração de H_2SO_4 foi fixada em cada um deles, em tempo de reação de 60 minutos e nas quatro temperaturas supracitadas. O segundo investigou a influência das três variáveis estudadas (temperatura, tempo e soluções de H_2SO_4) nas características do *hydrochar*, além de propor e validar o tratamento otimizado com base nos rendimentos sólido e energético. De modo geral, os resultados indicaram redução do rendimento sólido de 90,72 para 43,21%, conforme houve aumento da temperatura e adição de H_2SO_4. O *hydrochar* produzido em temperatura intermediária (190 °C) foi responsável pela maior parcela no incremento do poder calorífico superior (PCS), 33%, em relação ao PCS da biomassa bruta. A estrutura da superfície dos *hydrochars* foi modificada e apresentou microesferas de carbono abundantes, principalmente na maior concentração de H_2SO_4. As condições de tratamento otimizado foram: temperatura de 185 °C, tempo de reação de 30 minutos e 0,038 mol L^{-1} de H_2SO_4. Esses resultados evidenciam a eficácia da metodologia simplificada e do sistema de reatores, enfatizando os papéis cruciais do H_2SO_4 e da temperatura na definição das características e do desempenho dos *hydrochars*.

Palavras-chave: Bioenergia, Catalisador, Hidrotratamento térmico, Otimização, Resíduos florestais.

GENERAL ABSTRACT

The initiative to use renewable energy sources has been promoted throughout the world, certified under the Zero Carbon policy. Therefore, there is growing interest in the development of alternative sources for the production of renewable energy, such as biomass. In this context, hydrothermal carbonization (HTC) is a promising conversion method to valorize biomass constituents. Thus, the main objective of the study was to verify the performance of *Eucalyptus grandis* sawdust in the production of *hydrochar* through HTC in simplified reactors, improving the effects of production parameters to maximize solid and energy yields. The HTC process was carried out in laboratory stainless steel reactors, where the biomass was inserted together with different solutions in a ratio of 1:10 (solid/liquid). Thus, HTC was conducted at all possible temperatures between temperatures of 150, 170, 190 and 220 °C, occurrence times of 30, 60 and 90 minutes and water solutions and concentrations of 0.1 and 0.2 mol L^{-1} sulfuric acid (H_2SO_4). The different *hydrochars* produced were thoroughly evaluated, through immediate chemical, elementary and structural analyses, as well as investigations into combustion behavior and potential emissions. The optimization of process conditions was carried out using response surface methodology (RSM). This thesis was divided into two papers. The first presents the potential of the methodology used and investigates the properties of *hydrochars* in three different experiments, in which the concentration of H_2SO_4 was introduced in each of them, in an occurrence time of 60 minutes and at the four temperatures mentioned above. The second investigated the influence of the three scientific variations (temperature, time and H_2SO_4 solutions) on the characteristics of the *hydrochar*, in addition to proposing and validating the optimized treatment based on solid and energy yields. In general, the results indicated a reduction in solid yield from 90.72 to 43.21 %, as the temperature increased and H_2SO_4 was added. *Hydrochar* produced at high temperature (190 °C) was responsible for the largest share in the increase in higher calorific value (PCS), 33 %, in relation to the PCS of raw biomass. The surface struture of the *hydrochars* was modified and presented abundant carbon microspheres, especially at the highest concentration of H_2SO_4. The optimized treatment conditions were: temperature of 185 °C, occurrence time of 30 minutes and 0.038 mol L^{-1} of H_2SO_4. These results highlight the effectiveness of the simplified methodology and reactor system, emphasizing the crucial roles of H_2SO_4 and temperature in defining the characteristics and performance of *hydrochars*.

Keywords: Bioenergy; Catalyst; Forestry Waste; Hydrothermal treatment; Optimization.

SUMÁRIO

PRIMEIRA PARTE

1 INTRODUÇÃO

Muito esforço tem sido empenhado no desenvolvimento de soluções energéticas sustentáveis para substituir os combustíveis fósseis, a fim de abrandar o ritmo das alterações climáticas e evitar uma crise energética (Chen *et al.*, 2023). Portanto, abordar esse problema tornou-se um desafio global, que também proporciona oportunidades globais.

Na Conferência das Nações Unidas sobre o Clima de 2022, no Egito (COP 27), os governos foram solicitados a reavaliar e melhorar as suas metas de redução de emissões para 2030, enfatizando a necessidade de incorporar energias renováveis e de baixas emissões para diversificar as fontes e os sistemas energéticos (United Nations Environment Programme (UNEP), 2022). Assim, a produção de parcela significativa de energia a partir de fontes renováveis, como solar, eólica e biomassa é atualmente, a meta e o desejo de muitos países ao redor do mundo (Heidari *et al.*, 2019; Sharma, Panigrahi e Dubey, 2019).

Entre as possíveis soluções, a energia da biomassa (bioenergia) tem mostrado grande potencial e promessa no que diz respeito à redução líquida de emissões e à redução de resíduos (Chen *et al.*, 2023). Entre 2010 e 2022, o uso de bioenergia moderna aumentou em média cerca de 3% ao ano e está em tendência ascendente. No entanto, mais esforços são necessários para acelerar sua implantação, a fim de avançar no Cenário Emissões Líquidas Zero, que exige aumento da implantação de 8% ao ano entre 2022 e 2030, assegurando simultaneamente que a produção de bioenergia não incorre em consequências sociais e ambientais negativas (IEA, 2023).

Nesse cenário, o Brasil, segundo o relatório da REN21 (United Nations, 2020), publicado em 2020, sobre o status global das fontes renováveis foi considerado o terceiro país no mundo em capacidade total de bioenergia per capita, excluindo a energia hidrelétrica. E de acordo com dados do Balanço Energético Nacional (BEN), ano base 2022 (BEN, 2023) (Figura 1), 47,4% de toda Oferta interna de energia no país provém de fontes renováveis, sendo 21% desse valor dependente da biomassa e seus derivados, confirmando seu elevado potencial no setor.

Figura 1 – Oferta interna de energia no Brasil, ano base 2022.

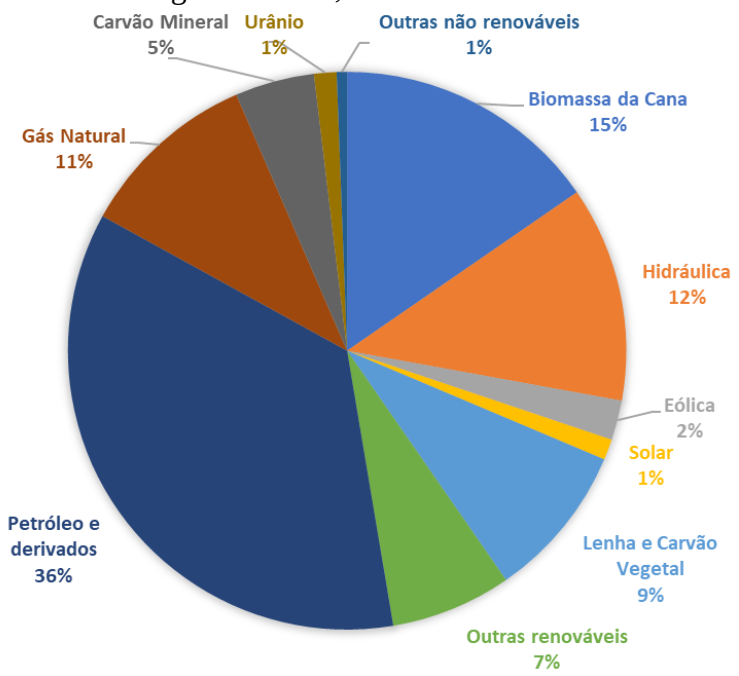

Fonte: Balanço Energético Nacional, ano base 2022 (BEN, 2023).

Como centro da economia de base biológica, a biomassa é uma das fontes de recursos renováveis mais indicadas para produzir bioenergia e produtos de alto valor agregado (Moncada B, Aristizábal M e Cardona A, 2016); e possui extensas fontes, incluindo resíduos agrícolas, florestais, da pesca e da aquicultura, fração orgânica de resíduos sólidos urbanos, lodo de esgoto e algas (Camia *et al.*, 2018).

Em se tratando de biomassa lignocelulósica, a utilização sustentável de resíduos agroflorestais, convertendo-os em produtos valiosos, oferece benefícios consideráveis, tanto ambientais quanto econômicos. Além disso, resíduos subutilizados podem causar impactos ambientais negativos, como a emissão de grandes quantidades de compostos orgânicos voláteis no caso de combustão e contaminação das águas subterrâneas, no caso de aterro, além da emissão de metano.

Destaca-se a utilização de resíduos de madeira, que apresentam vantagens como: baixa perda por degradação, uma vez que, quando estabelecida rotações silviculturais não estão sujeitas a sazonalidade. O Brasil, segundo Relatório Anual do Ibá (Ibá, 2023), possuía em 2022, 9,94 milhões de hectares de florestas plantadas, sendo 76% (7,6 milhões de hectares) de plantios de *Eucalyptus*, confirmando o potencial de utilização dos resíduos gerados por essa cadeia produtiva.

A fim de promover o uso sustentável dos recursos de biomassa sólida e reduzir os impactos sociais e de saúde associados ao seu uso tradicional, várias atividades têm sido coordenadas no âmbito da iniciativa de Energia Sustentável para Todos das Nações Unidas, que visam garantir o acesso universal à energia limpa até 2030 (IEA, 2017). Desta forma, é de supra importância a ampla variedade de processos, como tecnologias de pré-tratamento, conversão alternativa e melhorias de rotas para aumentar o potencial de utilização da biomassa (Hoekman *et al.*, 2017), contribuindo para sua participação mais expressiva na matriz energética.

No que tange à valorização da biomassa residual, a carbonização hidrotérmica (HTC) é uma rota promissora dadas as suas vantagens sobre outros processos termoquímicos (Cavali *et al.*, 2023) e demonstra potencial para converter ampla gama de matérias-primas em biocombustível sólido (*hydrochar*), denso em energia, com propriedades físico-químicas melhoradas em comparação ao material de origem e subprodutos líquidos e gases, em menor quantidade (Kambo, Minaret e Dutta, 2018). Sendo, a formação do *hydrochar* altamente depende dos diferentes parâmetros do processo, como tempo de reação, pressão e temperatura (Funke e Ziegler, 2010).

A HTC visa valorizar totalmente os constituintes da biomassa (Atallah *et al.*, 2019), assim, sua implementação pode ser realizada seguindo uma abordagem de biorrefinaria, considerando as possíveis aplicações do *hydrochar* e a identificação, recuperação e caracterização dos compostos intermediários, de alto valor comercial (subprodutos líquidos e gases) (Kumar e Yaashikaa, 2019). A HTC poderia funcionar como a primeira etapa de uma biorrefinaria, e essa abordagem concordaria completamente com os princípios da bioeconomia circular (Cavali *et al.*, 2023).

As instalações de biorrefinaria tem sido apontadas como resposta para os atuais problemas de eliminação de resíduos e como solução para fornecer um amplo espectro de produtos de valor agregado, como biocombustíveis, biomateriais e bioquímicos a partir de resíduos de biomassa, abundantes na natureza e renováveis (Kumar e Yaashikaa, 2019; Wang *et al.*, 2019).

No entanto, devido à relativa novidade do processo de HTC, os mecanismos de reação detalhados para diferentes matérias-primas não são totalmente compreendidos. Assim, considerando o interesse emergente pela HTC, torna-se necessário fornecer a análise de como os fatores temperatura, tempo de reação e a adição de catalisador podem afetar as propriedades do combustível sólido, *hydrochar*, para determinada matéria-prima.

Ademais, apesar do potencial tecnológico da HTC, ainda há escassez de informações sobre condições estatisticamente otimizadas para a obtenção de *hydrochar* de melhor qualidade para aplicações energéticas (Afolabi, Sohail e Cheng, 2020).

Assim, o objetivo geral deste trabalho foi avaliar o desempenho da serragem de *Eucalyptus grandis* para produção de biocombustível sólido, denominado *hydrochar*, por meio de tratamentos hidrotérmicos.

E os objetivos específicos foram:

a) Realizar a caracterização físico-química da serragem de *Eucalyptus grandis*, visando à HTC.
b) Avaliar o efeito da temperatura e do tempo de reação em experimentos com diferentes concentrações de catalisador ácido na produção de *hydrochars* de serragem de *Eucalyptus grandis*.
c) Avaliar a influência da adição de ácido na qualidade do *hydrochar*.
d) Avaliar a qualidade estrutural, as propriedades energéticas, o rendimento e as propriedades físico-químicas dos *hydrochars* produzidos.
e) Avaliar a combustibilidade dos *hydrochars* via a análise termogravimétrica;
f) Otimizar os efeitos da temperatura, e da concentração de ácido sulfúrico (H_2SO_4) via a metodologia de superfície de respostas.
g) Produzir e caracterizar o *hydrochar* na condição otimizada da HTC.
h) Validar o modelo otimizado quanto aos rendimentos sólido e energético.

Desta forma, a tese foi estruturada em dois artigos, conforme apresentados a seguir:

- Artigo I: Hydrotreatment of *Eucalyptus* sawdust: the influence of process temperature and H_2SO_4 catalyst on hydrochar quality, combustion behavior and related emissions.
- Artigo II: Hydrothermal carbonization of *Eucalyptus grandis* sawdust: process and catalytic H_2SO_4 conditions optimization for cleaner biofuel production using response surface methodology.

2 REFERENCIAL TEÓRICO

2.1 Perspectivas de utilização da biomassa como fonte de energia

Para reduzir a dependência de combustíveis fósseis sem comprometer a segurança energética, é imperativo aumentar a participação e o acesso à energia renovável, limpa e acessível (Afolabi, Sohail e Cheng, 2020). Por isso, a procura por fontes de energia renováveis tem sido aspecto fundamental e abordado por vários países, visando não somente diminuir a dependência do petróleo, mas, também, minimizar os problemas ambientais causados pela utilização de seus derivados.

A utilização crescente de energia proveniente da biomassa, bioenergia, é dita como decisiva para permitir a substituição parcial de combustíveis fósseis no futuro próximo. Portanto, a prospecção de fontes alternativas que tenham alta capacidade de geração de bioenergia e possam auxiliar a reduzir os níveis de emissões é essencial para o desenvolvimento sustentável (Alves *et al.*, 2020). Desta forma, a utilização de resíduos lignocelulósicos (fontes de biomassa de baixo custo e renováveis) como recurso de combustível ganhou notável atenção no desenvolvimento de uma sociedade de energia renovável, verde e limpa (Kambo, Minaret e Dutta, 2018).

A principal razão do recente interesse na produção de bioenergia é o suprimento potencialmente ilimitado de biomassa disponível, devido à sua renovabilidade. Assim, a biomassa é o único recurso de carbono que ocorre naturalmente e está disponível em quantidades o suficiente para substituir o recurso mundial primário de energia, combustíveis fósseis (Tumuluru *et al.*, 2012), capaz de ser transformada em combustíveis sólidos, líquidos e gasosos.

Além disso, a utilização da biomassa possui potencial econômico no cenário em que o preço dos combustíveis advindos do petróleo sobe em futuro próximo. A biomassa pode ser produzida em muitos países, diminuindo assim as relações de dependência energética que podem resultar em conflitos geopolíticos (Román *et al.*, 2018).

No entanto, existem algumas desvantagens na utilização da biomassa como recurso sustentável que precisam ser superadas, como sua heterogeneidade, presença de contaminantes, alto teor de umidade, baixa densidade energética (Ahmed *et al.*, 2019) e a inconveniência de armazenamento e transporte (Cheng *et al.*, 2022; Zhang, S. *et al.*, 2018), uma das principais restrições para a indústria de bioenergia em larga escala, tornando-a, muitas vezes, inadequada

para a conversão direta de energia por combustão e/ou gaseificação (Heidari *et al.*, 2020; Zhu *et al.*, 2015).

Portanto, a efetiva aplicação da biomassa lignocelulósica requer o uso de tratamentos que promovam o fracionamento dos seus principais constituintes (celulose, hemiceluloses e lignina). As pesquisas por novas tecnologias para obtenção de bioenergia visam melhorar as características energéticas do produto final, obtendo combustível mais atrativo e limpo (Carrasco *et al.*, 2020). Assim, vários processos de pré-tratamento térmico tem sido explorados para converter a biomassa em biocombustíveis sólidos, que se assemelham ao carvão em termos de propriedades físicas e químicas (Hoekman *et al.*, 2017).

Além disso, a utilização do conceito de biorrefinaria para integrar processos químicos, termoquímicos e biotecnológicos, bem como rotas catalíticas para obter produtos de maior valor agregado, é um dos desafios contemporâneos mais importantes.

Sob a égide das políticas de energia verde, as biorrefinarias de biomassa são consideradas plataformas equivalentes às refinarias tradicionais baseadas no petróleo e desempenham papel vital na produção de alternativas aos combustíveis fósseis e outros produtos de base biológica. Diferentes plataformas baseadas em biomassa, como gás de síntese, açúcares (C5/6), óleo vegetal, óleo de algas, soluções orgânicas, lignina e óleo de pirólise, poderiam ser acopladas de acordo com as necessidades do mercado para obter biorrefinarias integradas para a máxima exploração da matéria-prima e produzir ampla variedade de produtos (Moncada B, Aristizábal M e Cardona A, 2016).

A biorrefinaria é uma boa estratégia para a utilização sustentável em larga escala da biomassa na bioeconomia, uma vez que poderá resultar na produção de bioenergia e produtos de base biológica a custos competitivos, garantindo impactos socioeconómicos e ambientais ideais (IEA Bioenergy, 2022).

Em consonância com o Cenário Emissões Líquidas Zero, maior produção de bioenergia será exigida, no entanto, é necessário cuidados para garantir que isso não resulte em efeitos negativos para a sociedade ou para o ambiente. De acordo com considerações de sustentabilidade, não há expansão de terras agrícolas para bioenergia nem conversão de terras florestadas existentes em produção de culturas bioenergéticas neste Cenário. Assim, acredita-se que em 2030, 60% do fornecimento de bioenergia proverá de resíduos. Por isso, a inovação e a implantação de tecnologias de conversão de biocombustíveis serão necessárias para desbloquear totalmente o potencial de utilização dos resíduos (IEA, 2023).

A escolha da tecnologia mais apropriada para o desenvolvimento da bioenergia é impulsionada por uma série de fatores, como a matéria-prima disponível e suas propriedades,

escala de operação e vetor final de energia desejado. Isso resulta em diferentes tecnologias com diferentes nichos de mercado (Adams *et al.*, 2017).

2.2 Biomassa lignocelulósica

Embora a composição da biomassa dependa fortemente do tipo, maturidade e condições climáticas, pode-se dizer que ela contém cerca de 30–45% de celulose, 20–40% de hemiceluloses e 10–25% de lignina (Acharya, Dutta e Minaret, 2015), que estão fortemente ligadas entre si para formar a estrutura esquelética da planta, conforme apresentado na Figura 2. A celulose e as hemiceluloses estão conectadas principalmente por ligações de hidrogênio, enquanto a lignina e as hemiceluloses estão ligadas por ligações de hidrogênio, ligações iônicas, ligações covalentes e interações hidrofóbicas (Zhang *et al.*, 2022).

Figura 2 – Principais componentes da biomassa lignocelulósica. Estruturas da celulose e hemiceluloses e principais precursores da lignina.

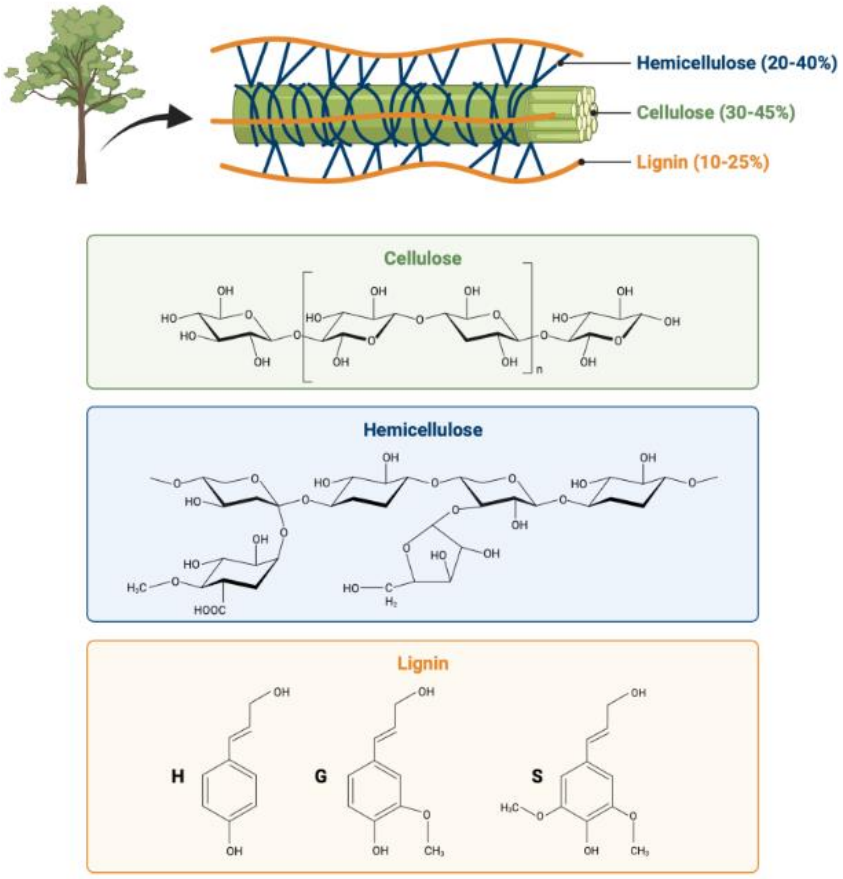

Legenda: H: Álcool p-cumarílico; G:Álcool conifelírico; S: Álcool sinapílico.
Fonte: Lugano (Lugano, 2023).

A celulose, componente mais abundante, consiste em polissacarídeo linear formado por unidades de anidro glicose unidas por ligação glicosídica do tipo β-(1,4). Devido à sua estrutura única de arranjo ordenado de feixes e estrutura altamente cristalina, a celulose é estável em muitas condições. Possui boa biocompatibilidade e grupos hidroxila ativos com razões O/C de 0,6–0,83 e H/C de 0,8–1,67 (Wu *et al.*, 2022).

A fração denominada hemiceluloses, é representada por diferentes heteropolímeros com massa molecular relativamente menor em comparação à celulose. São constituídas por diversos açúcares, principalmente pentoses (xilose e arabinose) e hexoses (manose, glicose e galactose) (Yu *et al.*, 2022) e caracterizada por possuírem cadeias facilmente hidrolisáveis. Dada a falta de ligações glicosídicas β-(1,4) repetidas e a natureza aleatória do polímero das hemiceluloses, estes não se formam tão cristalinos e resistentes em estrutura como a celulose e, portanto, são muito mais suscetíveis à extração hidrotérmica e hidrólise.

Por último, encontra-se a fração denominada lignina, que ligada à hemiceluloses, envolve a celulose e a protege de ataques hidrolíticos químicos ou enzimáticos (D. Fengel, 1989). A lignina, um heteropolímero amorfo, é mais resistente que a celulose e as hemiceluloses (Cavali *et al.*, 2020), por isso fornece resistência mecânica para biomassa, principalmente devido à sua matriz aromática (Wang *et al.*, 2017). Durante a HTC, as reações com a lignina apresentam duas fases, a primeira compreende uma reação rápida que degrada a lignina em fragmentos solúveis, e a segunda consiste em uma reação mais lenta onde esses fragmentos são repolimerizados. De acordo com a severidade da reação, a lignina pode ser separada em lignina não dissolvida e dissolvida, o primeiro levará ao *hydrochar* poli aromático, enquanto o último ao *hydrochar* fenólico (Wang *et al.*, 2018b).

Dentre as fontes de biomassa lignocelulósica que estão no foco das pesquisas e dos potenciais investimentos em bioeconomia, estão as florestas plantadas de rápido crescimento. Destaca-se o interesse na biomassa florestal como matéria prima para bioenergia no Brasil em função das florestas brasileiras serem certificadas como cultivos sustentáveis, muitas vezes realizados em áreas degradadas, o que significa que competem muito pouco por terras destinadas aos cultivos agrícolas de alimentos. Além disso, os produtos florestais não estão sujeitos a influências sazonais e podem ser colhidos durante o ano todo com elevada produtividade.

Salienta-se, ainda, o enorme interesse na valorização dos resíduos provenientes da biomassa florestal, como alternativa ao duplo propósito de aproveitar recursos e proteger o meio ambiente (Zhuang *et al.*, 2020).

Dentre diversas aplicações, as florestas plantadas são utilizadas para produção de madeira gerando grandes quantidades de resíduos, tanto durante as operações de colheita, quanto durante o processamento da madeira. Os resíduos do processamento de madeira compreendem os resíduos produzidos nas serrarias, como cascas, serragem e aparas (Braghiroli e Passarini, 2020). Estima-se a produção de resíduos nessas instalações em 238,7 milhões de m^3 de resíduos de madeira no mundo em 2022. No Brasil, a produção de resíduos de madeira é estimada em cerca de 19,1 milhões de m^3, sendo a indústria madeireira a maior responsável por essa produção (Food and Agriculture Organization of the United Nations, 2023).

Para evitar a carga ambiental causada pela má gestão dos resíduos florestais, estes materiais podem ser utilizados como matéria-prima em outros processos devido à sua composição lignocelulósica (Cavali *et al.*, 2023). A serragem de *Eucalyptus* spp. possui teores de celulose, hemiceluloses, lignina e cinzas variando de 42,7% a 44,7%, 16,1% a 19,0%, 23,0% a 32,2% e 0,2% a 1,0%, respectivamente (Morais *et al.*, 2015; Tavares *et al.*, 2022; Vallejo *et al.*, 2022).

Por se tratar de biomassa prontamente disponível, os resíduos madeireiros têm alto potencial para serem convertidos em valiosos produtos derivados de energia. Além disso, a utilização de resíduos de serragem, cavacos e chapas de madeira apresentam a vantagem de estarem comumente concentradas nas serrarias, evitando elevados custos de transporte. Com relação à serragem, vantajosamente não requer uma etapa de pré-tratamento físico para redução de tamanho (Cavali *et al.*, 2023). Neste contexto, a utilização de resíduos madeireiros apresenta inúmeras vantagens de utilização para a produção de bioenergia.

2.3 Conversão da biomassa

A importância da diversificação da matriz energética e a necessidade de fontes de energia mais sustentáveis é amplamente reconhecida. A biomassa é fonte renovável abundante para produzir biocombustíveis ou produtos de maior valor agregado por meio de diferentes processos. Além da tradicional conversão térmica da biomassa (combustão), existem três principais tecnologias de processo disponíveis: bioquímica, termoquímica e físico-química (Adams *et al.*, 2017).

Os processos termoquímicos compõem as principais vias de conversão para produzir energia a partir da biomassa lignocelulósica (Liu *et al.*, 2013), devido à sua versatilidade e flexibilidade, as tecnologias de conversão termoquímica recebem atenção especial dos

desenvolvedores de processos. Tais conversões podem ser divididas em processos secos e úmidos. Os processos secos, requerem umidade da biomassa entre 5 e 10% em massa e, por isso, geralmente, iniciam com a remoção do teor de umidade por meio de aquecimento, o que torna a conversão da matéria-prima com alto teor de umidade intensiva em energia e cara (Lucian, Volpe e Fiori, 2019), como a torrefação, pirólise e gaseificação.

Quanto aos processos úmidos, a matéria-prima pode apresentar teor de umidade entre 60 e 90 % em massa (Basso *et al.*, 2016). São considerados tratamentos alternativos valiosos para os resíduos de biomassa, pela sua flexibilidade e, a princípio, baixo investimento e custos operacionais (Lucian e Fiori, 2017; Munir *et al.*, 2023). Os processos úmidos são subdivididos em: carbonização hidrotérmica (HTC), liquefação hidrotérmica (HTL) e gaseificação hidrotérmica (HTG).

Com destaque para a carbonização hidrotérmica (HTC), que melhora substancialmente a eficiência da produção de bioenergia e vem sendo amplamente estudada e difundida (Lucian e Fiori, 2017; Lucian, Volpe e Fiori, 2019; Volpe *et al.*, 2018).

O processo de HTC envolve o aquecimento da biomassa em água sob pressão autógena, ou em alguns casos, na presença de produtos químicos, para aumentar a densificação de energia produzindo uma fração carbonácea, denominada *hydrochar*, produto mais estável e com maior teor de carbono do que a matéria-prima de origem.

No Brasil, esse método é conhecido como pré-hidrólise da biomassa, muitas vezes utilizada como pré-tratamento para outros processos, cujo objetivo é quebrar a estrutura da lignina, remover as hemiceluloses, reduzir a cristalinidade da celulose e aumentar a área superficial do produto obtido (Tian *et al.*, 2018).

De forma análoga à carbonização hidrotérmica a pré-hidrólise utiliza água, na presença ou ausência de catalisador. Quando aplicada com ácido diluído, a pré-hidrólise, é considerada a tecnologia de pré-tratamento mais próxima da comercialização devido à sua simplicidade, baixo custo e eficácia dos reagentes (Jung e Kim, 2015). Portanto, ao que tudo indica, a tecnologia HTC apresenta simultaneamente uma solução para o gerenciamento de resíduos de biomassa, tornando-a recurso valioso para a produção de energia renovável (Sharma, Sarmah e Dubey, 2020).

2.4 Carbonização Hidrotérmica - HTC

A HTC converte termicamente a biomassa em um produto sólido, *hydrochar*, com alto teor de carbono, na presença de água (Ahmed *et al.*, 2019; Sharma *et al.*, 2020); subprodutos

líquidos, onde os compostos mais voláteis e oxigenados, principalmente furanos e ácidos orgânicos se concentram durante a reação (Maniscalco, Volpe e Messineo, 2020) e uma pequena fração gasosa, constituída, principalmente CO_2 (Fiori *et al.*, 2014).

Também conhecida como pirólise úmida ou torrefação úmida, a HTC, é um processo termoquímico úmido, que utiliza água como meio de reação, considerada reagente não tóxico, ambientalmente correto, de baixo custo e que também está inerentemente presente em resíduos de biomassa (Libra *et al.*, 2011). Desta forma, o estágio de secagem com uso intensivo de energia, é dispensável (Lucian, Volpe e Fiori, 2019).

Pode ser aplicada a diversas fontes não tradicionais de biomassa, como a fração orgânica de resíduos sólidos urbanos, resíduos agrícolas úmidos, lodo de esgoto, algas, resíduos da aquicultura e a fontes tradicionais de biomassa (Afolabi, Sohail e Cheng, 2020; Libra *et al.*, 2011; Lu e Berge, 2014; Volpe *et al.*, 2016). Possui alta eficiência energética, condições de processo relativamente amenas e foi atestada por estudos sobre sua aplicação em nível industrial (Hitzl *et al.*, 2015; Lucian e Fiori, 2017).

Trata-se de um pré-tratamento que simula a coalificação natural da biomassa (Zhuang *et al.*, 2018). A associação do calor e pressão ao longo do tempo atuando em biomassas acumuladas no solo, continental ou marítimo, deram origem às reservas de combustíveis sólidos, líquidos e gasosos. Assim, aplicar altas pressões e temperaturas à matéria orgânica é uma forma de acelerar os caminhos naturais para formação de combustíveis (Libra *et al.*, 2011), em que ocorre aumento gradual de alteração da biomassa com o aumento da temperatura de carbonização.

Dentre os processos hidrotérmicos (Figura 3), a HTC é o processo no qual as condições operacionais de temperatura e pressão são as mais brandas, sendo uma das justificativas para seu empego na valorização de resíduos lignocelulósicos, permitindo sintetizar materiais à base de carbono de forma prática e eficaz (Ahmed Khan *et al.*, 2019).

Em comparação com pirólise, gaseificação e torrefação, a principal vantagem da HTC é utilizar matéria-prima úmida, sem secagem prévia, uma vez que a água atua como reagente, solvente e catalisador (Sharma, Sarmah e Dubey, 2020). No processo HTC, a biomassa reage com água em sistema fechado (reator), sob condições subcríticas, com pressão autógena, correspondente à temperatura de reação e mantida acima da pressão de saturação correspondente (10–50 bar) para garantir o estado líquido da água, (Zhang, Lin e Zhao, 2014), favorecendo sua capacidade de dissolver compostos polares (Heidari *et al.*, 2019).

Figura 3 – Classificação do processamento de carbonização hidrotérmica da biomassa com referência ao diagrama de fase pressão-temperatura da água.

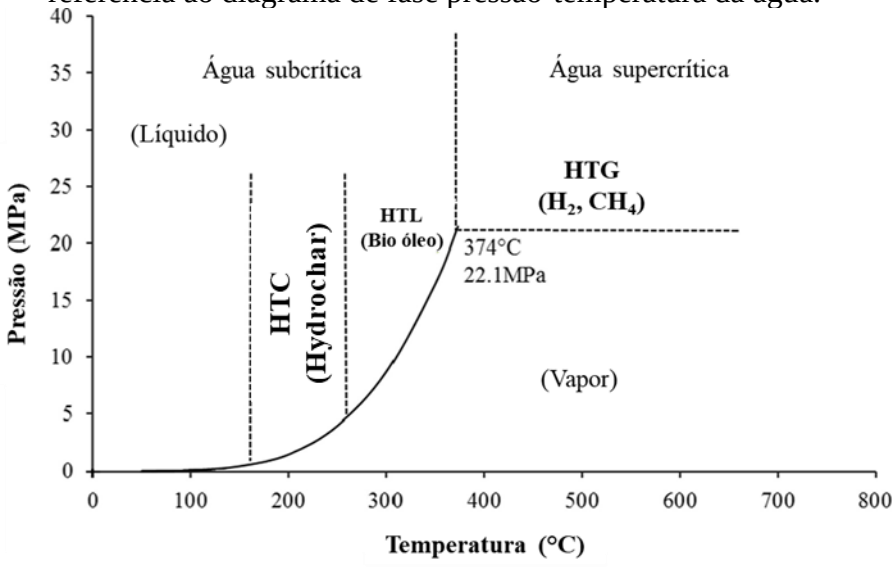

Fonte: Adaptado de Kambo e Dutta (Kambo e Dutta, 2015a).

A pressão geralmente não é controlada porque depende do vapor de saturação da água que é função da temperatura, e então a pressão autógena é comumente utilizada nas publicações disponíveis (Cavali *et al.*, 2023).

A temperatura varia geralmente de 150 a 280 °C, tempos de reação que variam de alguns minutos a várias horas (Funke e Ziegler, 2010; Libra *et al.*, 2011; Moscicki *et al.*, 2017; Peterson *et al.*, 2008) e em diferentes concentrações de matéria-prima para proporção de água.

Sob condições subcríticas, os constituintes da biomassa, são decompostos por uma infinidade de reações concorrentes, em que os mecanismos reacionais são conhecidos apenas parcialmente devido à grande complexidade dos diferentes tipos de biomassa e as diversas rotas reacionais possíveis (Funke e Ziegler, 2010; Heidari *et al.*, 2019; Lucian, Volpe e Fiori, 2019; Moscicki *et al.*, 2017). As principais reações são: hidrólise, desidratação, descarboxilação, aromatização e recondensação (Acharya, Dutta e Minaret, 2015; Basso *et al.*, 2016; Funke e Ziegler, 2010; Kambo, Minaret e Dutta, 2018), no entanto, cada HTC individual tem sua própria cinética de reação e é provavelmente catalisada uma pela outra (Reza *et al.*, 2013).

Diferentemente dos processos secos, a hidrólise, que exibe menor energia de ativação, é o mecanismo que inicia a degradação hidrotérmica da biomassa. Os principais componentes da biomassa são menos estáveis sob condições hidrotermais, o que leva a temperaturas de decomposição mais baixas quando comparadas àquelas das degradações pirolíticas secas (Bobleter, 1994).

Durante a hidrólise, a água reage com extrativos, hemiceluloses e celulose, rompendo as ligações éster e éter, principalmente ligações glicosídicas β-(1-4), resultando em ampla gama de produtos, incluindo oligômeros solúveis como sacarídeos da celulose e hemiceluloses (Reza, Uddin, *et al.*, 2014), com alguns intermediários, como 2-furfural, 5-hidroximetilfurfural (5-HMF), sendo posteriormente produzidos (Funke e Ziegler, 2010; Reza, Andert, *et al.*, 2014). A literatura menciona que a taxa de hidrólise é controlada por difusão e, portanto, é limitada por fenômenos de transporte dentro da estrutura fibrosa da biomassa (Reza *et al.*, 2013). Desta forma, o aumento da temperatura eleva a taxa de hidrólise.

A hidrólise é seguida por desidratação e descarboxilação (Funke e Ziegler, 2010; Reza, Andert, *et al.*, 2014). As reações de desidratação e desidrogenação implicam, respectivamente, na remoção dos grupos hidroxila e na ruptura dos ácidos carboxílicos de cadeia longa (Li *et al.*, 2020). Estruturas coloidais são destruídas, diminuindo a quantidade de grupos hidrofílicos e promovendo a formação de gases, principalmente CO_2 (Moscicki *et al.*, 2017). Outros gases como CO, CH_4 e H_2 (no caso do processo catalítico) também podem ser detectados (Sermyagina *et al.*, 2015). A diminuição na quantidade de grupos OH também causa redução na relação O/C. O decréscimo na quantidade de grupos hidroxila é o aspecto chave para tornar a biomassa submetida a HTC mais hidrofóbica, tornando a desidratação física mais fácil (Funke e Ziegler, 2010).

Simultaneamente, a reação de descarboxilação diminui a quantidade de grupos carboxila (COOH) e carbonila (C=O) diminuindo, ligeiramente, a razão O/C do *hydrochar*, seguido das reações de polimerização e aromatização (Funke e Ziegler, 2010; Reza, Werner, *et al.*, 2014). As reações de aromatização resultarão em estruturas poliméricas aromáticas que são estáveis sob condições hidrotérmicas e são consideradas os blocos de construção do *hydrochar* (Funke e Ziegler, 2010). É importante salientar que o principal problema na compreensão da química da HTC é que as reações não ocorrem em série e sua ordem, severidade e interações ainda não foram totalmente descobertas (Sevilla e Fuertes, 2009).

De maneira geral, à medida que a severidade da reação aumenta, a maioria dos compostos voláteis é liberada, aumentando o conteúdo de carbono e o poder calorífico (Li *et al.*, 2020). Dependendo da composição da biomassa bruta e das condições operacionais da HTC, diversos compostos como ácidos orgânicos, aldeídos, fenóis, furfurais, aminas aromáticas, entre outros compostos produzidos pela decomposição da biomassa, podem ser encontrados na fase líquida (Heidari *et al.*, 2019; Reza, Andert, *et al.*, 2014).

Normalmente, uma fração muito pequena de produtos gasosos (< 5–10%) é produzida sob condições de HTC, especialmente quando realizada abaixo de 260°C (Basso *et al.*, 2016;

Libra *et al.*, 2011; Yan *et al.*, 2010), portanto, espera-se que a maioria dos compostos orgânicos decompostos importantes estejam presentes no subproduto líquido.

A HTC é um processo exotérmico que reduz o teor de oxigênio e hidrogênio, descrito pelas relações atômicas H/C e O/C devido à desidratação e descarboxilação respectivamente, tornando assim as características do *hydrochar* mais próximas do carvão (Sevilla e Fuertes, 2009). Isso ocorre devido à diminuição no número de ligações O – C e H – C de baixa energia, e ao aumento no número de ligações C – C de alta energia, aumentando assim, a densidade de energia da matéria-prima de biomassa após a HTC (Zhao *et al.*, 2014). No entanto, a reação inicial da HTC (hidrólise) é endotérmica (Ibbett *et al.*, 2011). Portanto, a energia de ativação para hidrólise deve ser fornecida por aquecimento externo.

Nesse processo, a presença de umidade é necessária para facilitar o contato entre os diversos constituintes da matéria-prima (Djandja *et al.*, 2021) e atua como catalisador. A combinação de altas temperaturas e pressões altera as propriedades físicas e químicas da água, como: densidade, viscosidade, constante dielétrica e acidez (Yu, Lou e Wu, 2008).

Em temperaturas de 200 a 280°C, a constante iônica da água está sujeita a aumento significativo, e a água se comporta como solvente apolar (Reza *et al.*, 2013). A presença de água acelera o processo de carbonização da biomassa e, simultaneamente, afeta o rendimento do produto (Funke e Ziegler, 2010). A razão para o último é evidente, a água na biomassa serve tanto como meio de reação quanto como reagente (Sharma, Sarmah e Dubey, 2020). A 250 °C, a água pura tem capacidade catalítica cerca de 25 vezes mais do que à temperatura ambiente (Ahmad, Silva e Varesche, 2018).

Portanto, a água serve como agente de reação perfeito com a capacidade de conduzir as reações da HTC, em contraste com as reações tradicionais do processo de pirólise. Na pirólise, o teor de água presente na biomassa tem efeito negativo no processo, pois requer maior calor de vaporização (Akhtar e Amin, 2011). Assim, a HTC, aumenta as opções de uso de biomassa como matéria-prima juntamente com a economia geral do processo. Ademais, a utilização de água como meio reacional, apresenta várias vantagens, pois, é ecologicamente segura, amplamente disponível e relativamente de baixo custo. Sendo, o processo como um todo mais correto ambientalmente, em comparação com a pirólise devido a menor emissão de material volátil (Demir Cakan *et al.*, 2008; Titirici *et al.*, 2007).

À temperatura ambiente, a água sob autoionização produz íons hidrônio e hidróxido. O valor da constante de dissociação a 25 °C é $1{,}0 \times 10^{-14}$. No estado subcrítico, esse valor aumenta 3 vezes. A quebra e alteração da rede de ligações de hidrogênio ocasiona redução na viscosidade e densidade da água (Yang, 2007). A química iônica e a supressão de radicais livres são

promovidas sob condições subcríticas. O pH desta água será ligeiramente ácido e pode, portanto, catalisar as reações (Kambo e Dutta, 2015a).

A quantidade de água utilizada na reação HTC deve ser suficiente para garantir a dispersão completa da biomassa no meio reacional (Heidari *et al.*, 2019). Normalmente, a água é adicionada ao sistema em proporção de 3 a 10 vezes a massa seca da biomassa (Liu *et al.*, 2013; Reza *et al.*, 2013). Estudos indicam que a adição de mais água terá efeito positivo nas características físicas, como área de superfície e volume de poros. Por outro lado, a proporção água/biomassa mais baixa pode resultar em tempos de residência menores, polimerização mais precoce e maior rendimento de *hydrochar* (Heidari *et al.*, 2019).

As hemiceluloses geralmente se decompõem em torno de 160°C em água subcrítica e em torno de 200–300°C em condições ambientais, enquanto a celulose e a lignina começam a se decompor em 180–200°C e acima de 220°C em água subcrítica, e 300–400°C e acima de 600°C em condições ambientais, respectivamente (Kambo e Dutta, 2014).

A biomassa normalmente contém 40-60% de oxigênio. Portanto, excluir o oxigênio da biomassa é o objetivo mais importante para aumentar a densidade energética. O oxigênio pode ser removido seja por desidratação, em que o oxigênio é eliminado na forma de água ou por descarboxilação, em que é removido na forma de dióxido de carbono. A biomassa sofre reação de desidratação a valores mais elevados de pressão e temperatura, mesmo em excesso de água. Geralmente, as reações de desidratação são aceleradas pelo efeito catalítico de pequena quantidade de um ácido de Arrhenius, como H_2SO_4 (Peterson *et al.*, 2008).

A reação de desidratação por sua vez, compromete a reação de despolimerização por meio da hidrólise a temperatura elevada, devido à alta ionização da água nessa temperatura (Kumar, Olajire Oyedun e Kumar, 2018). Ao mesmo tempo, a natureza ácida e básica da água esclarece por que mais biomassa será convertida em biocombustível durante a HTC em comparação com a pirólise, na qual a água não está envolvida (Zhang, Xu e Champagne, 2010). Além disso, a natureza básica da água enfraquece certas ligações no material orgânico. Como resultado, novos fragmentos moleculares são aumentados, alterando o ambiente de reação.

As principais vias de reação envolvidas no processo de carbonização hidrotérmica ainda estão em discussão na comunidade científica (Titirici *et al.*, 2012). Uma rota possível foi discutida por Jatzwauck e Schumpe (Jatzwauck e Schumpe, 2015), segundo o qual o processo HTC está essencialmente dividido em três etapas. A primeira está relacionada principalmente à hidrólise da celulose, hemiceluloses e parte da lignina. Durante a segunda etapa, os intermediários gerados sofrem novo arranjo, resultando na geração de produtos gasosos. Como

alternativa à formação da fase gasosa, produtos intermediários podem se conglomerar para formar carvão secundário, durante a terceira etapa.

A outra rota mais discutida, em relação à evolução das reações de HTC, envolve duas vias principais: a transformação sólido-sólido, segundo a qual o *hydrochar* é gerado diretamente da desidratação da biomassa inicial, e a reação líquido-sólido na qual os orgânicos dissolvidos presentes na solução polimerizam de volta para formar novamente o material sólido, muitas vezes denominado carvão secundário (Knežević, Swaaij, Van e Kersten, 2009; Kruse e Dahmen, 2015; Volpe e Fiori, 2017).

Por meio dessas reações, é possível aumentar o teor de carbono da matéria-prima inicial, removendo a maioria dos compostos oxigenados mais voláteis (furanos e ácidos graxos de baixa massa molecular) que normalmente são movidos para a fase aquosa (Volpe, Goldfarb e Fiori, 2018).

Também é relatado na literatura que, durante a HTC, parte dos inorgânicos podem ser extraídos da matriz de biomassa para a água do processo e, portanto, são removidos do combustível sólido resultante (Reza *et al.*, 2013, 2015; Volpe, Goldfarb e Fiori, 2018), fato que promove no *hydrochar*, a redução de minerais (cinzas) e, por outro lado, aumenta seu poder calorífico (Gao *et al.*, 2019; Volpe *et al.*, 2018).

No entanto, ao mesmo tempo, o material orgânico também é dissolvido na água do processo, levando a diminuição do rendimento de massa total. Assim, se a perda de matéria orgânica for maior do que a redução dos elementos inorgânicos, o teor de cinzas aumentará após o processo de HTC (Hansen, Fendt e Spliethoff, 2022).

Ao trabalharem com a HTC de sete matérias-primas lignocelulósicas, Hansen et al. (Hansen, Fendt e Spliethoff, 2022), concluíram que a composição inorgânica da matéria prima tratada com HTC foi fundamentalmente alterada. Potássio (K) e Cloro (Cl) foram removidos em grande parte do biocombustível por dissolução de sais na água do processo, enquanto a remoção de Silício (Si), Cálcio (Ca) e Fósforo (P) foi limitada no material sólido. Essas mudanças levam à melhoria das propriedades do combustível no que diz respeito à tendência à corrosão, temperaturas de fusão das cinzas e emissões de partículas finas. Por outro lado, o teor de nitrogênio (N) no combustível aumentou após o tratamento, levando a maior risco de emissões de NO_x durante a combustão.

Além disso, a HTC também pode aumentar a área de superfície específica (Wilk e Magdziarz, 2017) e o volume diferencial dos poros (Gao *et al.*, 2019) do *hydrochar*. Mudanças na superfície durante o tratamento com HTC estão associadas à redução de compostos

orgânicos e volatilização, definindo a matriz de *hydrochar* (Başakçılardan Kabakcı e Baran, 2019; He, Giannis e Wang, 2013; Mendoza Martinez *et al.*, 2021).

O processo HTC pode ser classificado como direto ou catalítico. No processo direto, apenas água e matéria-prima são aquecidas em reator a diferentes faixas de temperatura, enquanto no processo catalítico, um catalisador é utilizado. Em geral, os catalisadores ácidos são os mais eficazes para hidrólise (Wang *et al.*, 2018b).

Por fim, a integração do HTC com outros processos renováveis/convencionais pode não só tornar todo o processo mais eficiente energeticamente, mas também pode resultar em produtos mais desejados (Heidari *et al.*, 2019). Como pode ser verificado nos estudos de Reza et al. (Reza, Uddin, *et al.*, 2014), que indicaram que a mistura de 10% de *hydrochar* de HTC e 90% de carvão de torrefação resultaria em pellet durável com maior densidade de energia. Isso ocorre porque o *hydrochar* preenche os espaços vazios e faz pontes sólidas entre as partículas de biomassa torrificada. A HTC pode ser combinada com pirólise e gaseificação (Castello, Kruse e Fiori, 2014; Erlach, Harder e Tsatsaronis, 2012). Liu et al. (Liu, Ma e Chen, 2018) mostraram que sua combinação com a pirólise melhora a capacidade de adsorção de contaminantes como Cr^{6+}, Cd^{2+} e atrazina.

2.4.1 *Hydrochar*

Semelhante ao biocarvão do processo de torrefação, o *hydrochar* é visto como o principal produto da HTC e pode ser efetivamente isolado da fração líquida devido à sua propriedade homogênea e hidrofóbica (Hoekman *et al.*, 2013), essa última, significa menores problemas de armazenamento e transporte (Kambo e Dutta, 2015a). Possui maior PCS devido à fixação de carbono e menor teor de material volátil, o que o torna, um biocombustível sólido melhor do que a matéria-prima de origem (Başakçılardan Kabakcı e Baran, 2019; Mendoza Martinez *et al.*, 2021).

O *hydrochar* pode variar de coloração marrom claro a preto (Ahmed *et al.*, 2019; Hoekman *et al.*, 2017), como pode ser observado na Figura 4, e portanto, mais escuro que a biomassa original. O escurecimento da coloração do *hydrochar* é uma evidência visual de carbonização.

Figura 4 – *Hydrochar* de serragem de *Eucalyptus grandis*.

Fonte: Da autora, 2023.

O *hydrochar* produzido por HTC com utilização de catalisador ácido diluído, apresenta porosidade na parede celular, pois o ácido penetra, causando ruptura das n-cadeias celulósicas constituintes, gerando o gás que desencadeia o processo de erupção na parede celular e deixa o material todo poroso, facilitando, em muito a difusão gasosa no processo de combustão (Lin *et al.*, 2020).

A formação do *hydrochar* pode ser descrita como a conversão de lignina e/ou celulose não dissolvida e fragmentos dissolvidos por meio da hidrocarbonização (Gao, P. *et al.*, 2016). Durante a HTC, a formação do *hydrochar* ocorre por duas vias: (1) carvão primário - formação direta de sólido para sólido e (2) carvão secundário - formado devido à polimerização da fração líquida (Hoekman *et al.*, 2017; Lucian, Volpe e Fiori, 2019).

Geralmente, o hydrochar produzido pela HTC detém 55-90% da massa original da matéria prima e 80-90% do conteúdo de energia (Yan *et al.*, 2009). E demonstra ter propriedades de combustão melhoradas em comparação com o carvão equivalente, oriundo da pirólise (Kambo e Dutta, 2015a), em grande parte devido ao seu conteúdo mineral reduzido. Comparando o hydrochar com outros materiais carbonáceos, ele estaria próximo ao linhito, porém sem as desvantagens desse tipo de carvão que apresenta altos teores de cinzas (5 a 25%) e enxofre (0,4 a 2,6%), fornecendo benefícios ambientais e de saúde.

2.4.2 Fatores que influenciam os produtos da Carbonização Hidrotérmica

Apesar do elevado interesse, o processo de produção de hydrochar ainda não atingiu as condições ideais para alto rendimento. Estudos anteriores sugerem que vários parâmetros operacionais influenciam o processo HTC (Nizamuddin *et al.*, 2017) e, por isso, precisam ser estudados, uma vez que, podem gerar grande variedade nas propriedades físico-químicas do hydrochar (Ahmed *et al.*, 2019). Compreender e contabilizar essas interações é importante ao desenvolver modelos para prever as propriedades dos hydrochars produzidos (Román *et al.*, 2018).

Além disso, existe grande interdependência entre as variáveis envolvidas no processo de HTC, como a temperatura, tempo de reação, uso de catalisador, proporção biomassa/água e tipo de biomassa. Geralmente, a temperatura de reação tem maior influência, no entanto, as outras variáveis podem ter relevância menor ou maior, dependendo das condições específicas da reação, ou seja, cada variável do processo pode influenciar de forma diferente as reações intermediárias e os produtos gerados, em termos de rendimentos e composição (Volpe e Fiori, 2017).

Portanto, é de suma importância definir as melhores condições para maximizar a eficiência de retenção de energia, a fim de obter um hydrochar valioso para fins energéticos (Maniscalco, Volpe e Messineo, 2020).

2.4.2.1 Efeito da Temperatura

A temperatura é sugerida como o parâmetro chave para o processo de HTC, oferecendo calor de desintegração para fragmentação das ligações presentes na estrutura da biomassa (Nizamuddin *et al.*, 2017), influenciando diretamente o rendimento do hydrochar e suas características (Zhang *et al.*, 2019).

À medida que a temperatura aumenta, o rendimento sólido e o conteúdo de oxigênio tendem a diminuir, enquanto aumenta a aromaticidade do hydrochar, melhorando tanto o conteúdo energético, quanto a termo estabilidade (Zhang, Y. *et al.*, 2018). Nesse aspecto, à medida que a temperatura da HTC aumenta, a água no estado subcrítico reforça a dissolução de compostos orgânicos da biomassa, resultando na queda de rendimento do hydrochar (Gao, Y. *et al.*, 2016). Fato que foi verificado por Volpe et al. (Volpe *et al.*, 2018), ao trabalharem com resíduos de azeitona. Os autores observaram que o rendimento sólido de hydrochar diminuiu

com o aumento da temperatura de HTC, apresentando valores entre 81,7 e 57,6% a 180 e 250 °C, respectivamente.

Diferentes estudos avaliaram o efeito da temperatura de reação no rendimento e propriedades do hydrochar (Arauzo, Olszewski e Kruse, 2018; Lucian, Volpe e Fiori, 2019), e concluíram que ela é a principal responsável pela degradação da biomassa e aumento do PCS. Como relatado por Lucian et al. (Lucian, Volpe e Fiori, 2019), que observaram aumento do PCS da poda de azeitona de 22,6 para 27,8 MJ kg^{-1} quando a temperatura de reação aumentou de 180 para 250 °C.

Outra explicação, é que em temperaturas mais altas, uma porção maior de biomassa participará da reação, enquanto em temperaturas baixas, a hemiceluloses é o principal composto degradado, assim, em temperaturas mais altas, ocorre maior decomposição e despolimerização da celulose e das hemiceluloses em subprodutos líquidos e gasosos, o que também aumenta a hidrofobicidade do hydrochar (Funke e Ziegler, 2010; Kambo e Dutta, 2015a).

Pela mesma razão, o PCS do hydrochar obtido pela HTC em temperaturas mais elevadas é superior ao obtido em temperaturas mais baixas. Visto que, o PCS da hemiceluloses, celulose e lignina são relatados na literatura na faixa de 14,7–18,2, 16,1–19 e 22,3–26,6 MJ kg^{-1}, respectivamente (Heidari *et al.*, 2019), assim a HTC em temperaturas mais altas removerá mais celulose e hemiceluloses e resultará em maiores frações de lignina.

A temperatura demonstra influenciar as taxas de carbonização, com temperaturas mais altas estando correlacionadas com a aceleração das reações de carbonização (Román *et al.*, 2018).

Além disso, reações pirolíticas adicionais podem se tornar cada vez mais influentes em temperaturas mais altas sob condições subcríticas (Funke e Ziegler, 2010). Nessas condições, a degradação da composição polimérica da biomassa resulta na formação de compostos intermediários como monômeros, furfurais e 5-Hidroxil Metil Furfural (HMF) (Reza *et al.*, 2013). Essas moléculas intermediárias são caracterizadas como materiais solúveis em água durante a análise da fibra, o que aumenta com o incremento da temperatura de reação da HTC (Kambo e Dutta, 2015a). A precipitação de tais compostos na estrutura porosa do hydrochar pode aumentar ainda mais a densidade de energia geral do produto sólido (Reza *et al.*, 2013).

Além do rendimento, a temperatura também influencia as demais características do hydrochar produzido pela HTC. Gao et al. (Gao, P. *et al.*, 2016), converteram casca de eucalipto via HTC, variando a temperatura na faixa de 220 a 300°C e variando o tempo de reação na faixa de 2 a 10h. Os autores verificaram que a temperatura de HTC desempenhou papel importante

no rendimento, nas propriedades físico-químicas e no comportamento térmico do hydrochar, enquanto o efeito do tempo de reação foi marginal. Temperaturas mais altas melhoraram a conversão hidrotérmica da casca de eucalipto, resultando em menor rendimento, mas em contrapartida, resultam em maior teor de carbono fixo, maior razão combustível, maior PCS e menores razões H/C e O/C. Com o aumento da temperatura de HTC, o rendimento sólido diminuiu de 46,4% para 40,0%, enquanto o PCS do hydrochar aumentou de 20,2 MJ kg^{-1} para 29,2 MJ kg^{-1}, respectivamente.

A pressão da reação HTC é uma variável que depende da temperatura, portanto, o que causa o chamado "efeito temperatura" é na verdade uma combinação de temperatura e pressão, uma vez que o aumento do primeiro parâmetro aumenta o último. E ao alterar a pressão, a temperatura de degradação também varia. Assim, não está claro se o efeito na carbonização se deve à temperatura, à pressão ou a ambas (Yu *et al.*, 2022).

2.4.2.2 Efeito do tempo de reação

Comparado à temperatura, o tempo de reação tem um impacto semelhante, porém em menor magnitude, na recuperação de produtos sólidos (Ahmed *et al.*, 2019) e o rendimento de hydrochar tende a ser maior quando os tempos de reação são curtos, diminuindo a medida que o tempo aumenta (Wang *et al.*, 2018b). HTC mais longo diminui o rendimento do hydrochar, bem como os grupos funcionais oxigenados na superfície devido às menores proporções atômicas H/C e O/C alcançadas (Malhotra e Garg, 2020; Zhang, Y. *et al.*, 2018).

O tempo de reação define não só a conversão geral da biomassa, mas também a composição do produto e influência o consumo de energia. Entretanto, alguns autores (Nizamuddin *et al.*, 2017), relataram que o tempo de reação só influencia as reações de hidrólise até certo intervalo de tempo, além do qual não tem nenhum impacto específico no processo, em determinada condição. Vários tempos de reação podem ser encontrados na literatura e variam de alguns minutos a várias horas (Heidari *et al.*, 2019).

Considerando a hidrólise como a primeira grande reação no processo de degradação da biomassa, ao realizar HTC com altas proporções sólido-líquido, o efeito do tempo de reação pode ser insignificante porque a quantidade de água pode não ser suficiente para decompor completamente a biomassa por hidrólise. Por outro lado, quando as proporções sólido-líquido são baixas, o efeito do tempo da HTC é mais significativo, regulando a distribuição dos produtos (Atallah *et al.*, 2019; Funke e Ziegler, 2010; Zhang *et al.*, 2019).

No entanto, González-Arias et al. (González-Arias *et al.*, 2020) ao realizarem HTC variando os tempos de reação de 3 a 9h em diferentes temperaturas para conversão da poda de oliveira, verificaram que ao aumentar o tempo de reação, o rendimento sólido tende a diminuir até certo ponto em que os polímeros dissolvidos na água do processo reagem entre si formando o que é conhecido como carvão secundário. Este comportamento é favorecido em tempos de reação mais elevados.

Román et al. (Román *et al.*, 2012), ao trabalharem com diferentes precursores, verificaram que a influência do tempo de reação era negativa ou não significativa. Outros autores indicam que não há clareza da influência do tempo no rendimento de hydrochar, podendo ser positivo, negativo ou nulo, a depender do precursor (Álvarez-Murillo *et al.*, 2015). Entretanto, ressaltam que, embora a temperatura e, por vezes a presença de catalisador, desempenhem o papel principal no rendimento, o efeito do tempo de reação não pode ser negligenciado.

Em relação ao PCS, Zhang et al. (Zhang *et al.*, 2015) realizaram HTC de espiga de milho a 250 °C e variaram o tempo de reação de 0,5 para 6 h em pequenos incrementos. Eles descobriram que o PCS do hydrochar aumentou de 24,3 MJ kg^{-1} em 0,5 h para 24,9 MJ kg^{-1} por 6 h. Assim, em comparação com a temperatura, o aumento do tempo de reação não apresentou efeito significativo no PCS do hydrochar.

Também é provável que a influência do tempo de reação nas características do produto da HTC seja dependente do tempo de aquecimento do reator e/ou da taxa de aquecimento. No entanto, poucos estudos relatam informações sobre taxa de aquecimento/tempo (Álvarez-Murillo *et al.*, 2016).

De acordo com Lucian et al. (Lucian, Volpe e Fiori, 2019), para baixas temperaturas, o tempo de reação pode até ter efeito positivo no rendimento sólido de hydrochar, corroborando com os resultados verificados por Chen et al. (Chen *et al.*, 2017). Os autores verificaram aumento no rendimento sólido quando a temperatura de reação foi fixada, respectivamente, em 180 e 190 °C para um tempo de reação de 6h, comparado aos rendimentos sólidos obtidos em 1h. O aumento no rendimento de hydrochar está associado ao rearranjo e polimerização de compostos orgânicos da fase líquida para a fase sólida (Volpe e Fiori, 2017).

Em contraste, tempos de reação mais curtos mostraram-se eficazes para a conversão de hydrochars e podem significar aumento na receita, permitindo que mais produto seja produzido em determinado intervalo de tempo (Saba, McGaughy e Toufiq Reza, 2019).

2.4.2.3 Efeito da matéria prima

Embora grupos funcionais aromáticos e ligações C–C e C–O aumentem gradualmente durante a degradação térmica (Wang *et al.*, 2020), características como energia de ignição, reatividade, PCS, estrutura morfológica e, portanto, os usos potenciais do produto final, dependem muito da composição da matéria-prima utilizada.

Por isso, a compreensão da natureza dos mecanismos que envolvem o processo de HTC depende principalmente do tipo de biomassa utilizada (Funke e Ziegler, 2010). Em geral, o efeito da composição da matéria-prima atua como parâmetro crucial na formação de hydrochar. Vários estudos indicam a influência do tipo de biomassa na qualidade e rendimento do hydrochar, bem como na sua porosidade (Kumar, Olajire Oyedun e Kumar, 2018; Wang *et al.*, 2018a). As proporções dos componentes bioquímicos da biomassa influenciam a via de degradação e a temperatura de reação (Funke e Ziegler, 2010).

Em relação ao rendimento de hydrochar, matéria-prima com maior estrutura de celulose-lignina serão menos afetadas pela mudança de temperatura e pressão do que aquelas com maior estrutura de hemicelulose-celulose (Güleç *et al.*, 2021), enfatizando, portanto, a influência da composição da matéria-prima na definição das condições de HTC. O tipo de material determina a taxa de reação inicial de hidrólise. Matéria-prima com constituinte polimérico facilmente degradado sofrerá carbonização mais rápida, no entanto, àquelas com constituinte polimérico recalcitrante, como a lignina, sofrerá carbonização mais lenta durante a degradação hidrotérmica. Além disso, a lignina tem se mostrado afetada em uma extensão muito limitada pelo processo de HTC e retida, quase que totalmente, nos hydrochars (Başakçılardan Kabakcı e Baran, 2019).

Como relatado por Kabakci e Baran (Başakçılardan Kabakcı e Baran, 2019), ao trabalharem com diferentes tipos de biomassa, sob temperatura de 220 °C e tempo de reação de 90 minutos, cujos resultados encontram-se no Quadro 1, cada biomassa apresentou características diferentes após a HTC. A razão mais importante para este fato é que as biomassas utilizadas no estudo contêm celulose, hemiceluloses, lignina, matéria inorgânica e substâncias orgânicas solúveis em diferentes proporções (Kumar, Olajire Oyedun e Kumar, 2018) e cada uma dessas estruturas se comportam de maneira diferente em condições hidrotérmicas.

Quadro 1 – Propriedades de amostras de biomassa lignocelulósica e seus hydrochars correspondentes.

Propriedades	Serragem de madeira		Casca de noz		Bagaço de azeitona		Semente de damasco		Casca de avelã	
	Cru	HC	Cru	HC	Cru	HC	Cru	HC	Cru	HC
Material volátil [a]	79,8	72,5	57,1	55,5	73,1	65,3	78,6	69,3	54	49,3
Carbono Fixo [a]	10,5	18,3	33,4	42,4	24,7	27,7	17,1	19,6	36,5	35,8
Cinzas [a]	7,4	6,7	4,3	0	0,1	5,5	2,7	9,3	5,1	11,8
C [a]	45,6	52,0	44,6	53,7	46,6	61,1	48,9	57,6	45,7	53,5
H [a]	6,1	4,8	5,6	5,3	5,9	6,4	5,9	5,7	5,3	5,1
N [a]	0,09	0,04	0,66	0,87	1,40	0,90	0,25	0,33	1,70	1,50
Extrativos [a]	1,9	ND	0	ND	1,7	ND	4	ND	0	ND
Lignina Klason [a]	28,5	ND	69,9	ND	48,9	ND	40,2	ND	58,9	ND
PCS [b]	18,60	20,61	17,53	21,46	19,66	25,56	19,74	23,64	17,07	20,99
SY [a]	-	55,7	-	64,8	-	65,8	-	60,8	-	65,8

Legenda: Cru = biomassa in natura; HC = hydrochar; [a] % massa seca; [b] MJ kg^{-1}; SY = Rendimento sólido. Fonte: Adaptado Kabakci e Baran (Başakçılardan Kabakcı e Baran, 2019).

Quanto maior o teor de lignina e menor o de hemiceluloses, maior a resistência da biomassa à degradação nas condições do processo de HTC. De acordo com Yang et al. (Yang, Shimanouchi e Kimura, 2015), a lignina é o constituinte químico da biomassa que mais contribui para o rendimento do hydrochar.

2.4.2.4 Efeito do catalisador

Normalmente, acredita-se que o processo de HTC seja auto catalítico pelo desenvolvimento de ácidos orgânicos, como ácido láctico, ácido levulínico e ácido fórmico da biomassa, causando uma redução no pH (Jain, Balasubramanian e Srinivasan, 2016). Porém, estudos constataram que a adição de ácidos, bases e sais pode ter efeito significativo no grau de carbonização, a fim de melhorar as propriedades físico-químicas dos produtos da HTC em condições de pressão, temperatura e tempo de reação menores (Antero *et al.*, 2020; Chen *et al.*, 2021; Jais *et al.*, 2021; MacDermid-Watts, Pradhan e Dutta, 2021; Wikberg *et al.*, 2015).

Geralmente, os catalisadores ácidos são os mais eficazes para a hidrólise, enquanto os catalisadores básicos prejudicam a formação de hydrochar e apoiam a formação de líquido (Nizamuddin *et al.*, 2017). Catalisadores ácidos promovem a decomposição de macromoléculas, podem reduzir as emissões de dióxido de carbono, ao mesmo tempo que

avançam as reações de hidrólise e descarboxilação (Benavente, Fullana e Berge, 2017), melhoram a taxa de reação HTC, mas, também, melhoram a proporção de combustível e a eficiência de recuperação de energia em até 0,4 e 36,3%, respectivamente (Sztancs *et al.*, 2021).

Este é um parâmetro bastante importante a considerar, uma vez que os catalisadores podem ser seletivos aos diferentes produtos formados durante a reação e podem favorecer a decomposição da biomassa, modificando a rota da reação e aumentando principalmente o nível de hidrólise (González-Arias *et al.*, 2021), influenciando o rendimento e as características do hydrochar (Antero *et al.*, 2020; He *et al.*, 2022; Jais *et al.*, 2021).

O efeito da HTC da celulose em diferentes concentrações primárias de ácidos e bases utilizando H_2SO_4, NaOH, $Ca(OH)_2$ e HCl como aditivos foi estudado por Lu et. al (Lu e Berge, 2014). O resultado mostra que esses aditivos aceleram a dissolução da celulose sólida e uma vez aumentada a concentração do aditivo, a conversão da glicose é acelerada.

Wikberg et al. (Wikberg *et al.*, 2015) relataram aumento do rendimento sólido em pH mais baixo para HTC de lignina Kraft de madeira de coníferas a 240 °C por 22h na presença de H_2SO_4. Eles atribuíram isso à dissolução de maior quantidade de lignina na fase líquida que então repolimerizou no hydrochar ao longo do tempo.

No entanto, Reza et al. (Reza *et al.*, 2015) relataram uma diminuição no rendimento sólido durante avaliação do efeito de pH da água de reação na HTC da palha de trigo a 200 e 260 °C na presença de CH_3COOH e KOH. Eles atribuíram esta observação ao aumento da degradação dos componentes da biomassa pelo CH_3COOH.

Os catalisadores podem quebrar as ligações C - C e C - O nas frações individuais (celulose, hemiceluloses e lignina) e na matriz lignocelulósica, facilitando a formação de carvão secundário (Evcil *et al.*, 2020). Assim, a formação de hydrochar pode ser aumentada utilizando catalisadores ácidos que facilitam a hidrólise, uma vez que, a adição de ácidos na HTC fornece mais íons de hidrogênio (H^+) para catalisar a hidrólise e acelera outras reações, como desidratação, descarboxilação, aromatização e polimerização (Antero *et al.*, 2020; Nizamuddin *et al.*, 2017), em condições fracamente ácidas (Ameen *et al.*, 2022). Em altas concentrações, no entanto, o H^+ fica excessivamente disponível, podendo levar a uma reação exagerada, diminuindo o rendimento e afetando as características do hydrochar (Jais *et al.*, 2021).

Os padrões para a seleção de um bom catalisador exigem que eles sejam termicamente estáveis, eficazes, de baixo custo e tenham alta seletividade para o rendimento necessário (Ameen *et al.*, 2022; Antero *et al.*, 2020), além disso, a concentração adequada dependerá dos demais parâmetros (temperatura, tempo, relação sólido-líquido) da HTC.

Ademais, catalisadores podem ser usados para controlar as emissões, como NO_x. Foi demonstrado que a substituição da água pura por solução aquosa mais ácida e básica, usando catalisadores, pode aumentar a remoção de nitrogênio (Zhao *et al.*, 2014). Este fato ocorre porque as reações químicas catalíticas convertem rapidamente o NO_x em nitrogênio e água (Nizamuddin *et al.*, 2017).

Ghanim et al. (Ghanim, Kwapinski e Leahy, 2017) estudaram o efeito da adição de H_2SO_4 e CH_3COOH. Ambos tiveram efeito na remoção do teor de cinzas, no entanto, H_2SO_4 também produziu aumento no conteúdo de carbono fixo. A obtenção de menor teor de cinzas devido à remoção de metais alcalinos e alcalino-terrosos melhorou o poder calorífico dos hydrochars obtidos.

Catalisadores homogêneos, ou seja, aqueles que são dissolvidos e alimentados no reator, como KOH ou H_2SO_4, oferecem a vantagem de não sofrerem problemas de coqueificação e inativação, como os catalisadores heterogêneos são propensos a fazer. No entanto, esses catalisadores devem ser recuperados e reutilizados no final do processo para que este seja mais econômico (Peterson *et al.*, 2008).

2.4.3 Vantagens do processo de Carbonização Hidrotérmica

Uma das principais vantagens do HTC sobre os demais processos termoquímicos é que a etapa de secagem inicial, não é necessária, uma vez que, na HTC, a umidade residual desempenha papel duplo, tanto como solvente quanto como catalisador (Fang *et al.*, 2018). A eliminação da pré-secagem representa economia de energia, pois a secagem é um processo extensivo e altamente energético. No entanto, a pós-secagem do hydrochar é necessária para aplicações energéticas. Além disso, a água como meio de reação é ecologicamente segura, de baixo custo, e prontamente disponível (Funke e Ziegler, 2010).

Por ser conduzida em ambiente aquoso, a HTC pode utilizar matérias-primas úmidas, incluindo resíduos verdes e outros materiais (Peterson *et al.*, 2008). Assim, um dos principais benefícios da utilização da HTC é a sua elevada flexibilidade na escolha da matéria-prima (Heidari *et al.*, 2019) e por esse motivo, não representa qualquer ameaça à produção de alimentos (Zhang *et al.*, 2009). Além do mais, embora a HTC produza um "fluxo de resíduos" aquoso, este material contém níveis substanciais de produtos químicos orgânicos potencialmente valiosos, como açúcares, furanos, furfurais e ácidos orgânicos (Funke e Ziegler, 2010).

Outra vantagem é que, em consequência da alta transferência de calor no ambiente aquoso, o processo HTC prossegue mais rapidamente do que a torrefação, por exemplo. Em níveis comparáveis de severidade de processo (temperatura), o hydrochar produzido por HTC tem maior densificação de energia do que o produto sólido obtido a partir da torrefação via seca (Yan *et al.*, 2009).

Kambo e Dutta (Kambo e Dutta, 2015b) compararam os processos de torrefação e HTC, juntamente com seus respectivos produtos sólidos, e concluíram que a HTC é superior na produção de produto sólido com maior conteúdo de energia, melhor moagem, maior hidrofobicidade e maior remoção de metais alcalinos e alcalino-terrosos.

A remoção de compostos inorgânicos pode ser considerada como vantagem importante do processo de HTC. Alguns estudos indicam que a HTC permite a produção de hydrochar de estrutura porosa (Funke *et al.*, 2021) podendo causar a lixiviação de metais alcalinos e alcalinos terrosos (Kambo e Dutta, 2015a; Reza *et al.*, 2013) e, portanto, produz quantidade menor de óxidos.

Adicionalmente, o fato da água ser mantida no estado líquido, operando no ponto de saturação ou acima dele, minimiza amplamente a mudança de entalpia associada ao calor latente de vaporização da água, consiste em outra vantagem do processo. A grande mudança de entalpia associada ao calor latente (2260 J/g) significa que o aquecimento da água a 100°C sob pressão requer seis vezes menos energia do que gerar vapor a 100°C. Tecnologias de conversão que exigem a pré-secagem da matéria prima, como a pirólise, precisam superar o calor latente da vaporização para remover a água antes do processamento (“Biller e Ross_2016_ Produção de biocombustível por hidrocarbonização.pdf”, [s.d.]).

Ademais, a HTC é compatível o suficiente para ser combinado com outros processos, permitindo assim que produtos com determinadas características em termos de morfologia, porosidade, química e propriedades eletrônicas sejam produzidos para aplicações específicas como geração de energia (Carrasco *et al.*, 2020), nanopartículas (para fabricação de compósitos), purificação de água (Tran *et al.*, 2017), captura de carbono e correção do solo (Puccini *et al.*, 2018).

Outros destaques estão relacionados a altos rendimentos sólidos e qualidade do produto final em relação ao PCS, funcionalidade de superfície ajustáveis, presença de ligantes naturais, comportamento condutor, facilidade de operação, baixo custo e eficiência energética do processo (Lin *et al.*, 2015; Reza, Andert, *et al.*, 2014; Román *et al.*, 2012).

Por fim, a possível escalabilidade do processo até o nível industrial (Hitzl *et al.*, 2015), bem como as condições de processo relativamente suaves, tornam a HTC uma solução válida

para o futuro próximo para a transformação de ampla gama de biomassa em materiais valiosos (Hitzl *et al.*, 2015; Lucian e Fiori, 2017).

2.4.4 Otimização do processo de HTC

A HTC é indicada como tecnologia para valorização dos resíduos de biomassa. No entanto, sugere-se que o processo HTC deva ser otimizado para cada tipo de biomassa (Lu e Berge, 2014). A otimização das condições operacionais da HTC para a recuperação do combustível hydrochar é crucial, principalmente do ponto de vista do desenvolvimento do processo. E segundo Picone (Picone, Volpe e Messineo, 2021), um dos principais desafios da HTC é otimizar os parâmetros do processo e investigar sua influência nas diferentes biomassas.

Um processo HTC ideal e econômico deve ser caracterizado pela menor temperatura e tempo de reação possíveis, para o máximo rendimento de hydrochar e maior poder calorífico (Afolabi, Sohail e Cheng, 2020).

Neste contexto, a Metodologia de Superfície de Respostas (RSM), tem sido empregada com sucesso para otimizar processos de HTC de diferentes biomassas (Akbari *et al.*, 2022; Jais *et al.*, 2021; Wang *et al.*, 2022). Trata se de uma abordagem comprovada e amplamente divulgada para investigar os efeitos interativos combinados entre variáveis independentes (de entrada) em um processo. Eles são particularmente úteis na otimização de processos para produzir respostas (saídas) para todas as combinações possíveis de entradas dentro de um espaço experimental para permitir a identificação de condições ótimas (Afolabi, Sohail e Cheng, 2020).

2.4.5 Aplicações do Hydrochar

A utilização do hydrochar depende de suas propriedades físico-químicas, enfatizando a importância de caracterizar adequadamente esse material de acordo com diferentes técnicas (Sharma *et al.*, 2020).

A aplicação que está despertando o interesse de pesquisadores em todo o mundo é sua capacidade de agir como combustível neutro, sendo fonte de carbono com alta densidade energética (Ma *et al.*, 2022; Zhang *et al.*, 2020). Como o hydrochar apresenta melhora do comportamento térmico de combustão em comparação com a matéria-prima in natura, ele pode ser coqueimado com carvão para geração de energia (Kruse, Funke e Titirici, 2013).

Ainda quanto a utilização energética, a HTC seguida de processos de compactação pode melhorar significativamente as características de transporte, armazenamento e manuseio do hydrochar, que pode ser utilizado na forma de pellets e briquetes (Kambo e Dutta, 2015a).

No entanto, além do uso como biocombustível sólido, o hydrochar pode ser utilizado na produção de carvão ativado para tratamento de água (Khataee *et al.*, 2017); na correção e retenção de nutrientes no solo, aumentando o suprimento de nutrientes para as plantas e diminuindo as perdas devido à lixiviação (Fregolente *et al.*, 2021; Islam *et al.*, 2021; Libra *et al.*, 2011); no sequestro de carbono (Baronti *et al.*, 2017; Hoekman *et al.*, 2013; Yan *et al.*, 2010); como pré-tratamento para digestão anaeróbica (Luz Codignole *et al.*, 2018), entre outras aplicações.

Esta versatilidade é importante para que os custos de produção sejam diluídos, pois o hydrochar produzido pode ser destinado ao mercado de maior interesse econômico do momento.

3 CONSIDERAÇÕES GERAIS

Neste estudo, foram produzidos hydrochars a partir de diferentes condições de hidrotratamento, com metodologia e reatores simplificados. Os resultados revelaram que o processo HTC realizado, pode gerar hydrochars com propriedades aprimoradas em comparação com a biomassa in natura, para sua utilização como biocombustível sólido.

A Metodologia de Superfície de Resposta (RSM) se mostrou eficaz para analisar e otimizar o processo de carbonização hidrotérmica (HTC) de serragem de *Eucalyptus grandis* por meio de três parâmetros do processo, simultaneamente.

A otimização de processos apresenta desafios como rendimentos e tendência de PCS em direções opostas. Ficou evidente que os fatores mais influentes no processo, dentro da faixa estudada, foram a concentração de ácido e a temperatura de reação.

Com base nos rendimentos sólido e energético, juntamente com a desejabilidade geral, o hidrotratamento otimizado foi conduzido a uma temperatura de 185 °C, tempo de reação de 30 min e 0,038 mol L^{-1} de H_2SO_4, visando minimizar o tempo de reação (custos de produção), uma vez que o tempo não demonstrou efeito significativo, enquanto maximiza essas características energéticas.

Contudo, as possibilidades promissoras em torno da HTC são atestadas pelo crescente interesse nos últimos anos. Além disso, o potencial de biorrefinaria da HTC pode tornar este processo muito lucrativo no futuro. Melhoraria os aspectos ambientais e econômicos da HTC, evitando a geração de resíduos e aumentando os rendimentos do processo, respectivamente. Esta abordagem contribuirá para o desenvolvimento de uma bioeconomia circular.

4 PERSPECTIVAS FUTURAS DA TESE

As abordagens apresentadas na tese constituem importantes passos para a consolidação da produção de hydrochar de maneira simplificada, com propriedades atrativas para o setor energético.

A produção de hydrochar por HTC, a partir de resíduos de serragem oferece inúmeros benefícios potenciais, como a redução do desperdício em aterros e a mitigação das emissões de gases com efeito de estufa. No entanto, existem vários desafios e limitações que precisam ser abordados, entre eles, estudos precisam avançar nos seguintes aspectos:

- Avaliar e validar os experimentos e modelos gerados em reatores de maior escala.

- Os produtos líquidos têm recebido atenção limitada, embora estes subprodutos contenham produtos de transição e exijam uma investigação mais detalhada. Esta pesquisa adicional é vital para compreender melhor o processo HTC em relação à formação de materiais ricos em carbono.

- Outro desafio está relacionado com a eficiência energética. Embora o processo de HTC possa converter resíduos em combustível de alto teor energético, o processo também requer insumos energéticos para aquecimento. Portanto, é fundamental avaliar a eficiência energética e a utilização de recursos do processo produtivo, assim como, identificar oportunidades para aumentar a eficiência e reduzir o consumo de recursos.

- É interessante que futuros estudos verifiquem o efeito dos extrativos durante o processo de HTC, principalmente em madeiras em que o teor de extrativos químicos pode chegar a 20%.

- Ainda existem mecanismos no processo HTC que precisam de mais estudos, a fim de se obter o maior controle sobre os parâmetros do processo, sua influência nas propriedades do produto final e, assim, suas possíveis aplicações. Por isso, mais pesquisas são necessárias para otimizar o processo de produção e reduzir o custo da produção de hydrochar.

- Mais estudos são necessários para melhorar e avaliar a implementação da HTC em diferentes cenários, como a ampliação de testes para diversas biomassas lenhosas e não lenhosas disponíveis no Brasil. Avaliações técnico-econômicas e avaliações de ciclo de vida são cruciais para alcançar bons resultados do ponto de vista social, ambiental e econômico.

REFERÊNCIAS BIBLIOGRÁFICAS

ACHARYA, B.; DUTTA, A.; MINARET, J. Review on comparative study of dry and wet torrefaction. **Sustainable Energy Technologies and Assessments**, v. 12, p. 26–37, 2015.
ADAMS, P.; BRIDGWATER, T.; LEA-LANGTON, A.; ROSS, A.; WATSON, I. **Chapter 8 - Biomass Conversion Technologies." Greenhouse Gas Balances of Bioenergy Systems**. [s.l: s.n.].
AFOLABI, O. O. D.; SOHAIL, M.; CHENG, Y. L. Optimisation and characterisation of hydrochar production from spent coffee grounds by hydrothermal carbonisation. **Renewable Energy**, v. 147, p. 1380–1391, 1 mar. 2020.
AHMAD, F.; SILVA, E. L.; VARESCHE, M. B. A. Hydrothermal processing of biomass for anaerobic digestion – A review. **Renewable and Sustainable Energy Reviews**, v. 98, n. September, p. 108–124, 2018.
AHMED KHAN, T.; KIM, H. J.; GUPTA, A.; JAMARI, S. S.; JOSE, R. Synthesis and characterization of carbon microspheres from rubber wood by hydrothermal carbonization. **Journal of Chemical Technology and Biotechnology**, v. 94, n. 5, p. 1374–1383, 1 maio 2019.
AHMED, T.; SAJIDAH, A.; JAMARI, S. S.; HASBI, M.; RAHIM, A.; PARK, J.; KIM, H. Biomass and Bioenergy Hydrothermal carbonization of lignocellulosic biomass for carbon rich material preparation : A review. v. 130, n. September, 2019.
AKBARI, HAMED; AKBARI, HESAM; FANAEI, F.; ADIBZADEH, A. Optimization of parameters affecting the hydrothermal carbonization of wastewater treatment plant sewage sludge. **Biomass Conversion and Biorefinery**, n. 4, 2022.
AKHTAR, J.; AMIN, N. A. S. A review on process conditions for optimum bio-oil yield in hydrothermal liquefaction of biomass. **Renewable and Sustainable Energy Reviews**, v. 15, n. 3, p. 1615–1624, 2011.
ÁLVAREZ-MURILLO, A.; ROMÁN, S.; LEDESMA, B.; SABIO, E. Study of variables in energy densification of olive stone by hydrothermal carbonization. **Journal of Analytical and Applied Pyrolysis**, v. 113, p. 307–314, 1 maio 2015.
ÁLVAREZ-MURILLO, A.; SABIO, E.; LEDESMA, B.; ROMÁN, S.; GONZÁLEZ-GARCÍA, C. M. Generation of biofuel from hydrothermal carbonization of cellulose. Kinetics modelling. **Energy**, v. 94, p. 600–608, 2016.
ALVES, J. L. F.; SILVA, J. C. G. DA; MUMBACH, G. D.; DOMENICO, M. DI; SILVA FILHO, V. F. DA; SENA, R. F. DE; MACHADO, R. A. F.; MARANGONI, C. Insights into the bioenergy potential of jackfruit wastes considering their physicochemical properties, bioenergy indicators, combustion behaviors, and emission characteristics. **Renewable Energy**, v. 155, p. 1328–1338, 1 ago. 2020.
AMEEN, M.; ZAMRI, N. M.; MAY, S. T.; AZIZAN, M. T.; AQSHA, A.; SABZOI, N.; SHER, F. Effect of acid catalysts on hydrothermal carbonization of Malaysian oil palm residues (leaves, fronds, and shells) for hydrochar production. **Biomass Conversion and Biorefinery**, v. 12, n. 1, p. 103–114, 2022.
ANTERO, R. V. P.; ALVES, A. C. F.; OLIVEIRA, S. B. DE; OJALA, S. A.; BRUM, S. S. Challenges and alternatives for the adequacy of hydrothermal carbonization of lignocellulosic biomass in cleaner production systems: A review. **Journal of Cleaner Production**, v. 252, 2020.
ARAUZO, P. J.; OLSZEWSKI, M. P.; KRUSE, A. Hydrothermal carbonization brewer's spent grains with the focus on improving the degradation of the feedstock. **Energies**, v. 11, n. 11, 2018.
ATALLAH, E.; KWAPINSKI, W.; AHMAD, M. N.; LEAHY, J. J.; ZEAITER, J. Effect of water-sludge ratio and reaction time on the hydrothermal carbonization of olive oil mill wastewater treatment: Hydrochar characterization. **Journal of Water Process Engineering**, v. 31, n. March, p. 8–15, 2019.
BARONTI, S.; ALBERTI, G.; CAMIN, F.; CRISCUOLI, I.; GENESIO, L.; MASS, R.; VACCARI, F. P.; ZILLER, L.; MIGLIETTA, F. Hydrochar enhances growth of poplar for bioenergy while marginally contributing to direct soil carbon sequestration. **GCB Bioenergy**, v. 9, n. 11, p. 1618–1626, 2017.
BAŞAKÇILARDAN KABAKCI, S.; BARAN, S. S. Hydrothermal carbonization of various lignocellulosics: Fuel characteristics of hydrochars and surface characteristics of activated hydrochars. **Waste Management**, v. 100, p. 259–268, 1 dez. 2019.

BASSO, D.; PATUZZI, F.; CASTELLO, D.; BARATIERI, M.; RADA, E. C.; WEISS-HORTALA, E.; FIORI, L. Agro-industrial waste to solid biofuel through hydrothermal carbonization. **Waste Management**, v. 47, p. 114–121, 2016.
BEN. **Balanço Energético Nacional Relatório Síntese 2023**. [s.l: s.n.].
BENAVENTE, V.; FULLANA, A.; BERGE, N. D. Life cycle analysis of hydrothermal carbonization of olive mill waste: Comparison with current management approaches. **Journal of Cleaner Production**, v. 142, p. 2637–2648, 2017.
Biller e Ross_2016_ Produção de biocombustível por hidrocarbonização.pdf. , [s.d.].
BOBLETER, O. Hydrothermal degradation of polymers derived from plants. **Progress in Polymer Science**, v. 19, n. 5, p. 797–841, 1994.
BRAGHIROLI, F. L.; PASSARINI, L. **Valorization of Biomass Residues from Forest Operations and Wood Manufacturing Presents a Wide Range of Sustainable and Innovative PossibilitiesCurrent Forestry Reports**Springer, , 1 jun. 2020.
CAMIA, A. *et al.* **Biomass production, supply, uses and flows in the European Union. First results from an integrated assessment**. [s.l: s.n.].
CARRASCO, S. *et al.* Experimental study on hydrothermal carbonization of lignocellulosic biomass with magnesium chloride for solid fuel production. **Processes**, v. 8, n. 4, 1 abr. 2020.
CASTELLO, D.; KRUSE, A.; FIORI, L. Supercritical water gasification of hydrochar. **Chemical Engineering Research and Design**, v. 92, n. 10, p. 1864–1875, 2014.
CAVALI, M.; LIBARDI JUNIOR, N.; SENA, J. D. DE; WOICIECHOWSKI, A. L.; SOCCOL, C. R.; BELLI FILHO, P.; BAYARD, R.; BENBELKACEM, H.; CASTILHOS JUNIOR, A. B. DE. **A review on hydrothermal carbonization of potential biomass wastes, characterization and environmental applications of hydrochar, and biorefinery perspectives of the processScience of the Total Environment**Elsevier B.V., , 20 jan. 2023.
CAVALI, M.; SOCCOL, C. R.; TAVARES, D.; ZEVALLOS TORRES, L. A.; OLIVEIRA DE ANDRADE TANOBE, V.; ZANDONÁ FILHO, A.; WOICIECHOWSKI, A. L. Effect of sequential acid-alkaline treatment on physical and chemical characteristics of lignin and cellulose from pine (Pinus spp.) residual sawdust. **Bioresource Technology**, v. 316, n. April, 2020.
CHEN, C.; LIANG, W.; FAN, F.; WANG, C. The Effect of Temperature on the Properties of Hydrochars Obtained by Hydrothermal Carbonization of Waste Camellia oleifera Shells. **ACS Omega**, 2021.
CHEN, W. H.; LEE, K. T.; HO, K. Y.; CULABA, A. B.; ASHOKKUMAR, V.; JUAN, C. J. Multi-objective operation optimization of spent coffee ground torrefaction for carbon–neutral biochar production. **Bioresource Technology**, v. 370, n. November 2022, p. 128584, 2023.
CHEN, X.; LIN, Q.; HE, R.; ZHAO, X.; LI, G. Hydrochar production from watermelon peel by hydrothermal carbonization. **Bioresource Technology**, v. 241, p. 236–243, 2017.
CHENG, C.; HE, Q.; ISMAIL, T. M.; MOSQUEDA, A.; DING, L.; YU, J.; YU, G. Hydrothermal carbonization of rape straw: Effect of reaction parameters on hydrochar and migration of AAEMs. **Chemosphere**, v. 291, n. June 2021, 2022.
D. FENGEL, G. W. **Wood: chemistry, ultrastructure, reactions**. Berlin, New York: Walter de Gruyter, 1989.
DEMIR CAKAN, R.; TITIRICI, M. M.; ANTONIETTI, M.; CUI, G.; MAIER, J.; HU, Y. S. Hydrothermal carbon spheres containing silicon nanoparticles: Synthesis and lithium storage performance. **Chemical Communications**, n. 32, p. 3759–3761, 2008.
DJANDJA, O. S.; YIN, L.; WANG, Z.; DUAN, P. From wastewater treatment to resources recovery through hydrothermal treatments of municipal sewage sludge : A critical review. v. 151, p. 101–127, 2021.
ERLACH, B.; HARDER, B.; TSATSARONIS, G. Combined hydrothermal carbonization and gasification of biomass with carbon capture. **Energy**, v. 45, n. 1, p. 329–338, 2012.
EVCIL, T.; SIMSIR, H.; UCAR, S.; TEKIN, K.; KARAGOZ, S. Hydrothermal carbonization of lignocellulosic biomass and effects of combined Lewis and Brønsted acid catalysts. **Fuel**, v. 279, n. December 2019, 2020.
FANG, J.; ZHAN, L.; OK, Y. S.; GAO, B. Minireview of potential applications of hydrochar derived from hydrothermal carbonization of biomass. **Journal of Industrial and Engineering Chemistry**, v. 57, p. 15–21, 25 jan. 2018.

FIORI, L.; BASSO, D.; CASTELLO, D.; BARATIERI, M. Hydrothermal Carbonization of Biomass : Design of a Batch Reactor and Preliminary Experimental Results. v. 37, p. 55–60, 2014.
FOOD AND AGRICULTURE ORGANIZATION OF THE UNITED NATIONS. **FAO.**
FREGOLENTE, L. G.; SANTOS, J. V. DOS; MAZZATI, F. S.; MIGUEL, T. B. A. R.; C. MIGUEL, E. DE; MOREIRA, A. B.; FERREIRA, O. P.; BISINOTI, M. C. Hydrochar from sugarcane industry by-products: assessment of its potential use as a soil conditioner by germination and growth of maize. **Chemical and Biological Technologies in Agriculture**, v. 8, n. 1, p. 1–13, 2021.
FUNKE, A.; ZIEGLER, F. **Hydrothermal carbonization of biomass: A summary and discussion of chemical mechanisms for process engineeringBiofuels, Bioproducts and Biorefining**, mar. 2010.
FUNKE, A.; ZIEGLER, F.; UNIVERSIT, T.; RECEBIDO, A.; INTERSCIENCE, W. discussão de mecanismos químicos. v. 177, n. 2010, p. 160–177, 2021.
GAO, L.; VOLPE, M.; LUCIAN, M.; FIORI, L.; GOLDFARB, J. L. Does hydrothermal carbonization as a biomass pretreatment reduce fuel segregation of coal-biomass blends during oxidation? **Energy Conversion and Management**, v. 181, n. September 2018, p. 93–104, 2019.
GAO, P.; ZHOU, Y.; MENG, F.; ZHANG, Y.; LIU, Z.; ZHANG, W.; XUE, G. Preparation and characterization of hydrochar from waste eucalyptus bark by hydrothermal carbonization. **Energy**, v. 97, p. 238–245, 2016.
GAO, Y.; YU, B.; WU, K.; YUAN, Q.; WANG, X.; CHEN, H. Physicochemical, pyrolytic, and combustion characteristics of hydrochar obtained by hydrothermal carbonization of biomass. **BioResources**, v. 11, n. 2, p. 4113–4133, 2016.
GHANIM, B. M.; KWAPINSKI, W.; LEAHY, J. J. Hydrothermal carbonisation of poultry litter: Effects of initial pH on yields and chemical properties of hydrochars. **Bioresource Technology**, v. 238, p. 78–85, 2017.
GONZÁLEZ-ARIAS, J.; BAENA-MORENO, F. M.; SÁNCHEZ, M. E.; CARA-JIMÉNEZ, J. Optimizing hydrothermal carbonization of olive tree pruning: A techno-economic analysis based on experimental results. **Science of the Total Environment**, v. 784, 2021.
GONZÁLEZ-ARIAS, J.; SÁNCHEZ, M. E.; MARTÍNEZ, E. J.; COVALSKI, C.; ALONSO-SIMÓN, A.; GONZÁLEZ, R.; CARA-JIMÉNEZ, J. Hydrothermal carbonization of olive tree pruning as a sustainableway for improving biomass energy potential: Effect of reaction parameters on fuel properties. **Processes**, v. 8, n. 10, 2020.
GÜLEÇ, F.; RIESCO, L. M. G.; WILLIAMS, O.; KOSTAS, E. T.; SAMSON, A.; LESTER, E. Hydrothermal conversion of different lignocellulosic biomass feedstocks – Effect of the process conditions on hydrochar structures. **Fuel**, v. 302, n. May, 2021.
HANSEN, L. J.; FENDT, S.; SPLIETHOFF, H. Impact of hydrothermal carbonization on combustion properties of residual biomass. **Biomass Conversion and Biorefinery**, v. 12, n. 7, p. 2541–2552, 1 jul. 2022.
HE, C.; GIANNIS, A.; WANG, J. Y. Conversion of sewage sludge to clean solid fuel using hydrothermal carbonization: Hydrochar fuel characteristics and combustion behavior. **Applied Energy**, v. 111, p. 257–266, 2013.
HE, Q.; CHENG, C.; RAHEEM, A.; DING, L.; SHIUNG, S.; YU, G. Effect of hydrothermal carbonization on woody biomass : From structure to reactivity. v. 330, n. August, p. 1–12, 2022.
HEIDARI, M.; DUTTA, A.; ACHARYA, B.; MAHMUD, S. A review of the current knowledge and challenges of hydrothermal carbonization for biomass conversion. **Journal of the Energy Institute**, v. 92, 2019.
HEIDARI, M.; SALAUDEEN, S.; NOROUZI, O.; ACHARYA, B.; DUTTA, A. Numerical comparison of a combined hydrothermal carbonization and anaerobic digestion system with direct combustion of biomass for power production. **Processes**, v. 8, n. 1, 2020.
HITZL, M.; CORMA, A.; POMARES, F.; RENZ, M. The hydrothermal carbonization (HTC) plant as a decentral biorefinery for wet biomass. **Catalysis Today**, v. 257, n. Part 2, p. 154–159, 2015.
HOEKMAN, S. K.; BROCH, A.; FELIX, L.; FARTHING, W. Hydrothermal carbonization (HTC) of loblolly pine using a continuous, reactive twin-screw extruder. **Energy Conversion and Management**, v. 134, p. 247–259, 2017.
HOEKMAN, S. K.; BROCH, A.; ROBBINS, C.; ZIELINSKA, B.; FELIX, L. Hydrothermal carbonization (HTC) of selected woody and herbaceous biomass feedstocks. **Biomass Conversion**

and Biorefinery, v. 3, n. 2, p. 113–126, 29 jun. 2013.
IBÁ. **Relatório Anual 2023**. [s.l: s.n.].
IBBETT, R.; GADDIPATI, S.; DAVIES, S.; HILL, S.; TUCKER, G. The mechanisms of hydrothermal deconstruction of lignocellulose: New insights from thermal-analytical and complementary studies. **Bioresource Technology**, v. 102, n. 19, p. 9272–9278, 2011.
IEA. Technology roadmap: delivering sustainable bioenergy. Paris, France; 2017. **Phyton**, v. 63, p. 87–91, 2017.
___. **Tracking Clean Energy Progress 2023**. Disponível em: <https://www.iea.org/reports/tracking-clean-energy-progress-2023>. Acesso em: 29 ago. 2023.
IEA BIOENERGY. Task 42 Biorefining in a Circular Economy Operating Agent. 2022.
ISLAM, MD AZHARUL; LIMON, M. S. H.; ROMIĆ, M.; ISLAM, MD ATIKUL. Hydrochar-based soil amendments for agriculture: a review of recent progress. **Arabian Journal of Geosciences**, v. 14, n. 2, 2021.
JAIN, A.; BALASUBRAMANIAN, R.; SRINIVASAN, M. P. Hydrothermal conversion of biomass waste to activated carbon with high porosity : A review. v. 283, p. 789–805, 2016.
JAIS, F. M.; IBRAHIM, S.; CHEE, C. Y.; ISMAIL, Z. High removal of crystal violet dye and tetracycline by hydrochloric acid assisted hydrothermal carbonization of sugarcane bagasse prepared at high yield. **Sustainable Chemistry and Pharmacy**, v. 24, n. September, 2021.
JATZWAUCK, M.; SCHUMPE, A. Kinetics of hydrothermal carbonization (HTC) of soft rush. **Biomass and Bioenergy**, v. 75, p. 94–100, 1 abr. 2015.
JUNG, Y. H.; KIM, K. H. Acidic Pretreatment. **Pretreatment of Biomass: Processes and Technologies**, p. 27–50, 1 jan. 2015.
KAMBO, H. S.; DUTTA, A. Strength, storage, and combustion characteristics of densified lignocellulosic biomass produced via torrefaction and hydrothermal carbonization. **Applied Energy**, v. 135, p. 182–191, 5 dez. 2014.
___. A comparative review of biochar and hydrochar in terms of production, physico-chemical properties and applications. **Renewable and Sustainable Energy Reviews**, v. 45, p. 359–378, 2015a.
___. Comparative evaluation of torrefaction and hydrothermal carbonization of lignocellulosic biomass for the production of solid biofuel. **Energy Conversion and Management**, v. 105, p. 746–755, 2015b.
KAMBO, H. S.; MINARET, J.; DUTTA, A. Process Water from the Hydrothermal Carbonization of Biomass: A Waste or a Valuable Product? **Waste and Biomass Valorization**, v. 9, n. 7, p. 1181–1189, 2018.
KHATAEE, A.; KAYAN, B.; KALDERIS, D.; KARIMI, A.; AKAY, S.; KONSOLAKIS, M. Ultrasound-assisted removal of Acid Red 17 using nanosized Fe3O4-loaded coffee waste hydrochar. **Ultrasonics Sonochemistry**, v. 35, p. 72–80, 1 mar. 2017.
KNEŽEVIĆ, D.; SWAAIJ, W. P. M. VAN; KERSTEN, S. R. A. Hydrothermal conversion of biomass: I, glucose conversion in hot compressed water. **Industrial and Engineering Chemistry Research**, v. 48, n. 10, p. 4731–4743, 2009.
KRUSE, A.; DAHMEN, N. Water – A magic solvent for biomass conversion. **The Journal of Supercritical Fluids**, v. 96, p. 36–45, 1 jan. 2015.
KRUSE, A.; FUNKE, A.; TITIRICI, M. M. Hydrothermal conversion of biomass to fuels and energetic materials. **Current Opinion in Chemical Biology**, v. 17, n. 3, p. 515–521, 2013.
KUMAR, M.; OLAJIRE OYEDUN, A.; KUMAR, A. A review on the current status of various hydrothermal technologies on biomass feedstock. **Renewable and Sustainable Energy Reviews**, v. 81, n. May 2017, p. 1742–1770, 2018.
KUMAR, P. S.; YAASHIKAA, P. R. Sources and operations of waste biorefineries. **Refining Biomass Residues for Sustainable Energy and Bioproducts: Technology, Advances, Life Cycle Assessment, and Economics**, p. 111–133, 2019.
LI, F.; ZIMMERMAN, A. R.; HU, X.; YU, Z.; HUANG, J.; GAO, B. One-pot synthesis and characterization of engineered hydrochar by hydrothermal carbonization of biomass with ZnCl2. **Chemosphere**, v. 254, 2020.
LIBRA, J. A.; RO, K. S.; KAMMANN, C.; FUNKE, A.; BERGE, N. D.; NEUBAUER, Y.; TITIRICI, M. M.; FÜHNER, C.; BENS, O.; KERN, J.; EMMERICH, K. H. Hydrothermal carbonization of biomass residuals: A comparative review of the chemistry, processes and applications of wet and dry

pyrolysis. **Biofuels**, v. 2, n. 1, p. 71–106, 2011.
LIN, Y.; GE, Y.; XIAO, H.; HE, Q.; WANG, W.; CHEN, B. Investigation of hydrothermal co-carbonization of waste textile with waste wood, waste paper and waste food from typical municipal solid wastes. **Energy**, v. 210, 2020.
LIN, Y.; MA, X.; PENG, X.; HU, S.; YU, Z.; FANG, S. Effect of hydrothermal carbonization temperature on combustion behavior of hydrochar fuel from paper sludge. **Applied Thermal Engineering**, v. 91, p. 574–582, 2015.
LIU, Y.; MA, S.; CHEN, J. A novel pyro-hydrochar via sequential carbonization of biomass waste: Preparation, characterization and adsorption capacity. **Journal of Cleaner Production**, v. 176, p. 187–195, 2018.
LIU, Z.; QUEK, A.; HOEKMAN, S. K.; BALASUBRAMANIAN, R. Production of solid biochar fuel from waste biomass by hydrothermal carbonization. v. 103, p. 943–949, 2013.
LU, X.; BERGE, N. D. Influence of feedstock chemical composition on product formation and characteristics derived from the hydrothermal carbonization of mixed feedstocks. **Bioresource Technology**, v. 166, p. 120–131, 2014.
LUCIAN, M.; FIORI, L. Hydrothermal carbonization of waste biomass: Process design, modeling, energy efficiency and cost analysis. **Energies**, v. 10, n. 2, 2017.
LUCIAN, M.; VOLPE, M.; FIORI, L. Hydrothermal carbonization kinetics of lignocellulosic agro-wastes: Experimental data and modeling. **Energies**, v. 12, n. 3, 2019.
LUGANO, G. **Lignocellulose Structure.** Disponível em: <https://app.biorender.com/biorender-templates/figures/likes/t-648f6560480945daa49e8bd2-lignocellulose-structure>.
LUZ CODIGNOLE, F.; VOLPE, M.; FIORI, L.; MANNI, A.; CORDINER, S.; MULONE, V.; ROCCO, V. Bioresource Technology Spent co ff ee enhanced biomethane potential via an integrated hydrothermal carbonization-anaerobic digestion process G RA P H I C A L AB S T R A C T. v. 256, n. February, p. 102–109, 2018.
MA, L.; GOLDFARB, J. L.; SONG, J.; CHANG, C.; MA, Q. Enhancing cleaner biomass-coal co-combustion by pretreatment of wheat straw via washing versus hydrothermal carbonization. **Journal of Cleaner Production**, v. 366, n. July, p. 132991, 2022.
MACDERMID-WATTS, K.; PRADHAN, R.; DUTTA, A. Catalytic Hydrothermal Carbonization Treatment of Biomass for Enhanced Activated Carbon: A Review. **Waste and Biomass Valorization**, v. 12, n. 5, p. 2171–2186, 2021.
MALHOTRA, M.; GARG, A. Hydrothermal carbonization of centrifuged sewage sludge : Determination of resource recovery from liquid fraction and thermal behaviour of hydrochar. v. 117, p. 114–123, 2020.
MANISCALCO, M. P.; VOLPE, M.; MESSINEO, A. Hydrothermal carbonization as a valuable tool for energy and environmental applications: A review. **Energies**, v. 13, n. 15, 2020.
MENDOZA MARTINEZ, C. L.; SERMYAGINA, E.; SAARI, J.; SILVA DE JESUS, M.; CARDOSO, M.; MATHEUS DE ALMEIDA, G.; VAKKILAINEN, E. Hydrothermal carbonization of lignocellulosic agro-forest based biomass residues. **Biomass and Bioenergy**, v. 147, 1 abr. 2021.
MONCADA B, J.; ARISTIZÁBAL M, V.; CARDONA A, C. A. Design strategies for sustainable biorefineries. **Biochemical Engineering Journal**, v. 116, p. 122–134, 2016.
MORAIS, D.; CARVALHO, D.; SEVASTYANOVA, O.; SOUZA, L.; PEREIRA, B.; LINDSTRÖM, M. E.; LUIZ, J. Assessment of chemical transformations in eucalyptus , sugarcane bagasse and straw during hydrothermal , dilute acid , and alkaline pretreatments. v. 73, p. 118–126, 2015.
MOSCICKI, K. J.; NIEDZWIECKI, L.; OWCZAREK, P.; WNUKOWSKI, M. Commoditization of wet and high ash biomass: wet torrefaction—a review. **Open Access Journal Journal of Power Technologies**, v. 97, n. 4, p. 354–369, 2017.
MUNIR, M. T.; UL SAQIB, N.; LI, B.; NAQVI, M. Food waste hydrochar: An alternate clean fuel for steel industry. **Fuel**, v. 346, n. February, 2023.
NIZAMUDDIN, S.; BALOCH, H. A.; GRIFFIN, G. J.; MUBARAK, N. M.; BHUTTO, A. W.; ABRO, R.; MAZARI, S. A.; ALI, B. S. An overview of effect of process parameters on hydrothermal carbonization of biomass. **Renewable and Sustainable Energy Reviews**, v. 73, n. December 2015, p. 1289–1299, 2017.
PETERSON, A. A.; VOGEL, F.; LACHANCE, R. P.; FRÖLING, M.; ANTAL, M. J.; TESTER, J. W. Thermochemical biofuel production in hydrothermal media: A review of sub- and supercritical water

technologies. **Energy and Environmental Science**, v. 1, n. 1, p. 32–65, 2008.
PICONE, A.; VOLPE, M.; MESSINEO, A. Process water recirculation during hydrothermal carbonization of waste biomass: Current knowledge and challenges. **Energies**, v. 14, n. 10, 2021.
PUCCINI, M.; CECCARINI, L.; ANTICHI, D.; SEGGIANI, M.; TAVARINI, S.; LATORRE, M. H.; VITOLO, S. Hydrothermal carbonization of municipal woody and herbaceous prunings: Hydrochar valorisation as soil amendment and growth medium for horticulture. **Sustainability (Switzerland)**, v. 10, n. 3, 2018.
REZA, M. T.; ANDERT, J.; WIRTH, B.; BUSCH, D.; PIELERT, J.; LYNAM, J. G.; MUMME, J. Hydrothermal Carbonization of Biomass for Energy and Crop Production. **Applied Bioenergy**, v. 1, n. 1, p. 11–29, 2014.
REZA, M. T.; ROTTLER, E.; HERKLOTZ, L.; WIRTH, B. Hydrothermal carbonization (HTC) of wheat straw: Influence of feedwater pH prepared by acetic acid and potassium hydroxide. **Bioresource Technology**, v. 182, p. 336–344, 2015.
REZA, M. T.; UDDIN, M. H.; LYNAM, J. G.; CORONELLA, C. J. Engineered pellets from dry torrefied and HTC biochar blends. **Biomass and Bioenergy**, v. 63, p. 229–238, 2014.
REZA, M. T.; WERNER, M.; POHL, M.; MUMME, J. Evaluation of integrated anaerobic digestion and hydrothermal carbonization for bioenergy production. **Journal of Visualized Experiments**, n. 88, p. 1–9, 2014.
REZA, M. T.; YAN, W.; UDDIN, M. H.; LYNAM, J. G.; HOEKMAN, S. K.; CORONELLA, C. J.; VÁSQUEZ, V. R. Reaction kinetics of hydrothermal carbonization of loblolly pine. **Bioresource Technology**, v. 139, p. 161–169, 2013.
ROMÁN, S.; LIBRA, J.; BERGE, N.; SABIO, E.; RO, K.; LI, L.; LEDESMA, B.; ALVAREZ, A.; BAE, S. Hydrothermal carbonization: Modeling, final properties design and applications: A review. **Energies**, v. 11, n. 1, p. 1–28, 2018.
ROMÁN, S.; NABAIS, J. M. V.; LAGINHAS, C.; LEDESMA, B.; GONZÁLEZ, J. F. Hydrothermal carbonization as an effective way of densifying the energy content of biomass. **Fuel Processing Technology**, v. 103, p. 78–83, 2012.
SABA, A.; MCGAUGHY, K.; TOUFIQ REZA, M. Techno-economic assessment of co-hydrothermal carbonization of a coal-Miscanthus blend. **Energies**, v. 12, n. 4, p. 1–17, 2019.
SERMYAGINA, E.; SAARI, J.; KAIKKO, J.; VAKKILAINEN, E. Hydrothermal carbonization of coniferous biomass: Effect of process parameters on mass and energy yields. **Journal of Analytical and Applied Pyrolysis**, v. 113, p. 551–556, 2015.
SEVILLA, M.; FUERTES, A. B. The production of carbon materials by hydrothermal carbonization of cellulose. **Carbon**, v. 47, n. 9, p. 2281–2289, 2009.
SHARMA, H. B.; PANIGRAHI, S.; DUBEY, B. K. Hydrothermal carbonization of yard waste for solid bio-fuel production: Study on combustion kinetic, energy properties, grindability and flowability of hydrochar. **Waste Management**, v. 91, p. 108–119, 15 maio 2019.
SHARMA, H. B.; SARMAH, A. K.; DUBEY, B. **Hydrothermal carbonization of renewable waste biomass for solid biofuel production: A discussion on process mechanism, the influence of process parameters, environmental performance and fuel properties of hydrocharRenewable and Sustainable Energy Reviews**Elsevier Ltd, , 1 maio 2020.
SHARMA, R.; JASROTIA, K.; SINGH, N.; GHOSH, P.; SRIVASTAVA, S.; SHARMA, N. R.; SINGH, J.; KANWAR, R.; KUMAR, A. A Comprehensive Review on Hydrothermal Carbonization of Biomass and its Applications. **Chemistry Africa**, v. 3, n. 1, p. 1–19, 2020.
SZTANCS, G.; KOVACS, A.; TOTH, A. J.; MIZSEY, P.; BILLEN, P.; FOZER, D. Catalytic hydrothermal carbonization of microalgae biomass for low-carbon emission power generation: the environmental impacts of hydrochar co-firing. **Fuel**, v. 300, n. January, 2021.
TAVARES, D.; CAVALI, M.; OLIVEIRA, V. DE; TANOBE, A.; ALBERTO, L.; TORRES, Z.; ROZENDO, A. S.; ZANDON, A.; SOCCOL, C. R. Lignin from Residual Sawdust of Eucalyptus spp .— Isolation , Characterization , and Evaluation of the Antioxidant Properties. p. 195–208, 2022.
TIAN, S. R.; LIU, Y. G.; LIU, S. B.; ZENG, G. M.; JIANG, L. H.; TAN, X. F.; HUANG, X. X.; YIN, Z. H.; LIU, N.; LI, J. Hydrothermal synthesis of montmorillonite/hydrochar nanocomposites and application for 17β-estradiol and 17α-ethynylestradiol removal. **RSC Advances**, v. 8, n. 8, p. 4273–4283, 2018.
TITIRICI, M. M.; THOMAS, A.; YU, S. H.; MÜLLER, J. O.; ANTONIETTI, M. A direct synthesis

of mesoporous carbons with bicontinuous pore morphology from crude plant material by hydrothermal carbonization. **Chemistry of Materials**, v. 19, n. 17, p. 4205–4212, 2007.
TITIRICI, M. M.; WHITE, R. J.; FALCO, C.; SEVILLA, M. Black perspectives for a green future: Hydrothermal carbons for environment protection and energy storage. **Energy and Environmental Science**, v. 5, n. 5, p. 6796–6822, 2012.
TRAN, H. N.; HUANG, F. C.; LEE, C. K.; CHAO, H. P. Activated carbon derived from spherical hydrochar functionalized with triethylenetetramine: Synthesis, characterizations, and adsorption application. **Green Processing and Synthesis**, v. 6, n. 6, p. 565–576, 2017.
TUMULURU, J. S.; HESS, J. R.; BOARDMAN, R. D.; WRIGHT, C. T.; WESTOVER, T. L. Formulation, pretreatment, and densification options to improve biomass specifications for Co-firing high percentages with coal. **Industrial Biotechnology**, v. 8, n. 3, p. 113–132, 2012.
UNITED NATIONS. **Renewables 2020 Global Status Report**. [s.l: s.n.].
UNITED NATIONS ENVIRONMENT PROGRAMME (UNEP). **"COP27 Ends with Announcement of Historic Loss and Damage Fund"**. Disponível em: <https://www.unep.org/news-and-stories/story/%0Acop27-ends-announcement-historic-loss-and-damage-fund>. Acesso em: 29 ago. 2023.
VALLEJO, F.; ALEJANDRO-MARTIN, S.; DÍAZ-ROBLES, L.; GONZÁLEZ, P.; CERECEDA-BALIC, F.; FADIC, X.; VIDAL, V.; BUCHNER, G.; POBLETE, J. Optimization of the Waste Lignocellulosic Biomass Hydrothermal Carbonization Process by Response Surface Methodology. **Chemical Engineering Transactions**, v. 94, p. 1309–1314, 2022.
VOLPE, M.; FIORI, L. From olive waste to solid biofuel through hydrothermal carbonisation: The role of temperature and solid load on secondary char formation and hydrochar energy properties. **Journal of Analytical and Applied Pyrolysis**, v. 124, p. 63–72, 2017.
VOLPE, M.; FIORI, L.; VOLPE, R.; MESSINEO, A. Upgrading of olive tree trimmings residue as biofuel by hydrothermal carbonization and torrefaction: A comparative study. **Chemical Engineering Transactions**, v. 50, p. 13–18, 2016.
VOLPE, M.; GOLDFARB, J. L.; FIORI, L. Hydrothermal carbonization of Opuntia ficus-indica cladodes: Role of process parameters on hydrochar properties. **Bioresource Technology**, v. 247, n. September 2017, p. 310–318, 2018.
VOLPE, M.; WÜST, D.; MERZARI, F.; LUCIAN, M.; ANDREOTTOLA, G.; KRUSE, A.; FIORI, L. One stage olive mill waste streams valorisation via hydrothermal carbonisation. **Waste Management**, v. 80, p. 224–234, 2018.
WANG, G.; ZHANG, J.; LEE, J. Y.; MAO, X.; YE, L.; XU, W.; NING, X.; ZHANG, N.; TENG, H.; WANG, C. Hydrothermal carbonization of maize straw for hydrochar production and its injection for blast furnace. **Applied Energy**, v. 266, n. December 2019, 2020.
WANG, R.; LIN, K.; PENG, P.; LIN, Z.; ZHAO, Z.; YIN, Q.; GE, L. Energy yield optimization of co-hydrothermal carbonization of sewage sludge and pinewood sawdust coupled with anaerobic digestion of the wastewater byproduct. v. 326, n. June, 2022.
WANG, S.; DAI, G.; YANG, H.; LUO, Z. Lignocellulosic biomass pyrolysis mechanism: A state-of-the-art review. **Progress in Energy and Combustion Science**, v. 62, p. 33–86, 2017.
WANG, T.; ZHAI, Y.; ZHU, Y.; LI, C.; ZENG, G. A review of the hydrothermal carbonization of biomass waste for hydrochar formation: Process conditions, fundamentals, and physicochemical properties. **Renewable and Sustainable Energy Reviews**, v. 90, n. December 2016, p. 223–247, 2018a.
___. **A review of the hydrothermal carbonization of biomass waste for hydrochar formation: Process conditions, fundamentals, and physicochemical propertiesRenewable and Sustainable Energy Reviews**Elsevier Ltd, , 1 jul. 2018b.
WANG, Y.; QIU, L.; ZHU, M.; SUN, G.; ZHANG, T.; KANG, K. Comparative Evaluation of Hydrothermal Carbonization and Low Temperature Pyrolysis of Eucommia ulmoides Oliver for the Production of Solid Biofuel. **Scientific Reports**, v. 9, n. 1, p. 1–11, 2019.
WIKBERG, H.; OHRA-AHO, T.; PILEIDIS, F.; TITIRICI, M. M. Structural and Morphological Changes in Kraft Lignin during Hydrothermal Carbonization. **ACS Sustainable Chemistry and Engineering**, v. 3, n. 11, p. 2737–2745, 2015.
WILK, M.; MAGDZIARZ, A. Hydrothermal carbonization, torrefaction and slow pyrolysis of Miscanthus giganteus. **Energy**, v. 140, p. 1292–1304, 1 dez. 2017.

WU, X.; GALKIN, M. V.; STERN, T.; SUN, Z.; BARTA, K. Fully lignocellulose-based PET analogues for the circular economy. **Nature Communications**, v. 13, n. 1, p. 1–12, 2022.
YAN, W.; ACHARJEE, T. C.; CORONELLA, C. J.; VÁSQUEZ, V. R. Thermal pretreatment of lignocellulosic biomass. **Environmental Progress and Sustainable Energy**, v. 28, n. 3, p. 435–440, out. 2009.
YAN, W.; HASTINGS, J. T.; ACHARJEE, T. C.; CORONELLA, C. J.; VÁSQUEZ, V. R. Mass and energy balances of wet torrefaction of lignocellulosic biomass. **Energy and Fuels**, v. 24, n. 9, p. 4738–4742, 2010.
YANG, W.; SHIMANOUCHI, T.; KIMURA, Y. Characterization of the residue and liquid products produced from husks of nuts from carya cathayensis sarg by hydrothermal carbonization. **ACS Sustainable Chemistry and Engineering**, v. 3, n. 4, p. 591–598, 2015.
YANG, Y. Subcritical water chromatography: A green approach to high-temperature liquid chromatography. **Journal of Separation Science**, v. 30, n. 8, p. 1131–1140, 2007.
YU, Y.; LOU, X.; WU, H. Production of mallee biomass in Western Australia: Energy balance analysis. **Energy and Fuels**, v. 22, n. 1, p. 190–198, 2008.
YU, Y.; XU, H.; YU, H.; HU, L.; LIU, Y. Formic acid fractionation towards highly efficient cellulose-derived PdAg bimetallic catalyst for H2 evolution. **Green Energy and Environment**, v. 7, n. 1, p. 172–183, 2022.
ZHANG, J. HONG; LIN, Q. MEI; ZHAO, X. RONG. The hydrochar characters of municipal sewage sludge under different hydrothermal temperatures and durations. **Journal of Integrative Agriculture**, v. 13, n. 3, p. 471–482, 2014.
ZHANG, L.; LIU, S.; WANG, B.; WANG, Q.; YANG, G.; CHEN, J. Effect of residence time on hydrothermal carbonization of corn cob residual. **BioResources**, v. 10, n. 3, p. 3979–3986, 2015.
ZHANG, L.; XU, C. (CHARLES); CHAMPAGNE, P. Overview of recent advances in thermo-chemical conversion of biomass. **Energy Conversion and Management**, v. 51, n. 5, p. 969–982, 2010.
ZHANG, N.; WANG, G.; ZHANG, J.; NING, X.; LI, Y.; LIANG, W.; WANG, C. Study on co-combustion characteristics of hydrochar and anthracite coal. **Journal of the Energy Institute**, v. 93, n. 3, p. 1125–1137, 2020.
ZHANG, S.; SU, Y.; XU, D.; ZHU, S.; ZHANG, H.; LIU, X. Effects of torrefaction and organic-acid leaching pretreatment on the pyrolysis behavior of rice husk. **Energy**, v. 149, p. 804–813, 2018.
ZHANG, T.; LI, W.; XIAO, H.; JIN, Y.; WU, S. Recent progress in direct production of furfural from lignocellulosic residues and hemicellulose. **Bioresource Technology**, v. 354, n. April, 2022.
ZHANG, Y.; GAO, X.; LI, B.; LI, H.; ZHAO, W. Assessing the potential environmental impact of woody biomass using quantitative universal exergy. **Journal of Cleaner Production**, v. 176, p. 693–703, 1 mar. 2018.
ZHANG, Y.; JIANG, Q.; XIE, W.; WANG, Y.; KANG, J. Effects of temperature, time and acidity of hydrothermal carbonization on the hydrochar properties and nitrogen recovery from corn stover. **Biomass and Bioenergy**, v. 122, p. 175–182, 1 mar. 2019.
ZHANG, Y.; MIN, B.; HUANG, L.; ANGELIDAKI, I. Generation of electricity and analysis of microbial communities in wheat straw biomass-powered microbial fuel cells. **Applied and Environmental Microbiology**, v. 75, n. 11, p. 3389–3395, 2009.
ZHAO, P.; SHEN, Y.; GE, S.; CHEN, Z.; YOSHIKAWA, K. Clean solid biofuel production from high moisture content waste biomass employing hydrothermal treatment. v. 131, p. 345–367, 2014.
ZHU, X.; LIU, Y.; QIAN, F.; ZHOU, C.; ZHANG, S.; CHEN, J. Role of Hydrochar Properties on the Porosity of Hydrochar-based Porous Carbon for Their Sustainable Application. **ACS Sustainable Chemistry and Engineering**, v. 3, n. 5, p. 833–840, 2015.
ZHUANG, X.; SONG, Y.; ZHAN, H.; BI, X. T.; YIN, X.; WU, C. Pyrolytic conversion of biowaste-derived hydrochar : Decomposition mechanism of speci fi c components. v. 266, n. January, 2020.
ZHUANG, X.; ZHAN, H.; HUANG, Y.; SONG, Y.; YIN, X.; WU, C. Bioresource Technology Conversion of industrial biowastes to clean solid fuels via hydrothermal carbonization (HTC): Upgrading mechanism in relation to coali fi cation process and combustion behavior. v. 267, n. May, p. 17–29, 2018.

SEGUNDA PARTE – ARTIGOS

ARTIGO 1 - HYDROTREATMENT OF *EUCALYPTUS* SAWDUST: THE INFLUENCE OF PROCESS TEMPERATURE AND H_2SO_4 CATALYST ON HYDROCHAR QUALITY, COMBUSTION BEHAVIOR AND RELATED EMISSIONS

Artigo publicado na Revista Fuel

doi.org/10.1016/j.fuel.2023.130643

Hydrotreatment of *Eucalyptus* sawdust: the influence of process temperature and H_2SO_4 catalyst on hydrochar quality, combustion behavior and related emissions

Nayara Tamires da Silva Carvalho [a], Edgar A. Silveira [b], Thiago de Paula Protásio [c], Paulo Fernando Trugilho [a] and Maria Lúcia Bianchi [d]

a. Federal University of Lavras (UFLA), Department of Forest Sciences, CP. 3037, CEP. 37200-000, Lavras-MG, Brazil.
b. University of Brasília, Mechanical Sciences Graduate Program, Laboratory of Energy and Environment, Brasilia-DF 70910-900, Brazil.
c. Federal Rural University of the Amazonia-UFRA, Campus Parauapebas, Parauapebas, CEP. 68515-000, Pará-PA, Brazil.
d. Federal University of Lavras (UFLA), Department of Chemistry (DQI), Universidade Federal de Lavras, CP. 3037, CEP. 37200-000, Lavras-MG, Brazil.

Abstract

Hydrothermal carbonization (HTC) presents a promising avenue for waste-to-energy conversion, owing to its cost-effectiveness, low emissions, and adaptability. This study employed HTC to convert *Eucalyptus grandis* sawdust residues into hydrochars (HC). HTC was conducted for 60 min in a high-pressure steel reactor within glycerin thermal bath equipment under different temperatures (150, 170, 190, and 220 °C) and reaction mediums (water and H_2SO_4 concentrations of 0.1 and 0.2 mol L^{-1}). The resulting HC underwent thorough analysis, encompassing proximate, ultimate, and morphological assessments and investigations into combustion behavior and potential emissions. Moreover, a new indicator, the hydrotreatment severity index (HSI), is proposed to provide a standardized measure of hydrotreatment severity and property predictions. Higher temperatures and increased H_2SO_4 concentrations were found to reduce solid yield (ranging from 43.21% to 90.72%) and induce morphological changes, including an abundance of carbon microspheres, particularly at higher acid concentrations. These modifications substantially improved higher heating values (HHV), up to 34% (HHV of 25.72 MJ kg^{-1} achieved at 220 °C with 0.2 mol L^{-1} H_2SO_4) compared to raw feedstock. Interestingly, the intermediate temperature of 190 °C contributed significantly, enhancing HHV by 33%. All HTC processes greatly enhanced the combustion performance and ignitability of hydrochars. The most favorable reactivity (S=7.61E7 $\%^2$ min^{-2} $°C^{-3}$) was observed at 220 °C with 0.2 mol L^{-1} H_2SO_4, along with an estimated CO_2 emissions of 2,058.46 kg per ton of hydrochar. These results underscore the efficacy of the simplified methodology and reactor system, emphasizing the critical roles of H_2SO_4 as catalyst and temperature in

shaping the characteristics and performance of hydrochars from a representative Brazilian residue, *Eucalyptus grandis.*

Keywords: Thermochemical conversion; Forestry Waste; Hydrotreatment severity index; Sulfuric acid; Solid biofuel.

Index Summary

Nomenclature

Ashes	ASH	Volatile matter	VM
Derivative Thermogravimetry	DTG	Waste-to-energy	WtE
Energy yield	EY	Weight loss	WL
Energy-mass-coefficient-index	EMCI		
Enhancement fator	EF	*Symbols*	
Eucalyptus	EUC	Atomic ratio of hydrogen to carbon	H/C
Extractives contente	EXT	Atomic ratio of oxygen to carbon	O/C
Fixed carbon	FC	Burnout index	D_f
Fuel ratio	FR	Burnout temperature	T_f
Greenhouse gas	GHG	Emiss. factor of chemically pure carbon	E_C
Hydrochar	HC	Emissions factor of carbon monoxide	E_{CO}
High-rank coal	HRC	Emissions factor of carbon dioxide	E_{CO_2}
Higher heating value	HHV	Emissions factor of methane	E_{CH_4}
Holocellulose	HOL	Emission factor of non-methane VOCs	E_{NMVOC}
Hydrothermal carbonization	HTC	Emissions factor of nitrogen oxides	E_{NO_X}
Hydrotreatment severity index	HSI	Exergy	ε
Lower heating value	LHV	Ignition temperature	T_i
Low-rank coal	LRC	Ignition time	t_i
Medium rank coal	MRC	Integrated combustion index	S
Scamming electron microscopy	SEM	Peak time	t_m
Specific chemical bioexergy	SCB	Temperature	T
Solid yield	SY	Time	t
Total lignin contente	LT	Time range at half value of (dm/dt) max	$\Delta t_{1/2}$
Thermogravimetry	TG		

1. Introduction

The increasing barriers to minimizing our dependence on fossil fuels and their effect on climate change have prompted a search for groundbreaking energy solutions. In this context, biomass residues emerge as a promising biofuel option to fulfill our daily energy needs, harnessing the potential of waste-to-energy (WtE) processes. WtE conversion technologies have gained momentum in recent decades [1]. Regarding the WtE thermochemical process, hydrothermal carbonization (HTC) is a promising technology for converting biomass waste into hydrochar [2,3].

HTC occurs through an intricate network of reactions involving solid-solid and solid-liquid conversions encompassing hydrolysis, dehydration, decarboxylation, and polymerization [4,5]. The HTC process upgrades the raw biomass, enhancing the hydrochar energy density,

increasing its HHV through carbon fixation, reducing volatile materials, and dissolving ashes in the liquid phase [6].

As the HTC treatment entails pressurized conditions, the process equipment can be more intricate and costly than conventional torrefaction [7]. On the other hand, HTC can be conducted more expeditiously than torrefaction and can accommodate a broad spectrum of raw materials, as the initial moisture level is not a concern [8]. Therefore, HTC could promote biomass valorization and improve its transport, storage and fuel characteristics [9].

In wood-based industries, upgrading waste streams from primary production offers not only a source of additional revenue but also an opportunity to meet internal heat and electricity demands for industrial processes. According to the FAO [10] database, world production of sawn wood reached almost 489.1 million m^3 in 2022. Moreover, the production of about 238.7 m^3 of wood waste can become an environmental problem if not disposed of properly. However, to avoid the environmental burden caused by inadequate handling of forest residues, these materials can be used as raw material in other processes due to their lignocellulosic composition.

Numerous studies have assessed hydrochar for pertinent applications across various domains (Table 1). However, its utilization hinges on physicochemical properties, underscoring the significance of appropriately characterizing this material through diverse techniques. As per Table 1, the most applied performance parameters for evaluating the quality of hydrochar produced under differing temperature and reaction time conditions are the product yield and HHV.

In the literature, no works were found proposing using simplified HTC reactors to produce quality hydrochar. Furthermore, although some studies have been conducted regarding the utilization of catalysts in hydrothermal carbonization, there remains ample room for research in this area [11]. For instance, it includes the assessment of different catalysts and feedstock, investigations into HTC chemistry, kinetics and heat transfer, energy and heat recovery, synergies between process parameters, reactor technologies, and technical and economic aspects [12].

Table 1. Summary of hydrotreatment studies indicating the reactor technology, performance indicators and contributions.

Reactor technology / Treatment conditions	**Analytical techniques/ Performance indicators**	**Contributions**	**Ref.**
Batch reactor (250 mL) Feedstock: Sewage sludge Temperature: 260 °C Time:120–240 min	Proximate analysis (VM, FC and ASH) Calorific analysis (HHV and EF) SEM, FTIR, TGA Kinetic Parameters	Comparison between hydrochar and pyrochar Combustion kinetics	[13]
Batch reactor with pressure control Feedstock: Giant bamboo, coffee wood and parchment, and *Eucalyptus* Temperature180–240 °C Time: 180 min Solid-liquid: 8:1	Proximate analysis (VM, FC and ASH) Calorific analysis (HHV and EF) SEM HTC liquid (NVR, pH and TOC) Plant performance indicators	Effect of operating conditions (SY, EF and composition) HTC Liquid Characterization HTC plant modelling	[14]
Batch reactor with constant pressure Feedstock: Corn silage, empty fruit bunches, grass clippings, olive pomace, sewage sludge, wheat straw, fir bark Temperature: 180–270 °C Time: 30–240 min	Proximate analysis (VM, FC and ASH) Calorific analysis (HHV) Ultimate analysis (CHNO-Cl) Ashes composition (XRF) Emission Factors	Properties that are relevant for the combustion of a fuel Inorganic composition	[15]
High-pressure reactor (GCF-1.5) Forest residues Temperature: 200–280 °C Time: 60 min Solid-liquid: 1:5	Proximate analysis (VM, FC and ASH) Calorific analysis (HHV and EF) SEM, FTIR e Raman, BET TG-DTG (combustion index)	Structural characteristics and fuel performance of hydrochar	[16]
Autoclave reactor (Hastelloy-100 mL) Wheat, straw, and *Eucalyptus* Temperature: 200–270 °C Time: 30–120 min Solid-liquid: 4g- 40, 50 e 60 mL	Proximate analysis (VM, FC and ASH) Calorific analysis (HHV and EF) Flask combustion ion chromatography SEM e XPS TG-DTG (combustion index)	Effects of experimental conditions on the chlorine (Cl) behavior during HTC and fuel properties	[17]
Autoclave-mechanical agitation (Buchi Glas Uster Limbo) Olive oil industry residues Temperature: 200–260 °C Time: 30–240 min Solid-liquid 5:1	Proximate analysis (VM, FC and ASH) Ultimate analysis (CHNO) Calorific analysis (HHV and EF) FTIR, BET, SEM Energy balance	Focuses on combustion properties and changes in the inorganic composition of fuels treated with HTC, considering the risk of emission of polluting substances	[18]
Batch reactor Feedstock: *Eucalyptus grandis* Temperature: 150–220 °C Time 60 min Catalytic: 0.1 and 0.2 mol L^{-1} H_2SO_4	Proximate analysis (VM, FC and ASH) Ultimate analysis (CHNO) Calorific analysis (HHV and EF) Structural and non-structural analysis (lignin, holocellulose and extractives) TG-DTG (combustion index) Hydrochar (SY and EY) Hydrotreatment severity index (HSI) Emission Factors	High-pressure steel reactors in glycerin bath; Hydrotreatment Severity Index; Catalytic conditions (H_2SO_4); Combustion behavior of *Eucalyptus* sawdust hydrochar produced under catalytic conditions; Insight on combustion emissions derived from hydrochar combustion	Study

The originality of this work stands on i) investigating the influence and synergy of treatment temperature and H_2SO_4 catalyst to produce hydrochar from a representative Brazilian residue, *Eucalyptus grandis*; ii) introducing an HTC performance parameter, the Hydrotreatment Severity Index (HSI) to provide a standardized measure of hydrotreatment severity, allowing for consistent evaluations across various conditions and feedstocks and establishing correlations between treatment conditions and hydrochar properties and iii) explore the combustion behavior of hydrochar derived from *Eucalyptus grandis* residues produced under H_2SO_4 catalytic conditions and iv) assess insights related to produced emissions (CO_2, CO, CH_4 and NO_x) during its combustion.

The calculated indices allowed for an extensive assessment of *Eucalyptus grandis* biomass in hydrochar production. The results offer insights into dimensionless and condition-based process parameters for hydro-treatments under catalytic conditions.

2. Material and Methods

2.1 Feedstock and Hydrochar Characterization

The biomass used in this study was sawdust obtained from the processing of a 22-year-old *Eucalyptus grandis* wood sourced from a plantation at the Federal University of Lavras (UFLA/Brazil) sited in 21°13'26.86"S and 44°58'12.44"W. The wood processing was carried out at the experimental milling and drying unit, also located at UFLA. Subsequently, the biomass was milled using a knife mill and sorted through 40–60 mesh sieves. Before hydrothermal carbonization, the biomass samples were dried at 103±2 ºC for 24h.

Table 2 presents the characteristics of *Eucalyptus grandis* feedstock and the related standards (detailed in supplementary material). The dry basis was considered for the calculations for all tests (raw biomass and hydrochar).

The structure of the raw biomass and produced hydrochar were examined using scanning electron microscopy (SEM). The images of the samples were taken at 300x magnification, with a voltage of 15 kV, using a TM-4000Plus-Hitachi, Japan.

Table 2. Raw feedstock (*Eucalyptus grandis*) properties. Structural (lignin) and non-structural (extractives) components, proximate (ASH, volatile matter, and fixed carbon), ultimate (CHNO) and calorific (HHV, LHV and SCB) analysis.

Analysis [a]		**Standard**
Moisture content (%)	10.86	ASTM E871-82 (2013)
Total lignin [b] (%)	28.80	Gomide e Demuner (1986) e Goldschimid (1971)
Extractives (%)	9.46	ASTM D1107-96 (2015)
Holocellulose (%)	61.75	Eq. (S1) (see supplementary material)
Proximate analysis		
ASH (%)	0.47	ASTM E872-82 (2019)
FC (%)	12.03	
VM (%)	87.50	
FR [c]	0.14	
Ultimate analysis		
C (%)	50.48	Vario Micro Cube universal analyzer
H (%)	5.91	
O (%)	42.01	
N (%)	1.61	
O/C	0.83	
H/C	0.12	
Calorific analysis (MJ kg^{-1})		
HHV	19.19	Digital calorimeter IKA C-200 ASTM E711-87
LHV [c]	17.97	$LHV = HHV - 206 \times (H)$ Eq. (1)
SCB [d]	20.09	

[a] db: dry basis; [b] based on dry mass extractives-free [19,20]; [c] calculated [21]; [d] calculated [22].

2.2 Reactor apparatus

The schematic diagram of the experimental workflow is shown in Fig. 1, along with a detailed representation of the reactor models.

The HTC experiments were carried out using glycerin bath equipment, Quimis brand, model Q213-22, with a power output of 3100 W. The equipment operates within a temperature range of 50–300 °C, featuring an electronic temperature control system using a programmable on-off control mechanism to maintain reaction temperature with a system precision of ±0.6 °C.

This study randomly utilized 20 laboratory-scale reactors (volume = 0.2 L) constructed with 316 stainless steel (see SM for specifications) according to designs for pressurized cylindrical vessels for hydrochar production. The reactors have an internal diameter of 52 mm and a height of 11 mm. During the experiment, the reactors remain entirely immersed in the heated glycerin. Heat permeates across the entire surface of the reactors through conduction to the mixture of water/acidified and biomass.

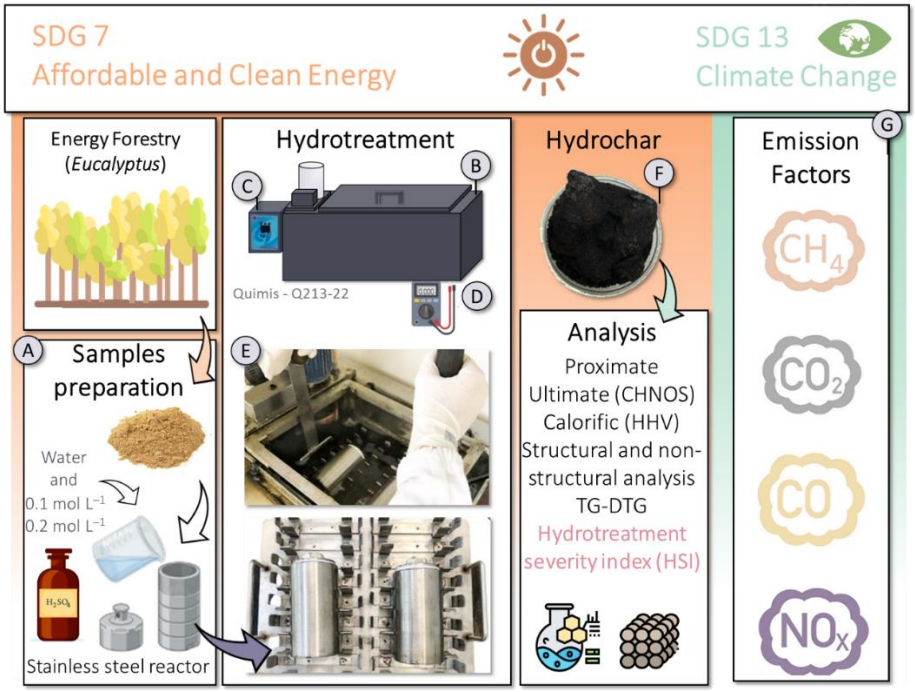

Figure 1. Workflow diagram and general scheme of the experimental system. A) Samples preparation, B) Heated glycerin bath, C) Temperature control, D) Wattmeter, E) Reactors, F) Hydrochar and G) Emission Factors.

2.3 Hydrotreatment conditions

The HTC process for each experimental run involved adding approximately 15 g of biomass into the reactor, along with distilled water or sulfuric acid (H_2SO_4) in a 1:10 ratio (solid on a dry basis/liquid), following the approach by Afolabi et al. and Otaviano et al. [23,24]. The reactor was adequately sealed and shaken to ensure complete wetting of the biomass. The reactors were inserted into the equipment after the glycerin bath reached the specified treatment temperature, which was maintained throughout the experiment.

The proposed high-pressure steel reactor is characterized by its simple construction without mechanical mixing and pressure measurement systems. The reactor's internal pressure was not measured during the HTC process, but according to previous studies, the pressure is autogenous and corresponds to the pressure of water under saturated conditions at the reaction temperature [23,25–27].

HTC was performed at 150, 170, 190, and 220 °C, with a reaction time of 60 min [28]. Three individual experiments were conducted: the control with water and the other two with concentrations of 0.1 and 0.2 mol L^{-1} of H_2SO_4, resulting in three treatments for each temperature, totaling 12 treatments.

After each experiment, the reactors were removed from the glycerin bath and placed in a cooling zone with running water at room temperature. Subsequently, the solid fraction was filtered and washed with 500 mL of distilled water. The solid samples were dried in an oven at 103±2 °C for 24h, weighed, and stored in plastic bags for further analyses.

Hydrothermal carbonization was repeated four times per treatment in each experiment, amounting to 48 hydrothermal carbonizations. In the subsequent discussion, the hydrochar is denoted as E_{i-j}, with i=0 (control), 1 and 2, attributed to the H_2SO_4 concentration (0; 0.1 and 0.2 mol L^{-1}) and j=150, 170, 190, and 220, related to the HTC temperatures.

2.4 Performance Indicator

The quality of hydrochar biofuel is primarily governed by its solid and energy yield and HHV. The solid yield of hydrochar ($SY(t)_T$), the fuel ratio (FR), the enhancement factor (EF), and the energy yield (EY) were calculated through Eqs. (2–5), respectively [29–31].

$$SY(t)_T = \frac{w_i(t)}{w_0} \times 100 \quad (2)$$

$$\text{FR} = \frac{FC}{VM} \quad (3)$$

$$EF = \frac{HHV_{Hydrochar}}{HHV_{raw}} \quad (4)$$

$$EY = SY \times EF \quad (5)$$

where $w_i(t)$ is the mass, on a dry basis, of the remaining solid after hydrothermal carbonization; w_0 is the mass, on a dry basis, of the raw material before the hydrothermal carbonization process; VM is the volatile matter content; FC is the fixed carbon content; $HHV_{Hydrochar}$ and HHV_{raw} refer to the higher heating value of the hydrochar and the raw material, respectively.

The difference between energy and solid yields is the energy-mass co-benefit index (EMCI), a performance metric to determine the optimal operational condition for biomass HTC [32–34]. The EMCI was calculated using Eq. (6):

$$EMCI = EY - SY \quad (6)$$

The present study introduces a new index to evaluate the hydrotreatment severity, the hydrotreatment severity index (HSI). The HSI is based on the torrefaction severity index (TSI), a dimensionless index based on the SY parameter first proposed by Chen et al. [35] and explored in previous works [36,37].

The HSI, described in Eq. (7), represents the ratio between the increment in SY for a specific hydrocarbonization condition and the SY of the most severe hydrocarbonization condition ($SY(E_2)_{220}$).

$$HSI = \frac{100 - SY(E_i)_T}{100 - SY(E_2)_{220}} \quad (7)$$

where E_i corresponds to the reaction medium of the specific treatment, T is the reaction temperature. Like the TSI [38], the dimensionless HSI (0–1) mitigates the measured SY variability. Therefore, the HSI is better suited for comparative studies, providing a standardized measure of hydrotreatment severity and allowing for consistent evaluations across various conditions and feedstocks. Additionally, the index established correlations between treatment conditions and hydrochar properties, which are essential for predicting and optimizing the outcomes of hydrotreatment processes.

Exergy finds extensive application in evaluating or approximating resource quantities, sustainable development, and the performance of energy conversion technologies [39]. Here, a simplified equation for exergy calculation, proposed by Song et al. [22], was applied to calculate the specific bioexergy of hydrochar as presented in Eq. (8).

$$\varepsilon_{biomass} = \beta \times HHV \quad (8)$$

Here, the coefficient β=1.047 represents the mean value derived from the ratio of specific chemical exergy of dry biomass to the higher heating value (HHV) on a dry basis, as discussed in Song et al.'s previous study [22]. This value was determined based on an analysis of correlations involving elemental composition, ashes and the chemical exergy of biomass [22].

2.5 Combustion behavior

Thermogravimetric measurements of raw material samples and produced HC were conducted using a TGA-60 apparatus from the Shimadzu brand. For the analyses, 5 mg per sample was utilized under an atmosphere of synthetic air (20±5% oxygen and 80±5% nitrogen), with a constant flow rate of 50 mL min^{-1} and a heating rate of 10 °C min^{-1} from 30–950 °C, as performed by Arauzo et al. [13].

The comprehensive combustibility (S) was determined with Eq. (9) [40–42].

$$S = \frac{DTG_{max} \times DTG_{mean}}{T_i^2 \times T_f} \quad (9)$$

Here DTG_{max} and DTG_{mean} are maximum and mean mass loss rate (% min^{-1}), T_i and T_f (°C) are the ignition and burnout temperatures, respectively.

2.6 Emission factors

To provide preliminary insights regarding the emissions from all hydrochar combustion, emission factors estimation characteristics of CO, CO_2, CH_4 and NO_x were calculated using the obtained ultimate analysis built on the factor's emission method [43–45]. The emissions factors (in kg kg^{-1}) of chemically pure carbon (E_C), carbon monoxide (E_{CO}), methane (E_{CH_4}), carbon dioxide (E_{CO_2}) and nitrogen oxides (E_{NO_x}) can be determined using Eqs. (10–14) [43–45].

$$E_C = C \times u_C \tag{10}$$

$$E_{CO} = \frac{MM_{CO}}{MM_C} \times E_C \times C_{CO/C} \tag{11}$$

$$E_{CH_4} = \frac{MM_{CH_4}}{MM_C} \times E_C \times C_{CH_4/C} \tag{12}$$

$$E_{CO_2} = \frac{MM_{CO_2}}{MM_C} \times \left(E_C - \frac{MM_C}{MM_{CO}} \times E_{CO} - \frac{MM_C}{MM_{CH_4}} \times E_{CH_4} - \frac{26.4}{31.4} \times E_{NMVOC} \right) \tag{13}$$

$$E_{NO_x} = \frac{MM_{NO_2}}{MM_N} \times E_C \times \frac{N}{C} \times N_{\frac{NO_x}{N}} \tag{14}$$

Here, C and N are the biomass's mass fractions of the elements. MM_C, MM_{CO}, MM_{CH_4}, MM_{CO_2} and MM_{NO_2} are the molar masses (g mol^{-1}). The dimensional factor u_C = 0.88 is the portion of C oxidized during the biomass combustion. $C_{CO/C}$ = 0.06 and $C_{CH_4/C}$ = 0.005 are the portion of C emitted as CO and CH_4. $C_{NO_x/C}$ = 0.122 is the part of N emitted as NO_x in the combustion process of biomass. E_{NMVOC} is the emission factor of non-methane VOCs (for biomass 0.009) [43–45].

3. Results and discussions

3.1 Hydrotreatment performance

Figure 2(a)–(f) shows the performance indexes used to evaluate the hydrotreatments. Considering thermochemical treatments, the weight loss (WL) and its corresponding solid yield (SY) are widely applied as performance indicators of treatment severity, allowing correlations with solid fuel properties [26].

The hydrochar was produced using water as the reaction medium at 150 °C ($E_{0\text{-}150}$) reported slight WL, with 90.72% SY. A significant SY decrease (up to 43.21%) was evidenced as the reaction's severity (higher temperatures and H_2SO_4 concentrations) increased, indicating that the experimental conditions had a significant effect in different proportions. The reduction in SY is attributed to the high volatilization and dissolution of organic matter in the process solution during the HTC process [15,46]. The lowest SY were obtained under the most severe hydrotreating conditions, varying between 43.88% and 43.21% ($E_{1\text{-}190}$ and $E_{2\text{-}190}$, respectively) and 45.85 and 45.42% ($E_{1\text{-}220}$ and $E_{2\text{-}220}$, respectively).

Martinez et al. [14] reported SY varying between 72.3-51.6% for hydrochar produced at 180–240 °C during 180 min from *Eucalyptus sp*.. In addition, Hansen et al. [15] explored HTC at 180-240 °C during 120 min of different residual biomass reports SY varying between 65–52% for olive pomace, 69-47% for wheat straw, 70-54% for spruce bark. As can be seen, both previous studies applied higher residence time and obtained higher SY. Therefore, it corroborates the present results and depicts the effect of H_2SO_4 as catalysts.

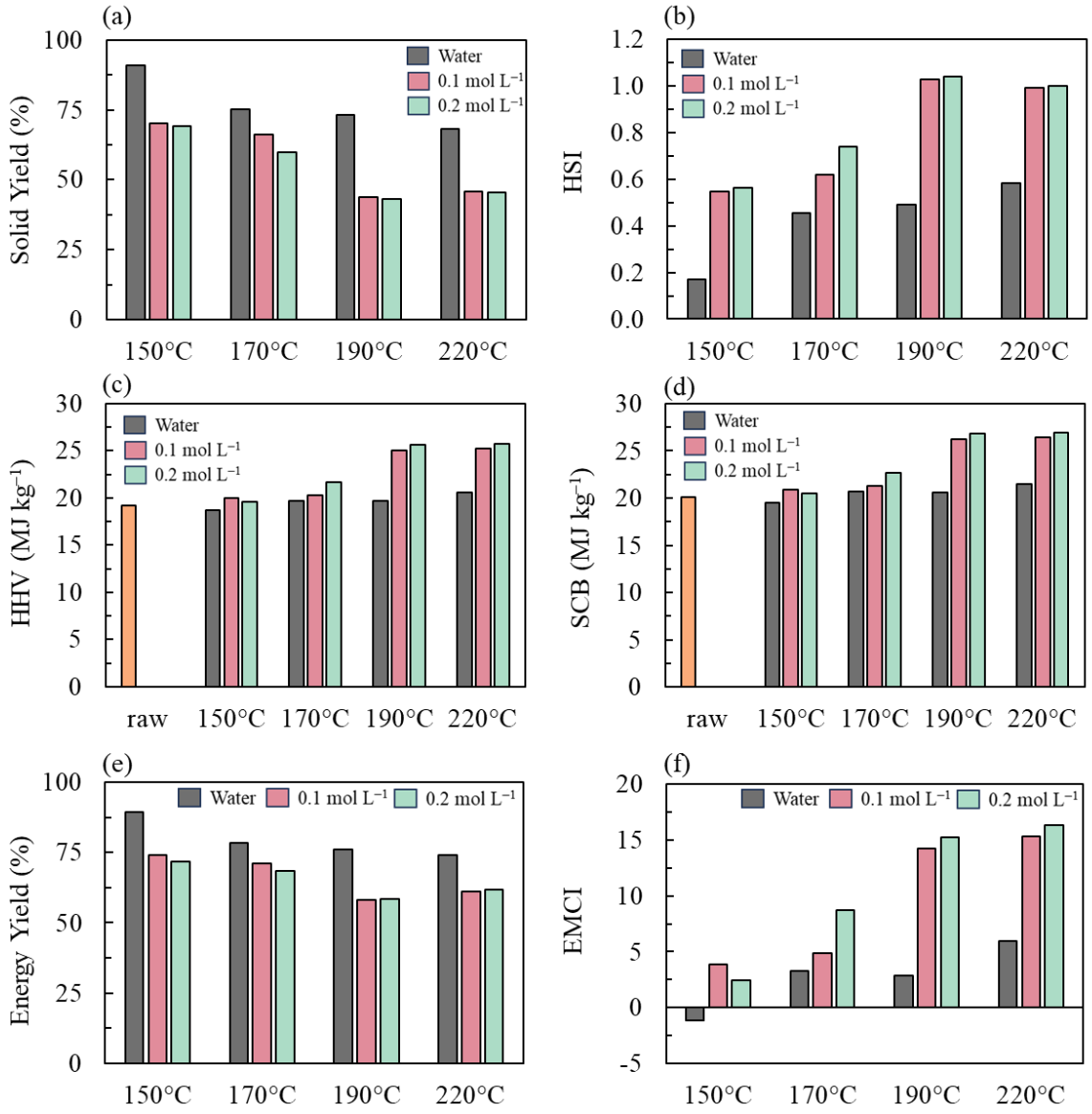

Figure 2. Indexes: (a) Solid yield (SY), (b) Hydrotreatment severity index (HSI), (c) Higher heating value (HHV), (d) Specific chemical bioexergy (SCB), (e) Energy Yield (EY) and (f) Energy-mass-coefficient-index (EMCI) of obtained hydrochar treatment at 150, 170, 190 and 220 °C, and holding time of 60 min, with reaction mediums of water, 0.1 mol L^{-1} and 0.2 mol L^{-1} H_2SO_4.

A slight increase in SY was observed comparing HTC at 190 and 220 °C (Fig. 2(a)) and might be attributed to a greater repolymerization from the liquid to the solid phase [4,47,48]. This rise can be explained based on the hydrochar formation pathways: (i) solid-solid conversion, in which the carbonaceous material, primary charcoal, results mainly from the dehydration of raw biomass; and (ii) a polymerization reaction, in which a solid carbonaceous

material is formed through retro-polymerization reactions of dissolved organics in the liquid phase, promoting an SY increase [49].

As for the different reaction mediums, it was observed that at the highest temperatures (190 and 220 °C), the 0.1 and 0.2 mol L^{-1} concentrations of H_2SO_4 showed no significant difference in SY. Therefore, increasing the concentration of H_2SO_4 was not a determining factor for the SY under these conditions. Ameen et al. [50] attributed the acceleration in dehydration, hydrolysis and coalification reactions to weakly acidic conditions. Funke et al. [4] also stated that the weak acidic condition increases the overall reaction rate in HTC.

The weight loss (so, the SY) intrinsically depends on raw biomass's structural and non-structural composition (lignin, holocellulose and extractives) [51,52]. For example, hardwood presents a lower weight loss than grasses when subject to the same treatment severity. Therefore, it is interesting to establish a dimensionless parameter to diminish the deviation of SY, considering the nature of biomass and the material thermal sensitivity of biomass degradation.

The HSI, Fig. 2(b), provides a dimensionless indicator for assessing the severity of the process and a new parameter for evaluating the correlation between hydrochar properties and treatment severity (see section 3.3). The values of HSI varied between 0.17–0.58, 0.55–0.99, and 0.56–1.00 with increasing temperatures from 150 to 220 °C in experiments carried out with water, 0.1 mol L^{-1} and 0.2 mol L^{-1} of H_2SO_4, respectively.

The HTC severity promoted the increase in the energy and exergy content (HHV and SCB) of the HC (Figs. 2(c) and (d)) [53]. The $E_{2\text{-}220}$ hydrotreatment resulted in the HC with the highest HHV of 25.72 MJ kg^{-1}, increasing the energy density by 34% compared to the raw material (19.19 MJ kg^{-1}), in line with the literature. For example, Yan et al. [54], working with loblolly pine at 260 °C, obtained a 36% increase in energy density. Oliveira et al. [55] obtained HHV between 19.5–21.3 MJ kg^{-1} (EF=1.09) when working with torrefaction of *eucalyptus* species treated at 160–230 °C for 5–15 hours. For instance, results indicate that the HTC process is more effective at upgrading the HHV than torrefaction.

The exergy content SCB of obtained HC varied between (19.55–26.93 MJ kg^{-1}) considering $E_{0\text{-}150}$ and $E_{2\text{-}220}$. Lamas et al. [56] determined the exergy of torrefied urban forest waste considering a blend of six species, reporting values ranging between 21.22–22.93 MJ kg^{-1}. In addition, Kartal and Özveren [57] statically investigated raw biomass characteristics and torrefaction parameters (200–300 °C and 15–60 min) to assess the chemical exergy of torrefied lignocellulosic biomass, reporting that torrefied products' chemical exergy appears to be centered between 20.11 and 23.99 MJ kg^{-1}, which are lower than HC of $E_{1 \text{ and } 2 - 190 \text{ and } 220}$.

The highest EY (Fig. 2(e)) was observed for $E_{0\text{-}150}$, with 89.57%, following a downward trend as the HTC temperature increased, in line with loblolly pine HTC [54]. At the highest temperature (220 °C) and in the reaction medium of 0.1 and 0.2 mol L^{-1} H_2SO_4, the EY showed a slight increase compared to the temperature of 190 °C, due to the higher HHV of these hydrotreatments, added to the slight increase in SY (Fig. 2(a)).

Typically, increased processing severity leads to decreased SY and a less pronounced reduction in EY due to energy densification (indicated by an increase in HHV). A higher EMCI explains a higher energy density with a lower solid volume [58], thus, an optimal condition. Increasing HTC severity resulted in a greater EMCI (Fig. 2(f)). The exception was $E_{0\text{-}150}$ HTC, with evidenced a –1.15 EMCI. A negative value indicates that the feedstock underwent degradation and did not exhibit an improvement in its HHV. Figure 2(f) depicted an increase of EMCI for higher catalyst concentrations, indicating greater energy density and reduced solid volume for treatments under catalytic conditions. The highest EMCI (16.37) was evidenced for the most severe HTC, $E_{2\text{-}220}$.

Compared to different thermochemical processes, Silveira et al. [59] reported EMCI ranging between 2–6 for torrefaction of urban forest waste conducted at 225-275 °C for 60 min. Evaristo et al. [32], exploring pyrolysis (500-700 °C, during 60 min) of spent coffee ground and brewers' spent grains, evidenced EMCI ranging between 5-10 and 15-23, respectively. Martinez et al. [14] exploring hydrothermal carbonization (180-240 °C, 180 min) of *Eucalyptus sp.* reported closer values to present results, with EMCI varying between 6.5-14, thus evidencing lower EMCI values compared to present results, even though the higher temperature (240 °C) and longer residence time (180 min). Therefore, the results show that the characteristics of the *Eucalyptus* hydrochar were improved by adding H_2SO_4.

3.2 Hydrochar assessment

Table 3 shows the proximate, ultimate and HHV results of the produced HC. The proximate results (see Table 2) of *Eucalyptus* feedstock (VM, FC and ASH content of 86.36%, 13.15% and 0.48%, respectively), its ultimate analysis (50.48%, 5.91%, 42.01% and 1.61% for carbon, hydrogen, oxygen and nitrogen content, respectively) and HHV (19.19 MJ kg^{-1}) are in line with *Eucalyptus* literature [60,61].

Considering the 12 experiments carried out, VM, FC, ASH, H/C and O/C varied between 85.43–49.63%, 14.41–48.98%, 0.07–1.39%, 1.29–0.76 and 0.59–0.26, respectively, depending on the severity of HTC. The comparison with raw feedstock indicates that the hydrotreatments

promoted significant changes in the composition of produced HC. Martinez et al. [14] reported VM, FC and ASH ranging between 79.1-56.5wt%, 20.8-43.4wt% and 0.1wt%, respectively, considering HTC conducted between 180–220 °C during 180 min.

The minor change in SY of $E_{0\text{-}150}$ (Fig. 2(a)) corroborates the minimal difference in its properties compared to feedstock. Compared to the raw biomass, the severest HTC exhibited a 36.73% decrease in VM and a corresponding increase in FC of 35.83%, in line with the 37% increase in HHV.

Table 3. Yield (in %), Proximate (volatile matter (VM), fixed carbon (FC), and ASH content in %), ultimate (CHONS, in %), calorific (HHV, LHV in MJ kg^{-1}), analysis of obtained hydrochar treatment at 60 min, temperatures of 150, 170, 190 and 220 °C with reactor mediums, control, 0.1 and 0.2 mol L^{-1} H_2SO_4, respectively.

Medium	**Control**				**0.1 mol L^{-1} H_2SO_4**				**0.2 mol L^{-1} H_2SO_4**			
Temp. (°C)	**150**	**170**	**190**	**220**	**150**	**170**	**190**	**220**	**150**	**170**	**190**	**220**
Yield (%)												
SY	90.72	75.15	73.25	68.22	70.14	66.26	43.88	45.85	69.28	59.72	43.21	45.42
Proximate (%)												
ASH	0.16	0.40	0.21	0.07	0.28	0.14	0.55	0.65	0.26	0.36	0.91	1.39
VM	85.43	84.27	82.09	77.85	81.62	77.21	55.01	54.18	78.15	71.06	52.96	49.63
FC	14.41	15.33	17.70	22.08	18.10	22.65	44.44	45.17	21.59	28.58	46.13	48.98
FR [a]	0.17	0.18	0.22	0.28	0.22	0.29	0.81	0.84	0.28	0.40	0.87	0.99
Ultimate (%)												
C	52.03	54.06	58.08	67.57	52.32	60.18	68.69	62.41	56.79	62.51	69.69	69.15
H	5.61	5.53	5.66	5.84	5.26	5.52	4.58	3.99	5.52	5.00	4.63	4.40
N	1.69	1.08	1.83	1.64	1.43	1.40	1.98	1.52	1.31	1.88	1.86	1.48
O [b]	40.51	38.93	34.23	24.89	40.71	32.76	24.21	31.44	36.10	30.25	22.92	23.58
S [c]	0.00	0.00	0.00	0.00	0.00	0.00	0.00	0.00	0.00	0.00	0.00	0.00
H/C ratio	1.29	1.23	1.17	1.04	1.21	1.10	0.80	0.77	1.17	0.96	0.80	0.76
O/C ratio	0.59	0.55	0.45	0.28	0.58	0.42	0.27	0.39	0.49	0.37	0.26	0.26
Calorific (MJ kg^{-1})												
LHV [d]	17.51	18.58	18.48	19.36	18.86	19.17	24.12	24.41	18.44	20.64	24.64	24.81
HHV	18.67	19.73	19.65	20.56	19.94	20.31	25.06	25.24	19.58	21.67	25.60	25.72
SCB [e]	19.55	20.66	20.57	21.53	20.88	21.26	26.24	26.43	20.50	22.69	26.80	26.93

[a] FC/VM; [b] O = 100 – C – H – N – ASH; [c] not detected; [d] calculated [21]; [e] calculated [22].

Regarding the ASH content (Table 3), a consistent behavior pattern could not be observed for different HTC conditions. During HTC, inorganics can be extracted from the biomass into the process water and thus removed from the resulting HC. However, at the same time, organic material is dissolved in the process water, leading to a decreasing yield. Therefore, if the loss of organic matter is greater than the reduction of inorganic elements, the ASH content increases after the treatment, as noted by Protásio et al. [62]. Similar results were reported by Hansen et

al. [15] and González-Arias et al.[63], who reported increased ASH content for higher treatment temperatures in most cases, resulting in inconsistent ASH behavior patterns.

The low ASH content of produced hydrochar can prevent the deposition of inorganic substances in combustion equipment and help prevent fouling and corrosion. This characteristic could indicate an advantage of the material as a solid fuel because the higher the ASH content of the solid fuel, the greater the energy losses due to the heating of mineral oxides during combustion [23,62].

Figure 3(a) translates the modification promoted by the HTC on raw biomass by co-relating the VM and FC for different treatment severities and catalytic conditions. In addition, it presents a FR colormap and literature data [13,15–17,64] for comparison. The correlation for FC and VM for all obtained hydrochar showed an excellent linear distribution with $R^2 > 0.99$.

Through the HTC, the degradation of hemicelluloses and cellulose occurs at lower temperatures (160–180 °C) due to subcritical water. At this temperature, the degradation results in CO, CO_2, and short-chain hydrochar, reducing the VM of produced HC [65].

With the increase in HTC temperature, the devolatilization rate accelerates, promoting dehydration and decarboxylation reactions, leading to a continuous reduction in the VM [66,67]. The VM, consisting of aliphatic hydrocarbons, carboxylic groups, and carbohydrates [68], migrate to the liquid and gaseous phases (primarily as CO_2) due to the mechanisms involved in HTC reactions. Higher temperatures also increase the decomposition of unreacted raw material into fragments, which undergo aromatization and repolymerization, thereby increasing the FC of the hydrochar [66,69]. Therefore, HTC benefits biomass combustion, reducing pollutants and combustion efficiency.

The influence of H_2SO_4 as a reaction medium is evident, catalyzing the degradation and promoting a pronounced reduction in VM and increase in FC as H_2SO_4 concentration increases. The significant effect of acid addition was also reported by Ghanim et al. [70], where the addition of acetic acid reduced the ASH content and increased FC, resulting in an increased FR and EY.

Figure 3(a) shows the literature's fuel ratio (FR) of produced HC and other raw materials. The FR relates the FC and VM, providing information on ease of ignitability and burning behavior. The HC obtained at 190 and 220 °C in a reaction medium of 0.1 and 0.2 mol L^{-1} H_2SO_4 showed higher FC and lower VM, hence a higher FR.

Compared to raw biomass, the FR of the hydrochar significantly increased from 0.15 to 0.99 in the more severe hydrothermal processing conditions ($E_{2\text{-}220}$). Results surpass the FR obtained by Lin et al. [17], which achieved an FR of 0.49 working with *Eucalyptus* residues at

a temperature of 235 °C and a time of 60 min. Therefore, H_2SO_4 as a catalyst improved hydrochar FR through HTC.

The Van Krevelen diagram is depicted in Fig. 3(b). Typical ranges for biomass, peat, lignite, and coal are also shown in the figure. Additionally, literature comparison [13,15–17,64] and the samples' specific bioexergy content (SBC colormap in MJ kg^{-1}) are presented.

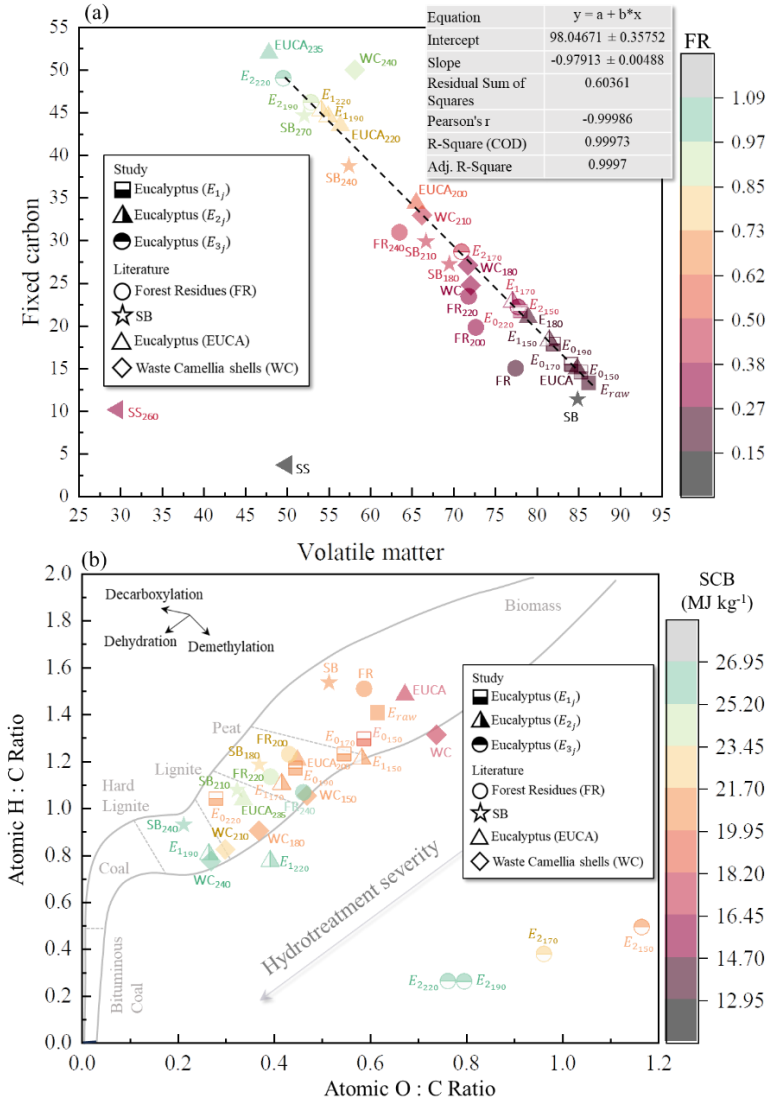

Figure 3. (a) Correlation between VM and FC. (b)Van Krevelen Diagram of obtained hydrochar experiment (Ei_j) at j =150, 170, 190 and 220 °C, and holding time of 60 min, with reaction medium of i = 0, 1 and 2 (water, 0.1 mol L^{-1} and 0.2 mol L^{-1} H_2SO_4, respectively). Literature for comparison: EUCA (180, 200, 235 °C) [17]; FR (200, 220, 240 °C) [16]; SB (180, 210, 240 and 270°C) [15]; SS (260°C) [13]; WC (150, 180, 210 and 240 °C) [64].

The dehydration process follows a path that decreases the H/C and O/C ratios from the upper-right corner to the lower-left corner, while decarboxylation moves from the lower-right corner to the upper-left corner, indicating a reduction in the O/C ratio and an increase in the

H/C ratio [71]. The *Eucalyptus grandis* feedstock is in the biomass region, along with some milder treatments ($E_{0\text{-}150}$, $E_{1\text{-}150}$, and $E_{0\text{-}170}$). As the HTC temperature increases, $E_{1\text{-}170}$ and $E_{0\text{-}190}$ transition into the peat region, $E_{0\text{-}220}$ enters the lignite region, and $E_{1\text{-}190}$ moves into the hard lignite region. The significance of dehydration in HTC becomes evident observing $E_{1\text{-}190}$ and $E_{0\text{-}220,}$ which shift to the left and exhibit fuel-like characteristics like lignite.

HTC is governed by hydrolysis, but some authors argue that the reactions of the process are not yet fully understood [12]. In brief, during the hydrolysis step, hemicelluloses, cellulose, and lignin are broken down into smaller fragments that enable subsequent reactions (dehydration and decarboxylation) to reduce the H/C and O/C ratios, crucial for obtaining a solid product similar to coal [72,73].

During HTC, both physical and chemical dehydration of biomass takes place. In physical dehydration, water is expelled from the biomass matrix primarily due to the reduction of its hydrophilic nature. In chemical dehydration, the hydroxyl group (-OH) is removed through the primary reaction mechanism, which reduces the atomic ratios of H/C and O/C. Decarboxylation reactions also transfer a small amount of carbon to the gaseous phase [74]. Lower atomic ratios of O/C and H/C indicate a higher degree of condensation and aromaticity [75]. Other reactions, such as decarboxylation, enable the degradation of carboxyl-carbonyl groups and release a significant portion of the gas phase, mainly composed of CO_2 and CO [12].

The carbon content increased from 52.03% to 69.69% as the reaction temperature increased, in line with Li et al. [76], which investigated the variability in properties of sawdust HC by varying the temperature (200–260 °C) and observed an increase in carbon content from 57 to 68%, along with an increase in HHV from 24 to 28 MJ kg^{-1}. Results also align with Śliz and Wilk [77], which reported carbon content varying between 56–67% considering HTC of acacia waste at 180 to 220 °C. Compared to the torrefaction process, Canabal et al. [78] obtained pellets with 66.5% carbon content from a blend of 60% Pine and 40% *Eucalyptus* torrefied at 300 °C for 60 minutes.

3.3 Hydrochar Properties Correlation

Figures 4 and 5 present the linear correlation and the correlation coefficients (R^2 values) considering the two performance indexes HTC temperature (Fig. 4) and HSI (Fig. 5) versus the proximate (VM, FC), ultimate (H/C and O/C atomic ratios) and energy properties (HHV and EY).

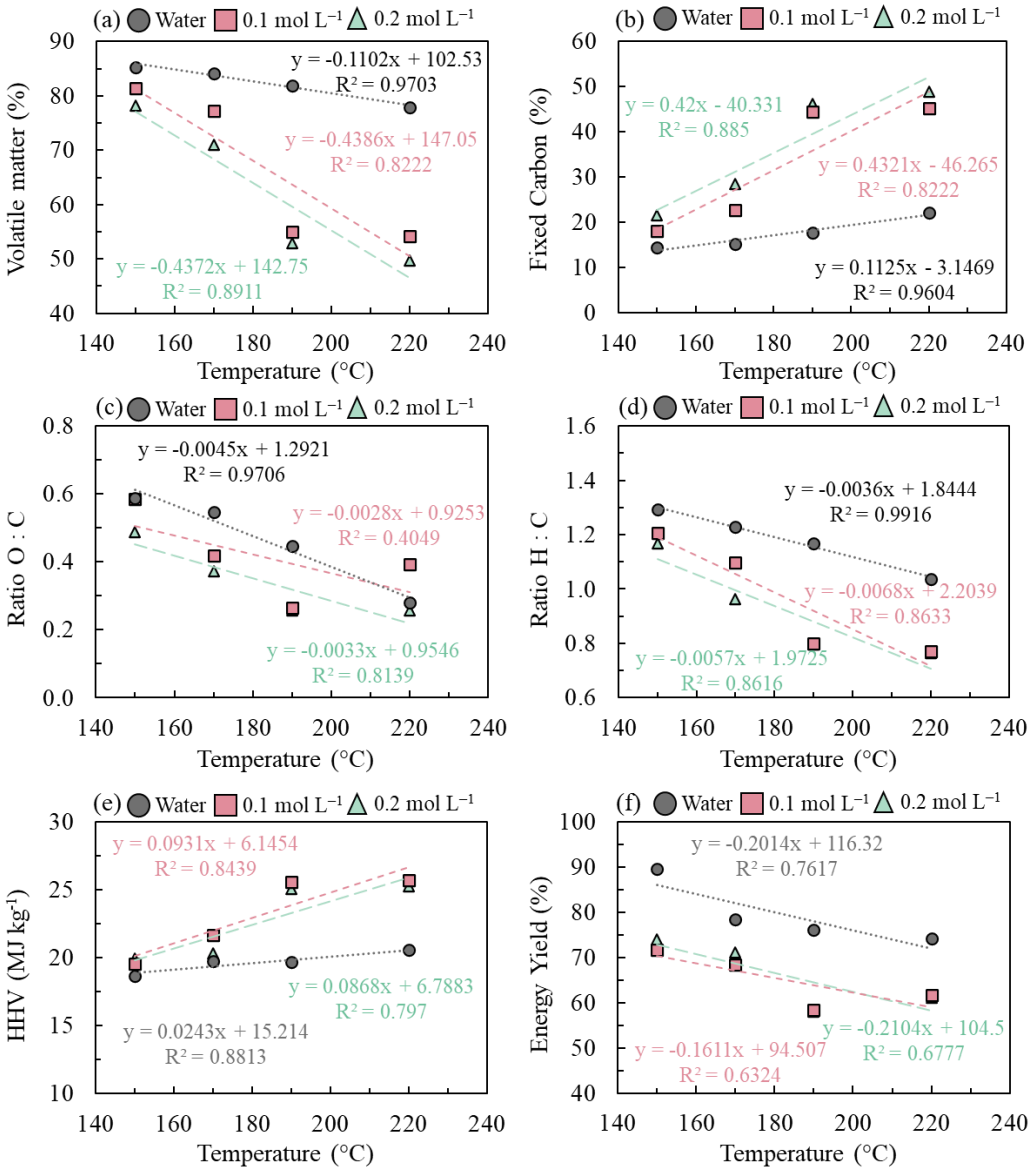

Figure 4. Correlations between HTC temperature and proximate (VM and FC), ultimate (H/C and O/C) and calorific (HHV and EY) for control, 0.1 mol L^{-1} and 0.2 mol L^{-1} H_2SO_4 reaction mediums.

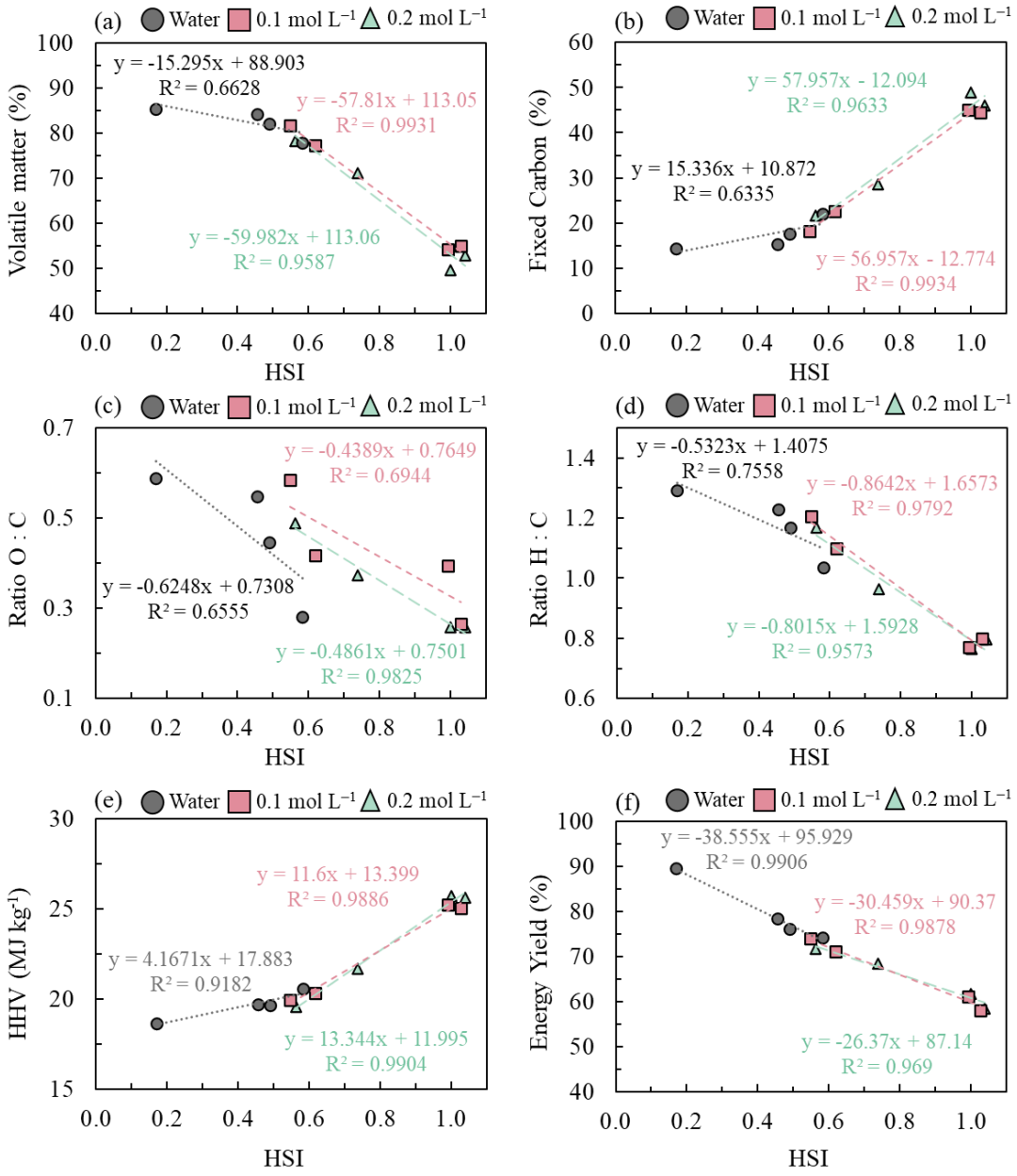

Figure 5. Correlations between HSI and proximate (VM and FC), ultimate (H/C and O/C) and calorific (HHV and EY) for control, 0.1 mol L^{-1} and 0.2 mol L^{-1} H_2SO_4 reaction mediums.

The VM, H/C, O/C and EY are well represented by a decrescent linear correlation with increasing temperature and HSI, while crescent linear correlations are reported for FC and HHV (Figs. 4 and 5). Tables S1 and S2 in the supplementary material provide detailed statistical results, presenting the coefficients of the linear correlation equation between the indexes and chemical properties. Tables S1 and S2 show that the yield property-based (HSI) reported significant correlations ($p \leq 0.05$) for almost all treatment temperatures and reaction mediums, except for control treatment (VM, FC, O/C and H/C). Exactly the treatments in which linear correlations with treatment temperature were statistically significant. Therefore, considering

the proximate, ultimate, and HHV of HC produced under catalytic conditions, the yield property-based (HSI) demonstrated better linear correlations, allowing better models for property prediction.

It is reported in the literature that acidic conditions, compared to neutral conditions, accelerate hydrolysis, dehydration and coalification [79]. The presence of a weak acid catalyst can increase the yield and carbon content of the hydrochar, while the oxygen and hydrogen content are reduced in the hydrochar due to the dehydration and decarboxylation reactions that occur during the HTC process [50].

3.4 Hydrochar morphology

Examining the SEM micrographs (Fig. 6) made it possible to identify morphological changes in the HC produced through HTC. The original biomass structure was observed to break down, and this effect was more pronounced for severe reaction conditions.

Surface changes (presence of heterogeneous pores and cavities) occur due to the reduction and volatilization of organic compounds [80], which can be characterized by the absence of hemicelluloses and cellulosic components and the high concentration of lignin [70]. In general, the proliferation of smaller fragments scattered irregularly around the porous/rough surfaces of the HC can be better observed in the E_1 (Fig.6 (b, e, h, k)) and E_2 (Fig.6 (c, f, i, l)) hydrotreatments, which, in turn, employ H_2SO_4 concentrations as the reaction medium and more prominently in the hydrothermal processing treatments conducted at higher temperatures [2,3,62].

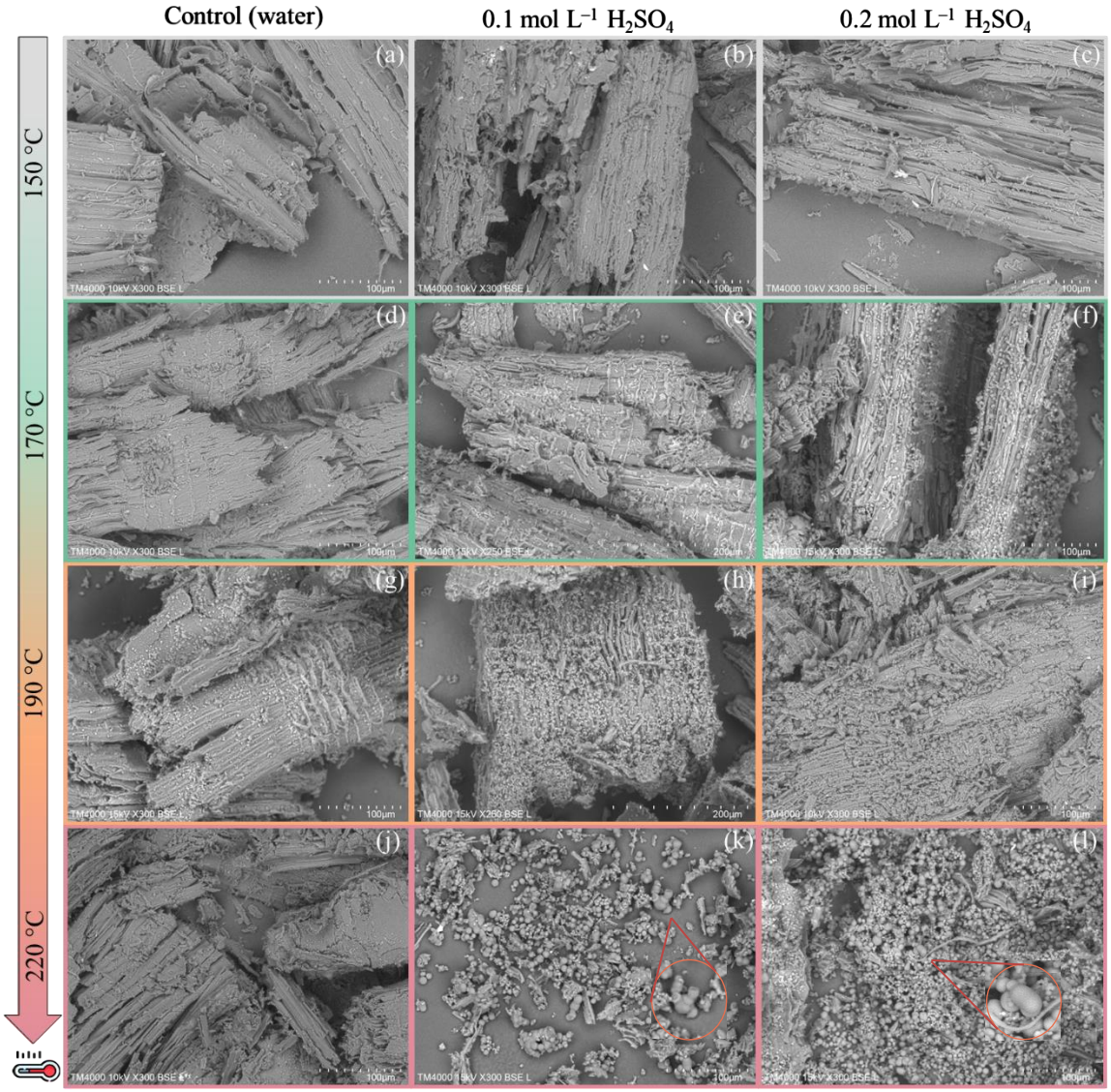

Figure 6. SEM images with 300X for hydrochar produced at 150 °C (a, b and c), 170 °C (d, e and f), 190 °C (g, h and i) and 220 °C (j, k and l) for control, 0.1 mol L^{-1} and 0.2 mol L^{-1} of H_2SO_4. Highlighted circles (k and l) show the occurrence of cohesion and fusion of carbon microspheres.

Notable modifications were observed for $E_{0\text{-}190}$ (Fig.6 (g), where the emergence of microspheres on the surface of the HC can be observed. The microspheres are characterized as secondary carbon [81] or "pseudo-lignin" by some researchers [82,83]. The microspheres observed in $E_{0\text{-}190}$ can also be seen in E_1 (0.1 mol L^{-1} of H_2SO_4) and E_2 (0.2 mol L^{-1} of H_2SO_4) at lower reaction temperatures (170 and 150 °C, respectively), indicating a significant effect of the acid concentrations on hydrochar formation since the presence of microspheres indicates that recondensation and repolymerization reactions have occurred.

The formation of microspheres is likely due to the decomposition of cellulose and hemicelluloses during HTC [84]. According to com Lei et al. [85], amorphous cellulose and some soluble lignin segments are hydrolyzed homogeneously, and the hydrolysis products subsequently recondense to form microspheres, indicating their association with the repolymerization process in hydrochar formation. At high temperatures, dissolved sugar monomers and other fragments in the liquid phase undergo polymerization reactions, forming carbonaceous spheres on the surface of lignocellulosic biomass hydrochar [14,86,87]. An increase in the quantity and size of microspheres can be observed for severe HTC, in line with Seville and Fuertes et al. [47].

The formation of carbon microspheres is also linked to the nucleation growth burst mechanism [88]. The concentration of aromatic clusters in the liquid continues to increase until a nucleation explosion occurs at a critical point of supersaturation. The growth of the nuclei thus formed continues to grow outward by diffusion [47]. Thus, hydrochar microspheres are formed by the nucleation growth mechanism (LaMer model [89,90]) attributed to diffusion of dissolved intermediates, e.g., HMF, on the carbon surface and reaction with reactive oxygen functional groups [90]. Also reported in the literature and verified in our study in Fig. 6(k,l) are phenomena of cohesion and fusion of carbon microspheres, which gradually agglomerated on the surface of the hydrochar and became more significant at higher HTC temperatures [51].

3.5 Combustion behavior

The TG and DTG curves and the two-dimensional TG contours for the produced HC with combustion temperature indications are shown in Fig. 7(a–i). The 2D contour plots offer a superior view from the surface formed using all the evolved TG curves for a specific condition. For example, considering control (water) treatment, the 2D contour was constructed (see Fig. S1 in supplementary material) using the four curves (E0-150, E0-170, E0-170 and E0-220). In essence, they provide an additional perspective and enhance the visualization of the thermal characteristics of the material throughout the temperature treatments.

In addition, the respective characteristic parameters reflecting the thermal behavior during the combustion process have been listed in Table 4 to assess the combustion performance of the produced HC.

Table 4. Combustion characteristic parameters of raw and hydrochar products for 150–220 ℃ and reaction mediums of control, 0.1 and 0.2 mol L^{-1} of H_2SO_4.

	T_i [a]	T_f [a]	T_p [a]	DTG_{mean} [b]	DTG_{max} [c]	S [d]
Raw	243.56	499.33	327.12	1.06	12.21	4.37
Control						
$E_{0\text{-}150}$	250.50	521.48	329.56	1.06	16.67	5.37
$E_{0\text{-}170}$	264.85	512.38	334.60	1.06	20.69	6.06
$E_{0\text{-}190}$	284.47	550.90	333.39	1.06	20.01	4.78
$E_{0\text{-}220}$	274.55	532.20	320.75	1.05	15.30	3.99
0.1 mol L^{-1}						
$E_{1\text{-}150}$	263.64	497.37	319.34	1.08	17.89	5.56
$E_{1\text{-}170}$	267.88	525.77	315.03	1.06	11.61	3.25
$E_{1\text{-}190}$	264.12	467.09	431.00	1.05	16.01	5.14
$E_{1\text{-}220}$	281.01	459.19	418.61	1.04	17.57	5.04
0.2 mol L^{-1}						
$E_{2\text{-}150}$	268.00	522.57	319.90	1.07	17.25	4.92
$E_{2\text{-}170}$	251.28	482.59	299.97	1.03	8.43	2.85
$E_{2\text{-}190}$	263.24	447.90	408.52	1.04	18.74	6.25
$E_{2\text{-}220}$	265.61	402.48	368.40	1.04	26.02	7.61

[a] T_i, T_f, T_p designated ignition, burnout and peak temperature, respectively in °C; [b] DTG_{mean} mean mass loss rate (% min^{-1}); [c] DTG_{max} maximum mass loss rate (% min^{-1}); [d] $\times 10^7$

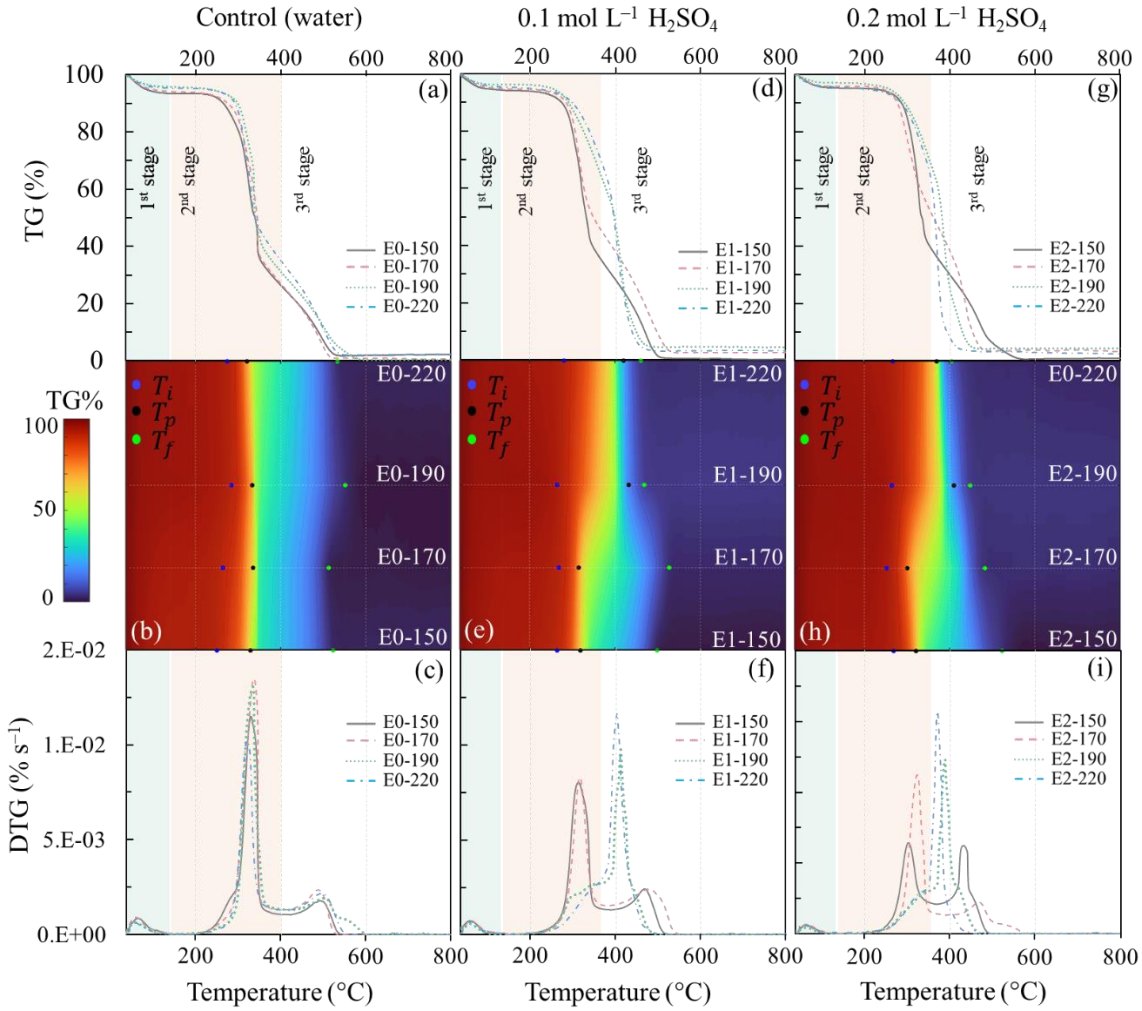

Figure 7. TG, 2D contour and DTG curves for the produced HC at 150, 170, 190 and 220 °C for control (a, b and c), 0.1 mol L^{-1} (d, e and f), and 0.2 mol L^{-1} (g, h and i) of H_2SO_4, respectively.

Overall, as the HTC temperatures increased, the conversion curves of the samples gradually shifted towards higher temperature regions, indicating that the hydrochar structure was more stable than raw biomass. A similar outcome was achieved by Zhang et al. [51]. The authors observed that when HTC conditions reached or exceeded 220 °C for 10 minutes, the formation of carbon microspheres increased the carbon content on the surface of the hydrochars. Consequently, this enhanced combustion efficiency leads to a rightward shift in the DTG curves.

In the hydrothermal treatments conducted with 0.1 and 0.2 mol L^{-1} H_2SO_4 (Figs. 7(d)–(f) and (g)–(i), respectively), the distinction between the TG and DTG curves became even more pronounced. These curves shifted towards higher temperature regions, particularly for the HC produced at 190 and 220 °C, highlighting the influence of the catalyst addition.

Figure 7 shows that the combustion of *Eucalyptus grandis* HC can be divided into three main stages: dehydration (1st stage in green), removal of volatile materials (2nd stage in orange), and fixed carbon combustion (3rd stage in white), in line with Liu et al. [91]. Figures 7(c), (f) and (i) exhibit two distinct, prominent DTG peaks within the temperature ranges of 300–350 °C and 380–550 °C, which aligns with prior studies that assessed HC from forest waste [16]. Shafie et al. [92] presented that following HTC, the initial peaks in the TG profiles are diminished due to the decomposition of cellulose and hemicelluloses during the HTC reaction, indicating the formation of new compounds with higher thermal stability, aligned with the results.

The increase in HTC temperature and H_2SO_4 concentration promoted a decrease in the height of the second peak. This behavior might be attributed to a reduction in volatile matter (VM), while the increase in the height of the third peak may be attributed to an increase in fixed carbon (FC) (see Table 3). At lower reaction temperatures, the primary peak is attributed to cellulose concentration; however, for HC obtained at higher reaction temperatures, this peak shifts to the right due to an increase in lignin concentration. The less severe HTC ($E_{0\text{-}150}$ in Fig. 7(c)) was the only one to present a prominent shoulder between 200–300 °C, a characteristic of hemicellulose degradation.

The third peak, between 380–550 °C, is associated with the lignin concentration and fixed carbon (FC) content (Table 3). Thus, as the severity of the hydrothermal treatment increased, the FC content followed the same trend, resulting in a higher maximum height of this peak [93].

The curves for hydrothermal treatments E_1 and E_2 at 190 and 220 °C exhibit a single peak between 300–500 °C. This might be attributed to the high lignin retained in these HC, as previously shown (Figs. 7(f) and (i)). In these cases, cellulose and hemicelluloses were likely almost entirely degraded, leaving lignin as the primary component.

Regarding $E_{0\text{-}220}$ and $E_{2\text{-}170}$, a slight oscillation in the TG curve was observed after the decline of the second peak, which may be related to the combustion of residual products within the hydrochar. These residual products require higher temperatures to be released during combustion [63].

T_i is the temperature at which the HC begins to burn and is related to the likelihood of fire or explosion. Therefore, higher values are beneficial for the handling, storing, and transporting of hydrochar [94]. Compared to the raw material, all hydrothermal treatments enhanced the combustion performance and ignitability of *Eucalyptus grandis* HC. The increase in T_i with process severity is closely linked to the VM content since T_i is higher as the VM percentage decreases. This, in turn, leads to an increase in FC, reducing the ignitability of the HC [93]. Lin

et al. [86] conducted HTC on pulp and paper sludge and reported that increasing the process temperature would raise the T_i of the hydrochar due to the reduction in VM.

Higher T_p values suggest a prolonged combustion process, while lower values indicate more heat released in a shorter period [51]. The 150 and 170 °C HC exhibit lower reactivity peaks than those produced at 190 and 220 °C. However, the higher reactivity peaks of 190 and 220 °C HC also had higher T_p values, shifting to the right in the DTG curve (T_p>368 °C). Although the VM decreases with increasing HTC severity, the T_f decreased as the HTC acid concentration increased. This suggests the formation of a secondary carbon phase (carbon microspheres), where volatile organics condense onto the primary carbon during HTC and devolatilize from the carbon surface during TGA [80].

The burnout temperature (T_f) is considered a crucial fuel parameter since fuels with high ignition temperatures require longer residence times or higher temperatures to achieve complete combustion. Apart from the $E_{2\text{-}220}$ hydrothermal treatment, the T_f of the HC increased compared to the feedstock, indicating that the process produced HC with a more stable chemical and thermal structure.

The combustibility index (S) indicate combustion performance and can be used to assess the reactivity of solid fuels by connecting ignition temperature, combustion speed, and burnout temperature [18]. As shown in Table 4, except for $E_{2\text{-}170}$, S values were above 3, indicating favorable combustion performance [95]. A study conducted by Ma et al. [96] considered S suitable for combustion when it exceeds 2E7 $\%^2$ min^{-2} $°C^{-3}$. The $E_{2\text{-}220}$ hydrothermal treatment yielded better combustion performance and reactivity results (S=7.61E7 $\%^2$ min^{-2} $°C^{-3}$).

3.6 Emissions assessment

The assessment of gas emissions associated with biomass combustion is often overlooked when evaluating the suitability of new raw materials for bioenergy purposes [45]. However, recent research has raised concerns about the climate change impacts of bioenergy as heterogeneous pathways of producing and converting biomass [97].

This underscores the importance of estimating gas emissions to provide valuable indicators for assessing the potential use of biomass [43]. Figure 8 presents the estimated emissions of pollutant gases based on the ultimate composition of feedstock and the produced HC.

Figure 8 indicates that the CO, CO_2, and CH_4 emissions exhibited a similar pattern, with a trend directly proportional to the increasing severity of the hydrothermal treatments. The results

revealed that the emission factors of the HC were higher than those of the raw biomass, reflecting the higher carbon content.

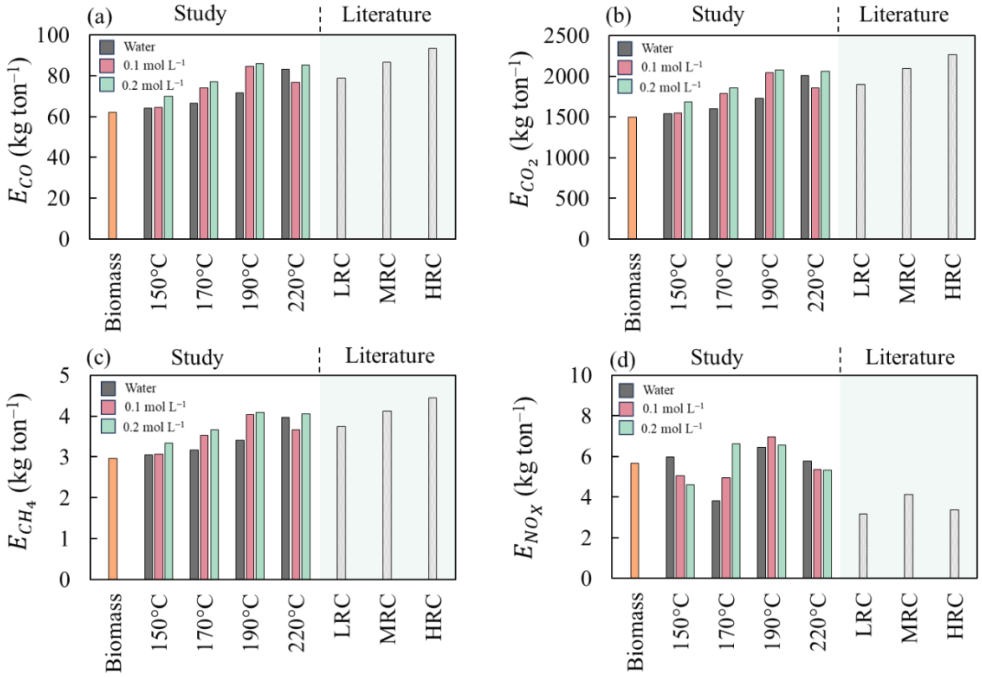

Figure 8. Emission factors for HTC treatments performed between 150–220 °C and reaction mediums of 0, 0.1 and 0.2 mol L^{-1} of H_2SO_4. (a) carbon monoxide (E_{CO}), (b) carbon dioxide (E_{CO_2}), (c) methane (E_{CH_4}) and (d) nitrogen oxides (E_{NOX}) in kg ton^{-1}. Data for comparison: low-rank coal (LRC), medium-rank coal (MRC) and high-rank coal (HRC) [98].

CO_2 emissions from *Eucalyptus grandis* HC's combustion are offset by biomass's carbon sequestration during its lifecycle. CO_2 emission factors ranged from 1,541.97 kg per ton ($E_{0\text{-}150}$) to 2,058.46 kg per ton ($E_{2\text{-}220}$), which are mostly comparatively lower than hard coal (1,969 kg per ton) [44].

The nitrogen content in the fuel is an indicator of NO_x emissions and atmospheric pollution during HC combustion. For the estimated NO_x emissions, observing a consistent behavior pattern was impossible. Initially, emissions decreased (150–170 °C), then increased with rising temperature (from 170 to 190 °C), and decreased again at 220 °C. A similar result was reported by Ren et al. [99], who found that biomass subjected to torrefaction has higher mass fractions of nitrogen than its raw biomass, and they also did not observe a clear trend in NO_x emission factors.

The initial decline in fuel nitrogen at low temperatures can be explained by removing nitrogen from water-soluble ammonium and nitrite salts. Furthermore, hydrolysis leads to the

dissolution of nitrogen [100] in the process water, causing even greater N removal at higher reaction temperatures. The apparent increase in nitrogen content in the HC is a result of more significant losses of other organic materials.

Most biomass fuels have low sulfur content; hence, they emit smaller amounts of SO_2 compared to coal when burned either alone or co-fired with coal [101]. In our study, the presence of sulfur in the raw material was not detected. Therefore, the level of SO_2 emissions, which depends on the sulfur content, was not determined. Therefore, using *Eucalyptus grandis* residues for hydrochar production can eliminate the emission of sulfur compounds during its combustion, giving it an advantage compared to other fossil fuels, for example.

4. Application and Prospects

The use of hydrochar for environmental purposes has recently received significant attention due to its physicochemical characteristics. HTC is suitable for increasing the energy density of biomass waste by increasing HHV due to carbon fixation, VM reduction and ash dissolution in the liquid phase. Consequently, hydrochar is a better solid biofuel than the raw feedstock [3,6,14].

The simplified HTC technology used in this study proved suitable for valorizing forestry residues and could be used, especially in developing countries such as Brazil. The use of this technology is aligned with the pillars of sustainable development, encompassing environmental, social and economic aspects.

However, perspectives and challenges in this field must be considered for sustainable development. Research gaps related to large-scale applications are the most pressing and require special attention and further exploration to optimize HTC processes [102]. Therefore, energy and environmental aspects such as gaseous emissions (combustion chamber associated with online emissions measurements) and secondary pollution must be considered when optimizing HTC-derived solid fuels for thermoelectric power plants [102]. Finally, more studies are still required to improve and evaluate the implementation of HTC and Co-HTC in different scenarios. LCA and techno-economic evaluations are crucial to attaining good results from social, environmental, and economic perspectives [3].

5. Conclusion

The hydrothermal carbonization (HTC) of *Eucalyptus grandis* residues emerges as a promising method, yielding hydrochar with significantly enhanced energy density and

characteristics compared to the raw material. The correlation between HTC severity and energy densification suggests the potential for tailoring hydrochar properties. The study's simplified methodology and reactors align with literature findings for various feedstocks. The impact of H_2SO_4 and temperature on hydrochar characteristics was underscored, confirming the significant effect of acid addition on hydrochar formation and properties. Notably, even at higher temperatures (190 and 220 °C), minimal acid addition (0.1 mol L^{-1} of H_2SO_4) suffices to improve hydrochar's energetic properties.

Hydrochar produced at 220 °C exhibits superior performance, displaying enhanced energy properties, pore structures, and carbon microspheres. While energy content increases at higher HTC temperatures, the bulk of the benefit is achieved at intermediate temperatures (190 °C), resulting in a 33% increase in HHV. However, careful consideration of process parameters is crucial, as higher temperatures entail greater control and pressure requirements, potentially introducing handling challenges and increased costs in commercial applications. Striking the right balance between energy benefits and practical feasibility is essential in the production of hydrochar from *Eucalyptus grandis* residues.

Acknowledgments

The research presented was supported by the Brazilian National Council for Scientific and Technological Development (CNPq), the Foundation for the Coordination and Improvement of Higher Level or Education Personnel (Capes), the Research Support Foundation of Minas Gerais state (FAPEMIG) and the Multi-User Biomaterials and Biomass Energy Laboratory of the Federal University of Lavras.

Appendix A. Supplementary data

Supplementary data to this article can be found online at https://doi.org/10.1016/j.fuel.2023.130643.

References

[1] Silveira EA, Macedo LA, Rousset P, Candelier K, Galvão LGO, Chaves BS, et al. A potassium responsive numerical path to model catalytic torrefaction kinetics. Energy 2022;239:122208. https://doi.org/10.1016/j.energy.2021.122208.

[2] Lin H, Zhang L, Zhang S, Li Q, Hu X. Hydrothermal carbonization of cellulose in aqueous phase of bio-oil: The significant impacts on properties of hydrochar. Fuel 2022;315:123132. https://doi.org/10.1016/j.fuel.2022.123132.

[3] Cavali M, Libardi Junior N, de Sena JD, Woiciechowski AL, Soccol CR, Belli Filho P, et al. A review on hydrothermal carbonization of potential biomass wastes, characterization and environmental applications of hydrochar, and biorefinery perspectives of the process. Sci Total Environ 2023;857. https://doi.org/10.1016/j.scitotenv.2022.159627.

[4] Funke A, Ziegler F. Hydrothermal carbonization of biomass: A summary and discussion of chemical mechanisms for process engineering. Biofuels, Bioprod Biorefining 2010;4:160–77. https://doi.org/10.1002/bbb.198.

[5] Kruse A, Funke A, Titirici MM. Hydrothermal conversion of biomass to fuels and energetic materials. Curr Opin Chem Biol 2013;17:515–21. https://doi.org/10.1016/j.cbpa.2013.05.004.

[6] Başakçılardan Kabakcı S, Baran SS. Hydrothermal carbonization of various lignocellulosics: Fuel characteristics of hydrochars and surface characteristics of activated hydrochars. Waste Manag 2019;100:259–68. https://doi.org/10.1016/j.wasman.2019.09.021.

[7] Kota KB, Shenbagaraj S, Sharma PK, Sharma AK, Ghodke PK, Chen WH. Biomass torrefaction: An overview of process and technology assessment based on global readiness level. Fuel 2022;324:124663. https://doi.org/10.1016/j.fuel.2022.124663.

[8] Hoekman SK, Broch A, Robbins C. Hydrothermal Carbonization (HTC) of Lignocellulosic Biomass. Energy & Fuels 2011;25:1802–10. https://doi.org/10.1021/ef101745n.

[9] Sharma HB, Sarmah AK, Dubey B. Hydrothermal carbonization of renewable waste biomass for solid biofuel production: A discussion on process mechanism, the influence of process parameters, environmental performance and fuel properties of hydrochar. Renew Sustain Energy Rev 2020;123. https://doi.org/10.1016/j.rser.2020.109761.

[10] Food and Agriculture Organization of the United Nations. FAO. For Prod Trade 2023. https://doi.org/Licença: CC BY-NC-SA 3.0 IGO.

[11] González J, Marta A, Jorge ES, Jiménez C, Baena FM, Zhang Z. Hydrothermal carbonization of biomass and waste : A review. Environ Chem Lett 2022:211–21.

[12] Heidari M, Dutta A, Acharya B, Mahmud S. A review of the current knowledge and challenges of hydrothermal carbonization for biomass conversion. J Energy Inst 2019;92.

[13] Arauzo PJ, Atienza-Martínez M, Ábrego J, Olszewski MP, Cao Z, Kruse A. Combustion characteristics of hydrochar and pyrochar derived from digested sewage sludge. Energies 2020;13. https://doi.org/10.3390/en13164164.

[14] Mendoza Martinez CL, Sermyagina E, Saari J, Silva de Jesus M, Cardoso M, Matheus de Almeida G, et al. Hydrothermal carbonization of lignocellulosic agro-forest based biomass residues. Biomass and Bioenergy 2021;147. https://doi.org/10.1016/j.biombioe.2021.106004.

[15] Hansen LJ, Fendt S, Spliethoff H. Impact of hydrothermal carbonization on combustion properties of residual biomass. Biomass Convers Biorefinery 2022;12:2541–52. https://doi.org/10.1007/s13399-020-00777-z.

[16] Liang W, Wang G, Xu R, Ning X, Zhang J, Guo X, et al. Hydrothermal carbonization of forest waste into solid fuel: Mechanism and combustion behavior. Energy 2022;246:123343. https://doi.org/10.1016/J.ENERGY.2022.123343.

[17] Lin Y, Ge Y, He Q, Chen P, Xiao H. The redistribution and migration mechanism of chlorine

during hydrothermal carbonization of waste biomass and fuel properties of hydrochars. Energy 2022;244. https://doi.org/10.1016/j.energy.2021.122578.

[18] Balmuk G, Cay H, Duman G, Kantarli IC, Yanik J. Hydrothermal carbonization of olive oil industry waste into solid fuel: Fuel characteristics and combustion performance. Energy 2023;278. https://doi.org/10.1016/j.energy.2023.127803.

[19] K. V. Sarkanen CHL. Lignins: occurrence, formation, structure and reactions. Wiley-Inte. California: 1971.

[20] GOMIDE, J. L.; DEMUNER BJ. Determinação do teor de lignina em material lenhoso: método Klarson modificado. O Pap 1986;47, n. 8:36–8.

[21] DIN EN 14918: Determination of calorific value., Berlim: 2010, p. CEN: 63 p.

[22] Song G, Shen L, Xiao J. Estimating Specific Chemical Exergy of Biomass from Basic Analysis Data. Ind Eng Chem Res 2011;50:9758–66. https://doi.org/10.1021/ie200534n.

[23] Afolabi OOD, Sohail M, Cheng YL. Optimisation and characterisation of hydrochar production from spent coffee grounds by hydrothermal carbonisation. Renew Energy 2020;147:1380–91. https://doi.org/10.1016/j.renene.2019.09.098.

[24] Otaviano CA MC, Paz-Cedeno FR, Pereira JFB MF. Hydrothermal pretreatment of Eucalyptus by-product and refining of xylooligosaccharides from hemicellulosic hydrolysate. Sep Purif Technol 2023;306. https://doi.org/10.1016/j.seppur.2022.122520.

[25] Álvarez-Murillo A, Román S, Ledesma B, Sabio E. Study of variables in energy densification of olive stone by hydrothermal carbonization. J Anal Appl Pyrolysis 2015;113:307–14. https://doi.org/10.1016/j.jaap.2015.01.031.

[26] Libra JA, Ro KS, Kammann C, Funke A, Berge ND, Neubauer Y, et al. Hydrothermal carbonization of biomass residuals: A comparative review of the chemistry, processes and applications of wet and dry pyrolysis. Biofuels 2011;2:71–106. https://doi.org/10.4155/bfs.10.81.

[27] Raheem A, Ding L, He Q, Hussain F, Hussain Z, Sajid M, et al. Effective pretreatment of corn straw biomass using hydrothermal carbonization for co-gasification with coal : Response surface Methodology – Box Behnken design 2022;324.

[28] He Q, Cheng C, Raheem A, Ding L, Shiung S, Yu G. Effect of hydrothermal carbonization on woody biomass : From structure to reactivity 2022;330:1–12.

[29] Silveira EA, Macedo LA, Candelier K, Rousset P, Commandré J-M. Assessment of catalytic torrefaction promoted by biomass potassium impregnation through performance indexes. Fuel 2021;304:121353. https://doi.org/10.1016/j.fuel.2021.121353.

[30] Silveira EA, Luz S, Candelier K, Macedo LA, Rousset P. An assessment of biomass torrefaction severity indexes. Fuel 2021;288. https://doi.org/10.1016/j.fuel.2020.119631.

[31] Macedo LA, Silveira EA, Rousset P, Valette J, Commandré J-M. Synergistic effect of biomass potassium content and oxidative atmosphere: Impact on torrefaction severity and released condensables. Energy 2022;254:124472. https://doi.org/10.1016/j.energy.2022.124472.

[32] Evaristo RBW, Ferreira R, Petrocchi Rodrigues J, Sabino Rodrigues J, Ghesti GF, Silveira EA, et al. Multiparameter-analysis of CO2/Steam-enhanced gasification and pyrolysis for syngas and biochar production from low-cost feedstock. Energy Convers Manag X 2021;12:100138. https://doi.org/10.1016/j.ecmx.2021.100138.

[33] Ghesti GF, Silveira EA, Guimarães MG, Evaristo RBWW, Costa M. Towards a sustainable waste-to-energy pathway to pequi biomass residues: Biochar, syngas, and biodiesel analysis. Waste Manag 2022;143:144–56. https://doi.org/10.1016/j.wasman.2022.02.022.

[34] Galvão LGOBSC, Morais MVG de, Vale AT do V, Caldeira-Pires A, Rousset P, Silveira EA. Combined thermo-acoustic upgrading of solid fuel: experimental and numerical investigation. 28th Eur. Biomass Conf. Exhib., 2020, p. 6–9. https://doi.org/10.5071/28thEUBCE2020-3DO.6.2.

[35] Chen WH, Huang MY, Chang JS, Chen CY. Thermal decomposition dynamics and severity of microalgae residues in torrefaction. Bioresour Technol 2014;169:258–64. https://doi.org/10.1016/j.biortech.2014.06.086.

[36] Santanna MS, Silveira EA, Caldeira-Pires A. Thermochemical pathways for municipal lignocellulosic waste as biofuel. 29th Eur. Biomass Conf. Exhib., 2021. https://doi.org/10.5071/29thEUBCE2021-3DV.6.8.

[37] Silveira EA, Santanna MS, Barbosa Souto NP, Lamas GC, Galvão LGO, Luz SM, et al. Urban lignocellulosic waste as biofuel: thermal improvement and torrefaction kinetics. J Therm Anal Calorim 2023;148:197–212. https://doi.org/10.1007/s10973-022-11515-0.

[38] Chen WH, Cheng CL, Show PL, Ong HC. Torrefaction performance prediction approached by torrefaction severity factor. Fuel 2019;251:126–35. https://doi.org/10.1016/j.fuel.2019.04.047.

[39] Chen WH, Aniza R. Specific chemical bioexergy and microwave-assisted torrefaction optimization via statistical and artificial intelligence approaches. Fuel 2023;333:126524. https://doi.org/10.1016/j.fuel.2022.126524.

[40] Wang C, Zhang X, Liu Y, Che D. Pyrolysis and combustion characteristics of coals in oxyfuel combustion. Appl Energy 2012;97:264–73. https://doi.org/10.1016/j.apenergy.2012.02.011.

[41] Zou H, Evrendilek F, Liu J, Buyukada M. Combustion behaviors of pileus and stipe parts of Lentinus edodes using thermogravimetric-mass spectrometry and Fourier transform infrared spectroscopy analyses: Thermal conversion, kinetic, thermodynamic, gas emission and optimization analyses. Bioresour Technol 2019;288. https://doi.org/10.1016/j.biortech.2019.121481.

[42] Qian W, Xie Q, Huang Y, Dang J, Sun K, Yang Q, et al. Combustion characteristics of semicokes derived from pyrolysis of low rank bituminous coal. Int J Min Sci Technol 2012;22:645–50. https://doi.org/10.1016/J.IJMST.2012.08.009.

[43] Maj G. Emission factors and energy properties of agro and forest biomass in aspect of sustainability of energy sector. Energies 2018;11. https://doi.org/10.3390/en11061516.

[44] Maj G, Najda A, Klimek K, Balant S. Estimation of energy and emissions properties of waste from various species of mint in the herbal products industry. Energies 2019;13. https://doi.org/10.3390/en13010055.

[45] Alves JLF, da Silva JCG, Mumbach GD, Domenico M Di, da Silva Filho VF, de Sena RF, et al. Insights into the bioenergy potential of jackfruit wastes considering their physicochemical properties, bioenergy indicators, combustion behaviors, and emission characteristics. Renew Energy 2020;155:1328–38. https://doi.org/10.1016/j.renene.2020.04.025.

[46] Sharma HB, Panigrahi S, Dubey BK. Hydrothermal carbonization of yard waste for solid bio-fuel production: Study on combustion kinetic, energy properties, grindability and flowability of hydrochar. Waste Manag 2019;91:108–19. https://doi.org/10.1016/j.wasman.2019.04.056.

[47] Sevilla M, Fuertes AB. The production of carbon materials by hydrothermal carbonization of

cellulose. Carbon N Y 2009;47:2281–9. https://doi.org/10.1016/j.carbon.2009.04.026.

[48] Wang T, Zhai Y, Zhu Y, Li C, Zeng G. A review of the hydrothermal carbonization of biomass waste for hydrochar formation: Process conditions, fundamentals, and physicochemical properties. Renew Sustain Energy Rev 2018;90:223–47. https://doi.org/10.1016/j.rser.2018.03.071.

[49] Volpe M, Fiori L. From olive waste to solid biofuel through hydrothermal carbonisation: The role of temperature and solid load on secondary char formation and hydrochar energy properties. J Anal Appl Pyrolysis 2017;124:63–72. https://doi.org/10.1016/j.jaap.2017.02.022.

[50] Ameen M, Zamri NM, May ST, Azizan MT, Aqsha A, Sabzoi N, et al. Effect of acid catalysts on hydrothermal carbonization of Malaysian oil palm residues (leaves, fronds, and shells) for hydrochar production. Biomass Convers Biorefinery 2022;12:103–14. https://doi.org/10.1007/s13399-020-01201-2.

[51] Zhang X, Li Y, Wang M, Han L, Liu X. E ff ects of Hydrothermal Carbonization Conditions on the Combustion and Kinetics of Wheat Straw Hydrochar Pellets and E ffi ciency Improvement Analyses 2020. https://doi.org/10.1021/acs.energyfuels.9b03754.

[52] Kumar M, Olajire Oyedun A, Kumar A. A review on the current status of various hydrothermal technologies on biomass feedstock. Renew Sustain Energy Rev 2018;81:1742–70. https://doi.org/10.1016/j.rser.2017.05.270.

[53] Wang R, Lin K, Peng P, Lin Z, Zhao Z, Yin Q, et al. Energy yield optimization of co-hydrothermal carbonization of sewage sludge and pinewood sawdust coupled with anaerobic digestion of the wastewater byproduct 2022;326.

[54] Yan W, Acharjee TC, Coronella CJ, Vásquez VR. Thermal pretreatment of lignocellulosic biomass. Environ Prog Sustain Energy 2009;28:435–40. https://doi.org/10.1002/ep.10385.

[55] Oliveira S De, Neiva DM, De C, Esteves B. Potential of Mild Torrefaction for Upgrading the Wood Energy Value of Different Eucalyptus Species 2018:1–8. https://doi.org/10.3390/f9090535.

[56] Lamas GC, S. Chaves B, Oliveira PP, Barbosa T, Gonzales T da S, Ghesti GF, et al. Effect of torrefaction on steam-enhanced co-gasification of an urban forest and landfill waste blend: H2 production and CO2 emissions mitigation. Int J Hydrogen Energy 2023. https://doi.org/https://doi.org/10.1016/j.ijhydene.2023.03.367.

[57] Kartal F, Özveren U. Investigation of the chemical exergy of torrefied biomass from raw biomass by means of machine learning. Biomass and Bioenergy 2022;159. https://doi.org/10.1016/j.biombioe.2022.106383.

[58] Chen D, Cen K, Gan Z, Zhuang X, Ba Y. Comparative study of electric-heating torrefaction and solar-driven torrefaction of biomass: Characterization of property variation and energy usage with torrefaction severity. Appl Energy Combust Sci 2022;9. https://doi.org/10.1016/j.jaecs.2021.100051.

[59] A. Silveira E, Santanna Chaves B, Macedo L, Ghesti GF, Evaristo RBW, Cruz Lamas G, et al. A hybrid optimization approach towards energy recovery from torrefied waste blends. Renew Energy 2023;212:151–65. https://doi.org/10.1016/j.renene.2023.05.053.

[60] Silveira EA, Luz SM, Leão RM, Rousset P, Caldeira-Pires A. Numerical modeling and experimental assessment of sustainable woody biomass torrefaction via coupled TG-FTIR. Biomass and Bioenergy 2021;146. https://doi.org/10.1016/j.biombioe.2021.105981.

[61] Silveira EA, Galvão LGO, Sá IA, Silva BF, Macedo L, Rousset P, et al. Effect of torrefaction

on thermal behavior and fuel properties of Eucalyptus grandis macro-particulates. J Therm Anal Calorim 2019;138:3645–52. https://doi.org/10.1007/s10973-018-07999-4.

[62] Protásio TP, Scatolino MV, Lima MDRA, Figueiredo ACC, Rodrigues C, Bufalino L, et al. Insights in quantitative indexes for better grouping and classification of Eucalyptus clones used in combustion and energy cogeneration processes in Brazil. Biomass and Bioenergy 2020;143. https://doi.org/10.1016/j.biombioe.2020.105835.

[63] González-Arias J, Baena-Moreno FM, Sánchez ME, Cara-Jiménez J. Optimizing hydrothermal carbonization of olive tree pruning: A techno-economic analysis based on experimental results. Sci Total Environ 2021;784. https://doi.org/10.1016/j.scitotenv.2021.147169.

[64] Chen C, Liang W, Fan F, Wang C. The Effect of Temperature on the Properties of Hydrochars Obtained by Hydrothermal Carbonization of Waste Camellia oleifera Shells. ACS Omega 2021. https://doi.org/10.1021/acsomega.1c01787.

[65] Gao Y, Wang X, Wang J, Li X, Cheng J, Yang H, et al. Effect of residence time on chemical and structural properties of hydrochar obtained by hydrothermal carbonization of water hyacinth. Energy 2013;58:376–83. https://doi.org/10.1016/j.energy.2013.06.023.

[66] Zhang Y, Jiang Q, Xie W, Wang Y, Kang J. Effects of temperature, time and acidity of hydrothermal carbonization on the hydrochar properties and nitrogen recovery from corn stover. Biomass and Bioenergy 2019;122:175–82. https://doi.org/10.1016/j.biombioe.2019.01.035.

[67] Ma P, Yang J, Xing X, Weihrich S, Fan F, Zhang X. Isoconversional kinetics and characteristics of combustion on hydrothermally treated biomass. Renew Energy 2017;114:1069–76. https://doi.org/10.1016/j.renene.2017.07.115.

[68] Peng X, Ye LL, Wang CH, Zhou H, Sun B. Temperature- and duration-dependent rice straw-derived biochar: Characteristics and its effects on soil properties of an Ultisol in southern China. Soil Tillage Res 2011;112:159–66. https://doi.org/10.1016/j.still.2011.01.002.

[69] Malhotra M, Garg A. Hydrothermal carbonization of sewage sludge: Optimization of operating conditions using design of experiment approach and evaluation of resource recovery potential. J Environ Chem Eng 2023;11. https://doi.org/10.1016/j.jece.2023.109507.

[70] Ghanim BM, Kwapinski W, Leahy JJ. Hydrothermal carbonisation of poultry litter: Effects of initial pH on yields and chemical properties of hydrochars. Bioresour Technol 2017;238:78–85. https://doi.org/10.1016/j.biortech.2017.04.025.

[71] Pala M, Kantarli IC, Buyukisik HB, Yanik J. Hydrothermal carbonization and torrefaction of grape pomace: A comparative evaluation. Bioresour Technol 2014;161:255–62. https://doi.org/10.1016/j.biortech.2014.03.052.

[72] Titirici M, Thomas A, Antonietti M. Back in the black : hydrothermal carbonization of plant material as an efficient chemical process to treat the CO 2 problem ? 2007:787–9. https://doi.org/10.1039/b616045j.

[73] Brunner G. The Journal of Supercritical Fluids Near critical and supercritical water . Part I . Hydrolytic and hydrothermal processes 2009;47:373–81. https://doi.org/10.1016/j.supflu.2008.09.002.

[74] Kambo HS, Dutta A. Strength, storage, and combustion characteristics of densified lignocellulosic biomass produced via torrefaction and hydrothermal carbonization. Appl Energy 2014;135:182–91. https://doi.org/10.1016/j.apenergy.2014.08.094.

[75] Danso-Boateng E, Shama G, Wheatley AD, Martin SJ, Holdich RG. Hydrothermal

carbonisation of sewage sludge: Effect of process conditions on product characteristics and methane production. Bioresour Technol 2015;177:318–27. https://doi.org/10.1016/J.BIORTECH.2014.11.096.

[76] Li L, Wang Y, Xu J, Flora JR V, Hoque S, Berge ND. Bioresource Technology Quantifying the sensitivity of feedstock properties and process conditions on hydrochar yield , carbon content , and energy content. Bioresour Technol 2018;262:284–93. https://doi.org/10.1016/j.biortech.2018.04.066.

[77] Śliz M, Wilk M. A comprehensive investigation of hydrothermal carbonization: Energy potential of hydrochar derived from Virginia mallow. Renew Energy 2020;156:942–50. https://doi.org/10.1016/j.renene.2020.04.124.

[78] Iglesias Canabal A, Proupín Castiñeiras J, Rodríguez Añón JA, Eimil Fraga C, Rodríguez Soalleiro R. Elemental composition of raw and torrefied pellets made from pine and pine-eucalyptus blends. Biomass and Bioenergy 2023;177. https://doi.org/10.1016/j.biombioe.2023.106951.

[79] Titirici MM, Funke A, Kruse A. Hydrothermal Carbonization of Biomass. Recent Adv Thermochem Convers Biomass 2015:325–52. https://doi.org/10.1016/B978-0-444-63289-0.00012-0.

[80] Lucian M, Volpe M, Gao L, Piro G, Goldfarb JL, Fiori L. Impact of hydrothermal carbonization conditions on the formation of hydrochars and secondary chars from the organic fraction of municipal solid waste. Fuel 2018;233:257–68. https://doi.org/10.1016/j.fuel.2018.06.060.

[81] Volpe M, Goldfarb JL, Fiori L. Hydrothermal carbonization of Opuntia ficus-indica cladodes: Role of process parameters on hydrochar properties. Bioresour Technol 2018;247:310–8. https://doi.org/10.1016/j.biortech.2017.09.072.

[82] Ko JK, Kim Y, Ximenes E, Ladisch MR. Effect of liquid hot water pretreatment severity on properties of hardwood lignin and enzymatic hydrolysis of cellulose. Biotechnol Bioeng 2015;112:252–62. https://doi.org/10.1002/bit.25349.

[83] Hu F, Jung S, Ragauskas A. Pseudo-lignin formation and its impact on enzymatic hydrolysis. Bioresour Technol 2012;117:7–12. https://doi.org/10.1016/j.biortech.2012.04.037.

[84] Sevilla M, Maciá-Agulló JA, Fuertes AB. Hydrothermal carbonization of biomass as a route for the sequestration of CO2: Chemical and structural properties of the carbonized products. Biomass and Bioenergy 2011;35:3152–9. https://doi.org/10.1016/j.biombioe.2011.04.032.

[85] Lei Y, Su H, Tian R. Morphology evolution, formation mechanism and adsorption properties of hydrochars prepared by hydrothermal carbonization of corn stalk. RSC Adv 2016;6:107829–35. https://doi.org/10.1039/c6ra21607b.

[86] Liu XV, Hoekman SK, Farthing W, Felix L. TC2015: Life cycle analysis of co-formed coal fines and hydrochar produced in twin-screw extruder (TSE). Environ Prog Sustain Energy 2017;36:668–76. https://doi.org/10.1002/ep.12552.

[87] Kannan S, Gariepy Y, Raghavan GSV. Optimization and Characterization of Hydrochar Derived from Shrimp Waste. Energy and Fuels 2017;31:4068–77. https://doi.org/10.1021/acs.energyfuels.7b00093.

[88] Liang JL, Liu YH, Zhang J. Effect of solution pH on the carbon microsphere synthesized by hydrothermal carbonization. Procedia Environ Sci 2011;11:1322–7. https://doi.org/10.1016/j.proenv.2011.12.198.

[89] Mer VK La. Nucleation in Phase Transitions. Ind Eng Chem 1952;44:1270–7. https://doi.org/10.1021/ie50510a027.

[90] Sun X, Li Y. Colloidal Carbon Spheres and Their Core/Shell Structures with Noble-Metal Nanoparticles. Angew Chemie - Int Ed 2004;43:597–601. https://doi.org/10.1002/anie.200352386.

[91] Liu F, Yu R, Ji X, Guo M. Hydrothermal carbonization of holocellulose into hydrochar: Structural, chemical characteristics, and combustion behavior. Bioresour Technol 2018;263:508–16. https://doi.org/10.1016/j.biortech.2018.05.019.

[92] Shafie SA, Al-attab KA, Zainal ZA. Effect of hydrothermal and vapothermal carbonization of wet biomass waste on bound moisture removal and combustion characteristics. Appl Therm Eng 2018;139:187–95. https://doi.org/10.1016/j.applthermaleng.2018.02.073.

[93] Chen X, Ma X, Peng X, Lin Y, Yao Z. Conversion of sweet potato waste to solid fuel via hydrothermal carbonization 2018;249:900–7.

[94] González-Arias J, Sánchez ME, Martínez EJ, Covalski C, Alonso-Simón A, González R, et al. Hydrothermal carbonization of olive tree pruning as a sustainableway for improving biomass energy potential: Effect of reaction parameters on fuel properties. Processes 2020;8. https://doi.org/10.3390/PR8101201.

[95] Parshetti GK, Quek A, Betha R, Balasubramanian R. TGA-FTIR investigation of co-combustion characteristics of blends of hydrothermally carbonized oil palm biomass (EFB) and coal. Fuel Process Technol 2014;118:228–34. https://doi.org/10.1016/j.fuproc.2013.09.010.

[96] Ma Q, Han L, Huang G. Evaluation of different water-washing treatments effects on wheat straw combustion properties. Bioresour Technol 2017;245:1075–83. https://doi.org/10.1016/j.biortech.2017.09.052.

[97] Röder M, Whittaker C, Thornley P. How certain are greenhouse gas reductions from bioenergy? Life cycle assessment and uncertainty analysis of wood pellet-to-electricity supply chains from forest residues. Biomass and Bioenergy 2015;79:50–63. https://doi.org/10.1016/j.biombioe.2015.03.030.

[98] Zhuang X, Song Y, Zhan H, Yin X, Wu C. Synergistic effects on the co-combustion of medicinal biowastes with coals of different ranks. Renew Energy 2019;140:380–9. https://doi.org/10.1016/j.renene.2019.03.070.

[99] Ren X, Sun R, Meng X, Vorobiev N, Schiemann M, Levendis YA. Carbon, sulfur and nitrogen oxide emissions from combustion of pulverized raw and torrefied biomass. Fuel 2017;188:310–23. https://doi.org/10.1016/j.fuel.2016.10.017.

[100] Kruse A, Koch F, Stelzl K, Wüst D, Zeller M. Fate of Nitrogen during Hydrothermal Carbonization. Energy and Fuels 2016;30:8037–42. https://doi.org/10.1021/acs.energyfuels.6b01312.

[101] Demirbaş A. Sustainable cofiring of biomass with coal. Energy Convers Manag 2003;44:1465–79. https://doi.org/10.1016/S0196-8904(02)00144-9.

[102] Zhuang X, Liu J, Zhang Q, Wang C, Zhan H, Ma L. A review on the utilization of industrial biowaste via hydrothermal carbonization 2022;154.

ARTIGO 2 - HYDROTHERMAL CARBONIZATION OF *EUCALYPTUS GRANDIS* SAWDUST: PROCESS AND CATALYTIC H_2SO_4 CONDITIONS OPTIMIZATION FOR CLEANER BIOFUEL PRODUCTION USING RESPONSE SURFACE METHODOLOGY

Artigo redigido conforme normas do periódico científico Energy, sendo uma versão preliminar, que pode sofrer alterações.

Hydrothermal carbonization of *Eucalyptus grandis* sawdust: process and catalytic H_2SO_4 conditions optimization for cleaner biofuel production using response surface methodology

Nayara Tamires da Silva Carvalho [a], Edgar A. Silveira [b], Thiago Protásio [c], Clara Lisseth Mendoza Martinez [d], Paulo Fernando Trugilho [a], Maria Lúcia Bianchi [e]

a. Federal University of Lavras (UFLA), Department of Forest Sciences, CP. 3037, CEP. 37200-000, Lavras-MG, Brazil.
b. University of Brasília, Mechanical Sciences Graduate Program, Laboratory of Energy and Environment, Brasilia-DF 70910-900, Brazil.
c. Federal Rural University of the Amazonia-UFRA, Campus Parauapebas, Parauapebas, CEP. 68515-000, Pará-PA, Brazil.
d. Lahti University of Technology LUT, Yliopistonkatu 34, FI-53850, Lappeenranta, Finland.
e. Federal University of Lavras (UFLA), Department of Chemistry (DQI), CP. 3037, CEP. 37200-000, Lavras-MG, Brazil.

Abstract

The utilization of biomass energy stands as a desirable approach to achieving global carbon neutrality. This study employed *Eucalyptus grandis* sawdust as a representative Brazilian biomass feedstock to explore its potential as an alternative energy source following hydrothermal carbonization (HTC) treatment. The investigation focused on identifying the optimal HTC condition and energetically characterizing the hydrochar obtained through the optimized process. Statistical analysis employing Response Surface Methodology (RSM) explored a Categorical Central Composite Design (CCD), guiding 20 experiments varying the hydroprocessing temperature (150–220 °C), time (30–90 min), and sulfuric acid concentration (0, 0.1, and 0.2 mol L^{-1}). The experimental design integrated three variables and six responses to maximize solid and energetic yields. RSM-CCD yielded statistically significant models, showcasing reduced quadratic models for the explored parameters. The optimized condition was determined as follows: a temperature of 185 °C, a reaction time of 30 min, and an H_2SO_4 concentration of 0.038 mol L^{-1}. Under these conditions, the hydrochar exhibited a Solid Yield (SY) of 67.62%, an Energetic Yield (EY) of 72.27%, and a Fuel Ratio (FR) of 0.25, highlighting maximum

yield and reduced energy consumption during production. Accordingly, experimental results validated model predictions with an error of less than 10%. This demonstrates that the experimental method is adequate and efficient. Therefore, hydrothermal carbonization emerges as a viable option for valorizing *Eucalyptus grandis* sawdust, considering its experimental validation and the potential for sustainable biomass residue utilization towards achieving carbon neutrality.

Keywords: Bioenergy; Forest by-products; Optimization; Power consumption; Renewable energy.

Index Summary

Nomenclature

Ashes	ASH		
Energy yield	EY	Lower heating value	LHV
Enhancement fator	EF	Solid yield	SY
Eucalyptus	EUC	Surface response methodology	RSM
Extractives contente	EXT	Total lignin content	LT
Fixed carbon	FC	Volatile matter	VM
Fuel ratio	FR	Weight loss	WL
Higher heating value	HHV		
Holocellulose	HOL	*Symbols*	
Hydrochar	HC	Atomic ratio of hydrogen to carbon	H/C
Hydrothermal carbonization	HTC	Atomic ratio of oxygen to carbon	O/C

1. Introduction

Establishing processes to address waste management while concurrently sourcing energy, chemicals, and materials represents a pivotal avenue toward sustainability. Biorefining is a promising approach for biomass's large-scale, sustainable utilization in the bioeconomy. It offers bioenergy production and bio-based products at competitive costs, thereby ensuring optimal socioeconomic and environmental impacts [1].

Bioenergy has garnered significant inclusion in energy strategies due to its potential for greenhouse gas mitigation. The scaling up of bioenergy technologies will likely be imperative to meet decarbonization targets, requiring increased biomass cultivation [2]. In this context, residual biomass is anticipated to hold substantial potential in meeting energy demands, serving as a source of solid fuel [3,4]. The generated waste comprises remnants from agro-industry, harvesting, such as branches, leaves, stumps, and manufacturing waste from wood production, including by-products from sawmills, such as bark, sawdust, and wood chips [5–8].

Biomass energy has garnered increasing attention due to its abundant availability and relatively straightforward utilization compared to other renewable energy sources, such as wind, hydropower, or solar energy [9,10]. Consequently, it has been applied as a feedstock in industrial-scale gasification, liquefaction, and biofuel production [11].

The valorization of residual biomass through hydrothermal carbonization (HTC) has attracted growing interest owing to its wide range of employable feedstocks and moderate reaction conditions. HTC is defined as a thermochemical process simulating natural coalification, converting biowaste into coal-like fuel (hydrochar) under moderate temperature (120–350 °C), reaction time (5–60 minutes), and autogenous pressure (2–16 MPa) [12]. Furthermore, the potential to enhance the hydrothermal reaction rate using catalysts is becoming an essential option as it can reduce the temperature and time required for hydroprocessing, thereby diminishing energy consumption and operational pressure [13].

It is extensively documented in the literature that the yield and quality of solid biofuel from HTC are contingent on various parameters, such as temperature, feedstock type, reaction time, pressure, and catalyst [14]. Therefore, optimizing these parameters is essential to achieve maximum efficiency when using hydrochar as an energy and environmentally sustainable feedstock.

In recent years, the Response Surface Methodology (RSM) has been widely employed in energy applications. The RSM technique comprehensively analyzes all influencing factors and optimal operational conditions. For example, Danso-Boateng et al. [15] utilized RSM to investigate the effect of the HTC process on fuel properties and the statistical significance of the results. Although this method does not explore the mechanisms underlying the reactions, implementing approaches like RSM allows for understanding each parameter's significance and interactions.

Table 1 compiles data from recent studies on HTC process optimization, encompassing various feedstocks, treatment conditions, and evaluations. Afolabi et al. [16] worked with spent coffee grounds and, based on DoE-RSM, identified a maximum hydrochar yield of 63.9% and a higher heating value of 31.6 MJ kg^{-1} under the ideal operational conditions of 216.4 °C and a 60 min reaction time. Akbari et al. [17] explored the impact of three independent variables: biomass-to-water ratio (10–30%), reaction time (15–45 min), and temperature (150–250 °C) on sewage sludge feedstock. The authors identified the optimum conditions for energy yield, which included an 8.9% weight, a reaction time of 33.4 minutes, and a temperature of 205.7 °C.

Moreover, Heidari et al. [18] developed a model to predict HTC outcomes (carbon content, mass yield, heating value, and energy recovery factor) based on the severity factor of HTC and the composition (cellulose, hemicellulose, and lignin content) of lignocellulosic biomass. Notably, no research has explored the hydroprocessing of *Eucalyptus grandis* sawdust using

RSM with three factors (temperature, time and H_2SO_4 as catalyst) to analyze, predict, and optimize HTC outcomes and validate the suggested models.

Table 1. Literature summary on optimization HTC from lignocellulosic biomass.

Feedstock	Treatment conditions	Assessment / Optimization	Suggested Optimization	Ref.
Spent coffee grounds	HTC Temp.: 180–220 °C Time: 1–5h	Solid yield (SY), higher heating values (HHV), energy yield (EY), proximate (FC, VM and ASH), ultimate (CHNOS) RSM validation: SY and HHV	Temp.: 216.4 °C Time: 1h	[16]
Sewage sludge	Temp.: 190, 220, 250 °C Time: 0.5, 2.25, 4 h pH: 3.9, 5, 6.1	Solid yield (SY), higher heating values (HHV), energy yield (EY), proximate (FC, VM and ASH), Ultimate (CHNOS) Box–Behnken Design	Temp.: 250 °C Time: 4h pH: 5	[19]
Sewage sludge	Temp.: 150, 200, 250 °C Time: 15, 30, 45 min Biomass:water: 5, 10,15% (P/P)	Solid yield (SY), higher heating values (HHV), energy yield (EY), proximate (FC, VM and ASH), ultimate (CHNOS) RSM validation: EY	Temp.: 205.7 °C Time: 33.4 min Biomass:water: 8.9 %	[17]
Pinewood	Temp.: 180, 220, 250 °C Time: 30, 60, 120, 180 min Biomass/water: 1:5	Higher heating values (HHV), ultimate (CHNOS)	Temp.: 220 °C Time: 60min	[20]
Coconut waste shell	Temp.: 180, 220 °C Time: 0 and 60 min	Solid yield (SY), higher heating values (HHV), energy yield (EY) RSM – CCD	Temp.: 200 °C Time: 0min	[21]
Eucalyptus grandis by-product	HTC Temp.: 150–220 °C Time: 30–90min H_2SO_4 concentration	Solid yield (SY), higher heating values (HHV), energy yield (EY), proximate (FC, VM and ASH) and ultimate (CNHO) / RSM analysis	Temp.: 185 °C Time: 30min H_2SO_4 concentration: 0.038 mol L^{-1}	This study

Therefore, for a potential industrial scale-up of this process, based on RSM analysis, this study provides a simultaneous optimization of the temperature, reaction time and varying concentrations of sulfuric acid. In this context, the originality of this work lies in i) a comprehensive experimental analysis to assess the HTC process of *Eucalyptus grandis* sawdust, ii) optimizing (RSM-CCD) the HTC process considering energy requirements and hydrochar quality by evaluating multiple hydrochar properties, and iii) conducting and validating the optimized hydroprocessing.

2. Material and Methods

2.1 Feedstock and Hydrochar Characterization

The research framework is depicted in Fig. 1. In this study, *Eucalyptus grandis* sawdust, obtained from wood processing, served as the primary feedstock. The source plantation was 22 years old and situated at the University Federal de Lavras (UFLA), at the geographic coordinates: Latitude 21°13’26.86” S e Longitude 44°58’12.44” W. The biomass was milled using a knife mill and sieved through 40–60 mesh screens. Before hydrothermal carbonization, the biomass samples were dried at 103±2 ºC for 24 hours.

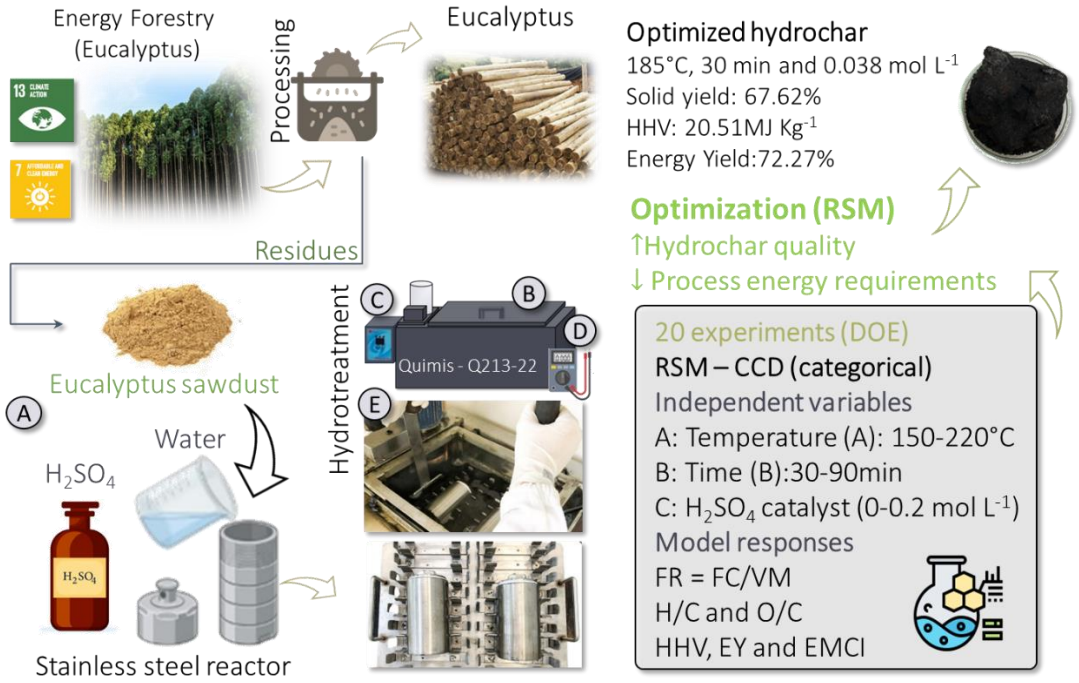

Figure 1. Research framework and general scheme of the experimental system. A) Samples preparation, B) Heated glycerin bath, C) Temperature control, D) Wattmeter and E) Reactors [22].

Table 2 provides detailed characteristics of the *Eucalyptus grandis* feedstock and associated standards (provided in the supplementary material). All calculations for tests, including raw biomass and hydrochar, were conducted on a dry basis.

Table 2. Raw feedstock (*Eucalyptus grandis*) properties. Structural (lignin) and non-structural (extractives) components, proximate (ASH, volatile matter – VM and fixed carbon – FC), ultimate (CHNO) and calorific (higher heating value – HHV) analysis [22].

Analysis [a]		**Standard**
Moisture content (%)	10.86	ASTM E871-82 (2013)
Total lignin (%)	28.80	Gomide e Demuner (1986) e Goldschimid (1971)
Extractives (%)	9.46	ASTM D1107-96 (2015)
Hollocellulose (%)	61.75	Eq. (S1) (see supplementary material)
Proximate analysis (%)		
ASH	0.47	ASTM E872-82 (2019)
FC	12.03	
VM	87.50	
FR [b]	0.14	
Ultimate analysis (%)		
C	50.48	Vario Micro Cube universal analyzer
H	5.91	
O	42.01	
N	1.61	
O/C	0.83	
H/C	0.12	
Calorific analysis (MJ kg^{-1})		
HHV	19.19	Digital calorimeter IKA C-200 ASTM E711-87

[a] db: dry basis; [b] Fuel ratio calculated as FR=FC/VM.

The solid yield of hydrochar (SY), the fuel ratio (FR), the enhancement factor (EF), and the energy yield (EY) were calculated through Eqs. (1–4), respectively [23–25].

$$SY = \frac{w_i}{w_0} \times 100 \quad (1)$$

$$\mathrm{FR} = \frac{FC}{VM} \quad (2)$$

$$EF = \frac{HHV_{Hydrochar}}{HHV_{raw}} \quad (3)$$

$$EY = SY \times EF \quad (4)$$

where w_i is the mass, on a dry basis, of the remaining solid after hydrothermal carbonization; w_0 is the mass, on a dry basis, of the raw material before the hydrothermal carbonization process; VM is the volatile matter content; FC is the fixed carbon content; $HHV_{Hydrochar}$ and HHV_{raw} refer to the higher heating value of the hydrochar and the raw material, respectively.

2.2 Hydrothermal Carbonization

Electric glycerin bath equipment was utilized to provide heat to maintain the reactor temperature. The HTC experiments were conducted in stainless steel laboratory reactors with an internal diameter of 52mm, a height of 11mm, and a volume of 0.2 L. During the experiments, the reactors were fully immersed in the heated glycerin, allowing heat to permeate across the entire surface of the reactors through conduction to the mixture of water/acidified water and biomass.

HTC treatments involved adding approximately 15g of *Eucalyptus grandis* sawdust, along with either distilled water or sulfuric acid (H_2SO_4) in a 1:10 ratio (solid on a dry basis/liquid), following the method described by [16,26].

The reaction was initiated after the glycerin bath reached the specified temperature, and the reactors were inserted into the equipment. After each experiment, the reactors were removed from the glycerin bath and placed in a cooling zone with running water at room temperature. Subsequently, the solid fraction was filtered and washed with 500 ml of distilled water, whereas the gas product was negligible and vented out. The solid samples were then dried in an oven at 103±2 °C for 24 hours, weighed, and stored in plastic bags for further analysis. After evaluating the hydrochars and conducting statistical analysis (see Section 2.3), HTC was performed under the optimized conditions to validate the adjusted models.

In the subsequent discussion, the hydrochar is denoted as $E_i j_k$, with i=0 (control), 1 and 2, attributed to the H_2SO_4 concentration (0, 0.1 and 0.2 mol L^{-1}); j=150, 185 and 220, related to the HTC temperatures and k=30, 60 and 90, related to the HTC times.

2.3 Statistical Analysis

Design of Experiments (DoE) techniques were employed to establish an interrelation between process factors and desired response values [18]. For this purpose, based on the

experimental conditions, the Central Composite Design (DOE-CCD) method was selected. In this way, the experiments were conducted to evaluate the influence of three parameters of HTC: temperature (A, 150–220 °C), reaction time (B, 30–90 minutes), and sulfuric acid concentration (C, 0 – 0.2 mol L^{-1}). The parameter ranges for both operational variables were selected based on prior studies [17,27]. The response variables taken in this project were solid yield (SY), energy yield (EY), HHV, FR, H/C and O/C, and the optimal operating condition was determined by combining the RSM results.

Therefore, the modeling was established to maximize SY, HHV, EY and FR and minimize treatment time, H/C, and O/C. The experimental variables (A, B, and C), the assignment of levels to the experimental variables (−1 and +1), and the assignment of model response values $R_1 - R_6$ are summarized in Table 3.

When using RSM to analyze response values, it is possible to obtain optimal operational conditions for individual responses. However, when both responses are equally important, selecting appropriate operating conditions that yield the best possible result for both parameters are crucial. Thus, Derringer's Desirability function can determine factor levels at which all responses reach optimal levels simultaneously [21]. All response variables were evaluated using the Design-Expert software (v.11). The agreement of the proposed models was assessed by the analysis of variance (ANOVA), considering a confidence level of 95%.

Table 3. Design of experiments (DOE) of HTC experiments considering a categorical central composite design.

Variable	**Unit**	**Level**			
		Minimum	**-1**	**+1**	**Maximum**
Temperature (A) [a]	°C	150	150	220	220
Time (B) [a]	min	30	30	90	90
H_2SO_4 concentration (C) [a]	mol L^{-1}	0.00	0.00	0.2	0.2
	Categorical (0;1)				
Model responses [b]					
R_1	R_2	R_3	R_4	R_5	R_6
SY	HHV	EY	FR	H/C	O/C

[a] Input Variables; [b] Output Variables.

3. Results and discussions

3.1 Process performance modeling

The studied variables (HTC temperature in °C (A), time in minutes (B), and sulfuric acid concentration in mol L^{-1} (C)) along with the experimental responses obtained from the 20 HTC experimental runs, based on the Central Composite Project (DOE-CCD) model, are compiled in Table 4, considering the average of at least two duplicate runs with errors controlled below 3%. In addition, Table S1 in the supplementary material provides the data used to calculate the FR (VM, ASH and FC), H/C and O/C (C, H, N and O).

Table 4. Experimental design describing independent variables and response results. HTC temperature (A, 150–220 °C), hydrotreatment time (B, 30–90 min) and H_2SO_4 concentration (C, 0–0.2 mol L^{-1}).

Run	A	B	C	SY [a]	HHV [b]	EY [a]	FR	H/C	O/C
1	220	30	0	71.03	19.68	73.93	0.23	1.1	0.43
2	220	90	0.2	45.90	25.50	61.91	0.97	0.28	0.77
3	150	60	0.1	70.14	19.94	73.98	0.22	1.21	0.58
4	150	90	0.2	71.51	19.56	73.97	0.27	0.57	1.17
5	150	30	0.2	70.39	19.70	73.32	0.24	0.54	1.21
6	220	90	0	65.58	21.54	74.71	0.33	0.94	0.39
7	185	30	0.1	43.83	24.57	56.93	0.67	0.83	0.25
8	185	60	0	73.25	19.65	76.13	0.22	1.17	0.45
9	185	60	0.1	42.62	24.73	76.13	0.78	0.82	0.40
10	185	60	0.1	41.38	25.27	55.30	0.85	0.79	0.46
11	185	60	0.1	44.16	25.10	58.61	0.81	0.80	0.23
12	185	60	0.1	43.59	25.03	67.69	0.81	0.80	0.30
13	185	60	0.1	43.88	25.06	58.15	0.81	0.80	0.27
14	185	90	0.1	47.39	24.71	61.92	0.81	0.82	0.26
15	185	60	0.1	43.88	25.06	58.15	0.81	0.80	0.27
16	150	90	0	84.04	18.06	92.67	0.17	1.30	0.49
17	150	30	0	94.54	19.07	95.30	0.16	1.34	0.53
18	220	60	0.1	45.85	25.24	61.19	0.84	0.77	0.39
19	220	30	0.2	43.92	25.32	58.82	0.92	0.21	0.77
20	185	60	0.2	43.21	25.60	58.49	0.87	0.26	0.80

[a] in (%); [b] in MJ kg^{-1}.

Table S1 in the supplementary material provides the data for calculating the FR (VM, ASH and FC), H/C and O/C (C, H, N and O). Table S2 in the supplementary material summarizes

the ANOVA results for each model obtained. Table 5 summarizes the respective prediction equations of terms (considering only the coefficients of statistically significant input variables in Table S2) for the responses of the six models in terms of coded factors (temperature (A), time (B), and sulfuric acid concentration (C)).

Table 5. Prediction equations of the six model's response in terms of coded factors (HTC temperature in °C (A), time in minutes (B), and H_2SO_4 concentration in mol L^{-1} (C).

Coef.	Reduced Quadratic Model [a]						Coded factors [b]
	SY	HHV	EY	FR	H/C	O/C	
β_0	44.24	24.86	58.09	0.7799	0.8189	0.3135	
β_1	-11.83	2.04	-6.87	0.223	-0.166	-0.123	$\times \boldsymbol{A}$
β_2	-0.929	-	-0.312	-	-	-	$\times \boldsymbol{B}$
β_3	-15.02	2.98	-7.62	0.216	-0.399	0.243	$\times \boldsymbol{C}$
β_{12}	-	-	1.98	-	-	-	$\times \boldsymbol{AB}$
β_{13}	-1.26	1	-	0.1437	-0.0025	-0.08	$\times \boldsymbol{AC}$
β_{23}	2.38	-	1.95	-	-	-	$\times \boldsymbol{BC}$
β_{11}	12.14	-1.93	8.4	-0.1983	0.1261	0.1375	$\times \boldsymbol{A^2}$
β_{33}	12.38	-1.89	8.12	-0.1833	-0.1489	0.2775	$\times \boldsymbol{C^2}$
β_{113}	4.59	-1.58	-	-	-	-	$\times \boldsymbol{A^2C}$

[a] reduced quadratic model follows; [b] Table 3.

The predicted and actual (experimental) data for the response variables obtained are presented in Fig. 2, depicting the regression fits (R^2). The reduced quadratic models demonstrate statistical significance (p <0.0001). High regression fit values were observed, with R^2 > 0.94. These results align with the literature that applied RSM to investigate the SY of coffee ground hydrochar (R^2 of 0.92) [16] and oat bark hydrochar presenting a SY (R^2 of 0.99) and HHV (R^2 of 0.98) [28].

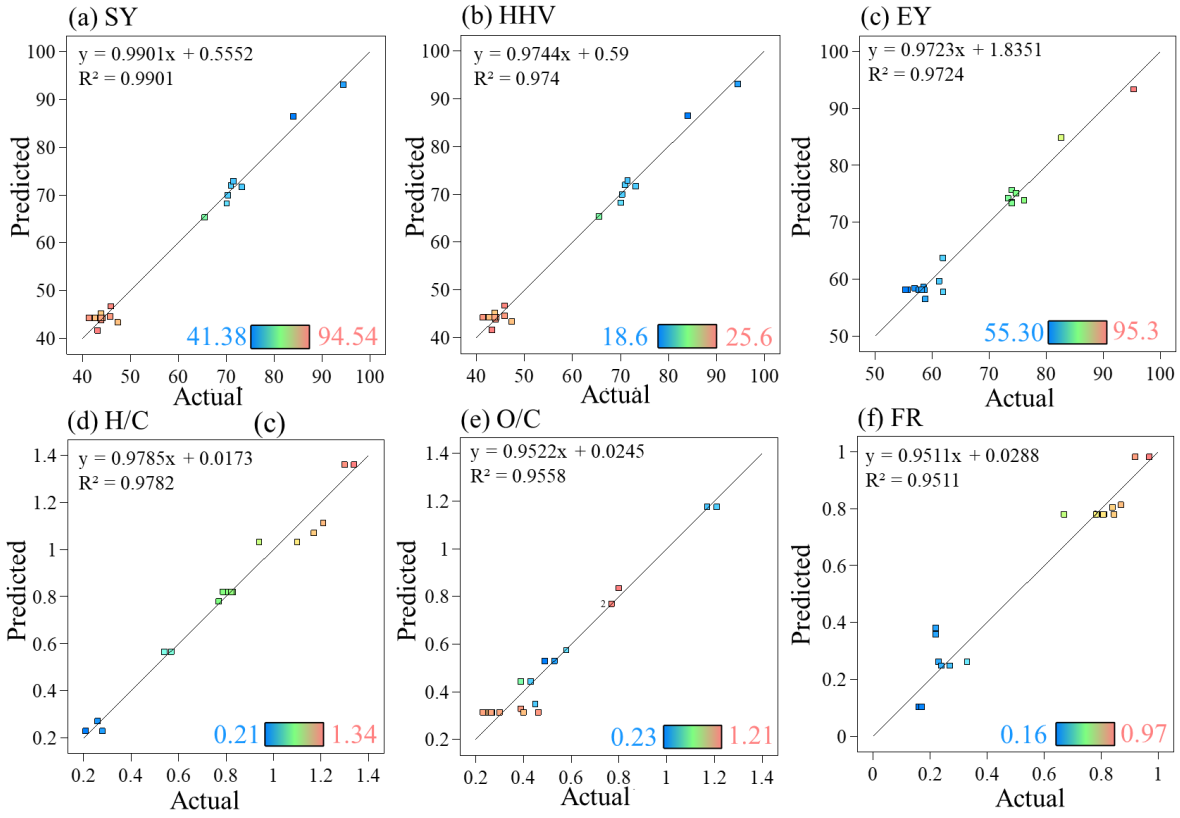

Figure 2. Correlation of predicted and experimental data. R_1=SY (%), R_2=HHV (MJ kg^{-1}), R_3=EY (%), R_4=H/C, R_5=O/C, R_6=FR.

3.2 Solid Yield of Hydrochar

The SY of hydrochar is an essential indicator during the HTC process, representing the percentage of solid products derived from the raw material. Three-dimensional (3D) and contour plots for each response model can be obtained from the correlations presented in Table 5. Figure 3 illustrates the response surface plot for SY.

Considering SY, the Table 5 indicates negative values for β_1 (-11.83), β_2 (-0.929), and β_3 (-15.02), adversely affecting SY and suggesting a greater dependency on H_2SO_4 than on temperature, followed by time. The SY ranged from 41.38 to 94.54% by mass and exhibited an expected trend, decreasing proportionally as the HTC temperature and H_2SO_4 concentration increased. A similar trend of reduction in hydrochar yield with an increasing reaction temperature of HTC of *Eucalyptus* bark was reported in the literature [29].

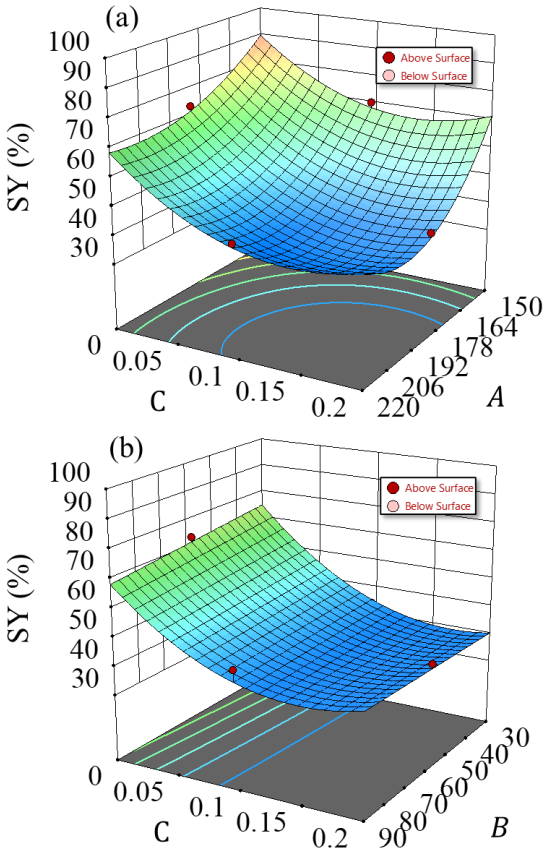

Figure 3. Response surface for model response SY (%) considering the model's independent parameters: *A* (temperature in °C), *B* (time in min) and *C* (concentration H_2SO_4 in mol L^{-1}).

Meanwhile, the time dependency showed a mild effect (comparing runs 4/5 in Table 4) for lower temperatures and only slightly more pronounced for the higher temperatures (comparing runs 1/6). A nearly flat curvature was observed for variable *B*, which showed no statistical significance for the SY model with a p-value of 0.204 (Table S2).

The SY slightly decreased with increasing time, from 71.03 to 65.58%, as the time extended from 30 to 90 minutes. Notably, longer reaction times will escalate energy consumption [18]. Therefore, if this parameter does not exert as much influence as the addition of sulfuric acid and temperature, it would be beneficial to set appropriate temperature and acid concentration based on the desired product characteristics, with a short residence time to minimize energy consumption.

Positive coefficients for temperature and squared H_2SO_4 terms (A^2 with β_{11} of 12.14 and C^2 with β_{33} of 12.38) suggest stabilizing SY reduction. Figure 3 revealed stabilization around 185 and 220 °C of HTC and between 0.05 and 0.2 mol L^{-1} of H_2SO_4, with no further reduction in SY. On the contrary, a slight increase was observed for higher temperatures, especially under severe conditions (220 °C and 0.2 mol L^{-1} of H_2SO_4). Aligned with Ameen et al. [30], they found that the hydrochar yield reduces with increasing temperature and time but increases with the presence of acid catalysts.

The HTC temperature governs biomass degradation, directly influencing the hydrochar yield and its characteristics [31]. Temperature plays a crucial role in biomass conversion through HTC, leading to lower hydrochar yields but with improved fuel characteristics [32].

The slightly higher SY under severe conditions can be attributed to the use of H_2SO_4 as a catalyst, which, in turn, promoted faster biomass degradation under HTC conditions, resulting in higher solid yields and carbon recoveries while concurrently creating a more stable carbonaceous structure. It can be inferred that using H_2SO_4 as a catalyst decomposed the lignin structure, allowing a more significant amount of lignin to dissolve in the liquid phase. These dissolved liquid precursors then polymerized into solid carbonaceous material, increasing the yield over time [33].

3.4 Proximate properties of hydrochar

Proximate properties are essential parameters for the characterization of hydrochar. These characteristics are of great value since hydrochar yields usually increase with the higher carbon content of the raw material, and its complexity influences the kinetics reactions [34]. It was required to determine the VM and ASH content to obtain the FR (FC/VM), obtaining the FC by difference. For a comprehensive assessment, Table S1 in the supplementary material presents the proximal analysis data of the 20 experiments performed. Figure 4(a) illustrates the

response surface of FR for the produced hydrochars. Figure 4(b) also depicts the ternary diagram of proximate properties.

Higher temperatures (A) and greater H_2SO_4 concentrations (C) promoted an increase in FR (a significant variable with p < 0.0001 in Table S2) with β_1 value of 0.223 and 0.216, respectively (Table 4), indicating a slight dependence on C (runs 2/6 and 8/20) than on A (runs 6/16), more noticeable for severe HTC (runs 2/4).

FR ranged from 0.16 to 0.97, showing statistical significance for both (A) and (C) (p<0.0001), as evident from the curvature in Fig. 4(a). As expected, the highest FR was attributed to more severe hydroprocessing (220 °C, 90 min, and 0.2 mol L^{-1} of H_2SO_4). FR increased with higher temperatures (β_1 of 0.223) and the highest H_2SO_4 concentration (β_2 of 0.216).

Figure 4(b) shows that increasing treatment severity (higher temperatures, catalyst concentration, longer times) leads to a decrease in volatile matter (VM), in line with [35,36]. During HTC, hemicelluloses and cellulose degrade at 160–180 °C due to subcritical water, producing CO, CO_2, short-chain hydrochar, and lowering VM, as outlined in Table S1. As HTC temperatures rise, devolatilization accelerates, fostering reactions that consistently diminish VM.

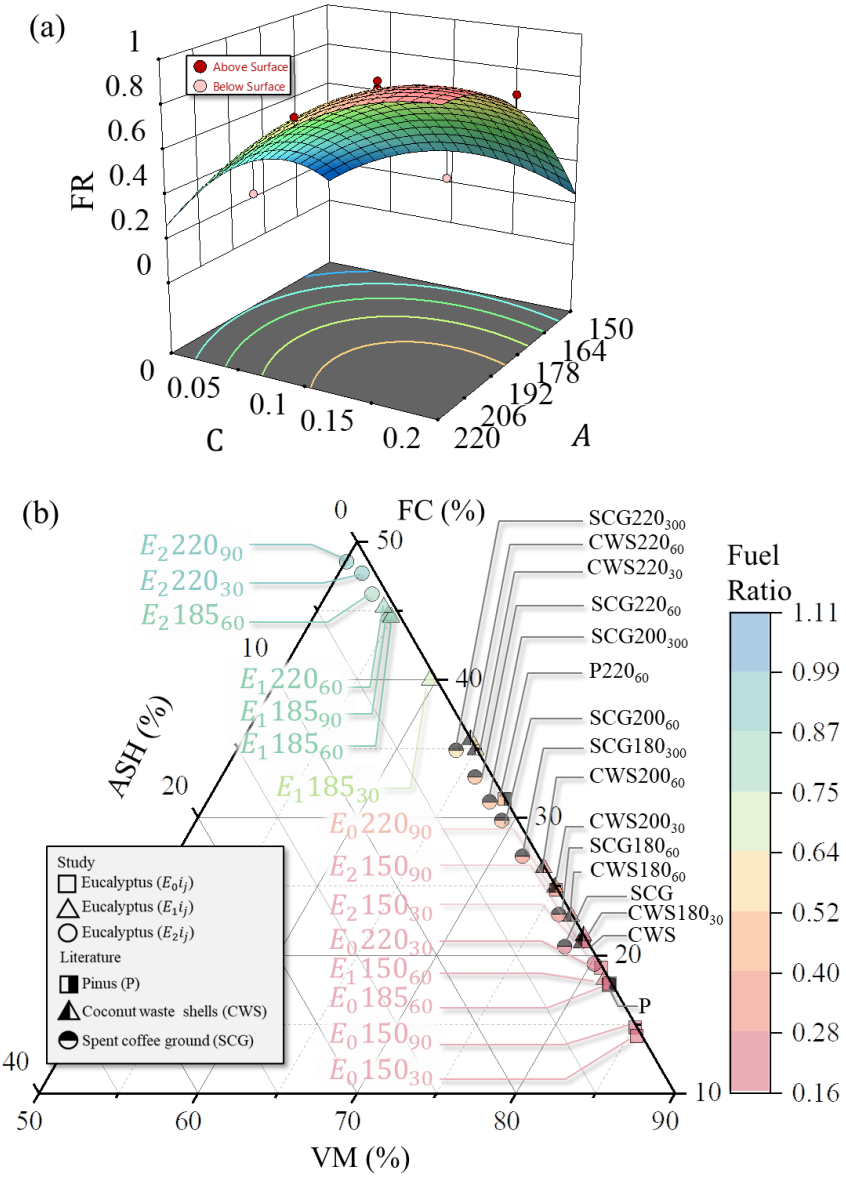

Figure 4. (a) FR response surface considering the model's independent parameters: A (temperature in °C) and C (H_2SO_4 concentration in mol L^{-1}). (b) Ternary diagram for hydrochars runs. Hydrochar is denoted as E_ij_k, with i=0 (control), 1 and 2, attributed to the H_2SO_4 concentration (0, 0.1 and 0.2 mol L^{-1}); j=150, 185 and 220, related to the HTC temperatures and k=30, 60 and 90, related to the HTC times. Literature comparison: Pinus (P) [20], Coconut waste shell (CWS) [21] and Spent coffee ground (SCG) [16].

Consistent with literature findings [37–39], the FC outcomes (Table S1 and Fig. 4(b)) correlate with increased temperatures, augmenting raw material decomposition through aromatization and repolymerization reactions, thus benefiting hydrochar combustion by enhancing efficiency (higher FC) and curtailing pollutants (lower VM).

The ASH content ranged between 0.07–1.33% (Table S1). Through HTC, inorganic elements migrate from biomass to process water, yielding a low-ash solid fuel (Fig. 4(b)). Simultaneously, organic material dissolves in the process water, possibly elevating ASH content if organic loss surpasses inorganic reduction. Furthermore, higher treatment temperatures often result in heightened ASH content [32,40,41]. As a result, various HTC conditions lead to inconsistent ASH content trends, as depicted in Table S1.

The impact of H_2SO_4 as a reaction medium is noticeable, catalyzing degradation and markedly reducing VM while increasing FC as H_2SO_4 concentration rises, leading to higher FR. This modification is evidenced by the pronounced increasing curvature in Fig. 3(a) and the shift to the top corner in the ternary diagram Fig. 4(b) as treatment temperature and catalyst concentration augments.

The FR response suggests that hydrochar produced under mild to severe conditions is a superior biofuel to those produced under light conditions. The 3D surfaces attempt an FR maximum value region after 185 °C and 0.1 mol L^{-1} (orange line in the contour map of Fig. 4(a)). The hydrochars in this study exhibit higher FR (Fig. 4(b)) compared to Pinus hydrochar from Heidari et al. [20], hydrochar from coconut waste shell (CWS) studied by Cheng et al. [21], and spent coffee ground (SCG) from Afolabi et al. [16] research.

3.5 Ultimate properties of hydrochar

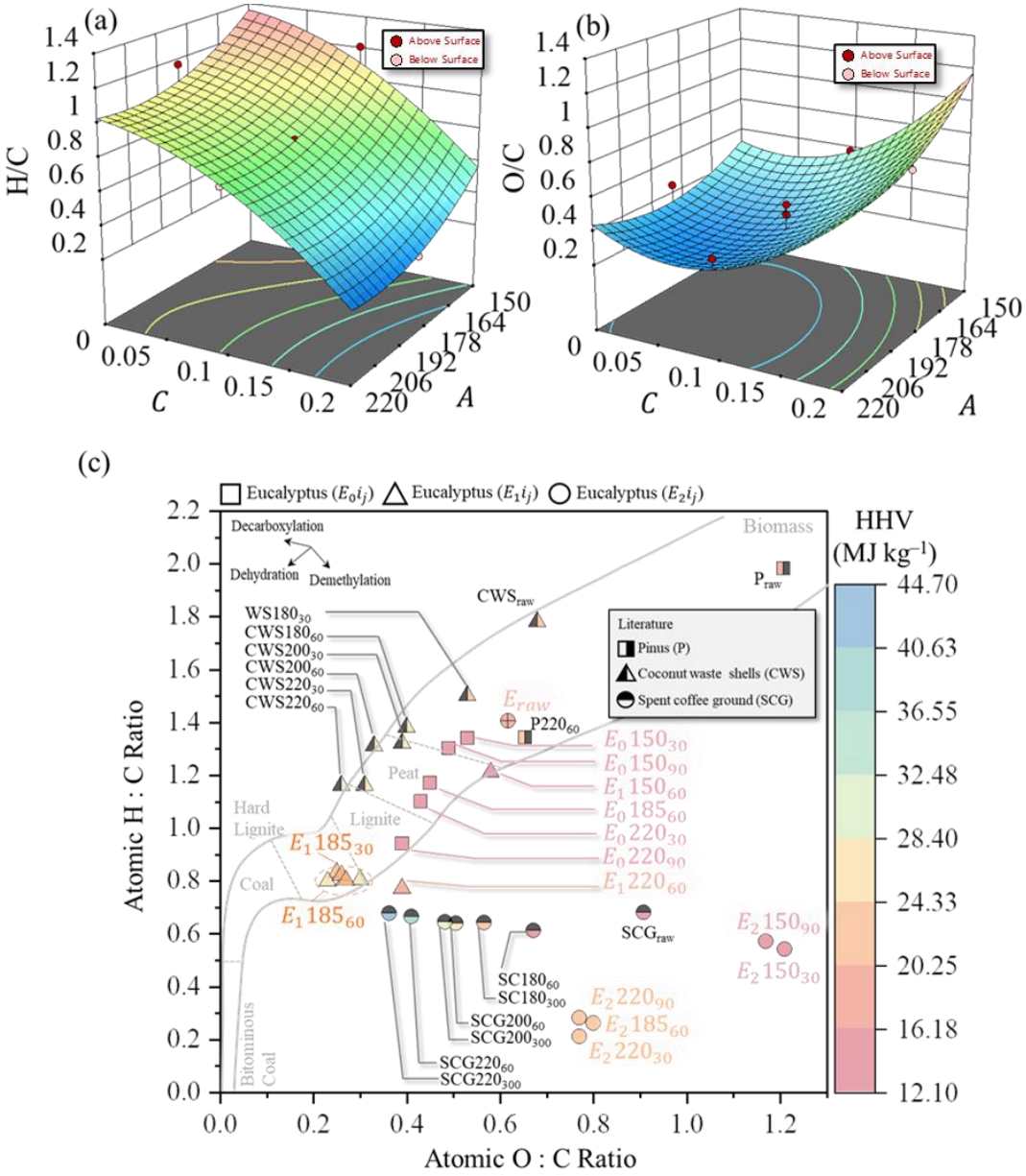

Figure 5. (a) H/|C and (b) O/C response surfaces considering the model's independent parameters: A (temperature in °C) and C (H_2SO_4 concentration in mol L^{-1}). (c) Van Krevelen diagram for produced hydrochars. Hydrochar is denoted as $E_i j_k$, with i=0 (control), 1 and 2, attributed to the H_2SO_4 concentration (0, 0.1 and 0.2 mol L^{-1}); j=150, 185 and 220, related to the HTC temperatures and k=30, 60 and 90, related to the HTC times. Literature comparison: Pinus (P) [20], Coconut waste shell (CWS) [21] and Spent coffee ground (SCG) [16].

From the ultimate analysis data, atomic ratios of H/C and O/C can be derived, which are crucial indices to examine the energy density of the fuel and are commonly used to assess the degree of carbonization of hydrochars. Figures 5(a) and (b) present the 3D response surfaces for H/C and O/C for *Eucalyptus grandis* hydrochar. Furthermore, the Van Krevelen diagram of the assessed data is shown in Fig. 5(c).

The Van Krevelen diagram (Fig. 5(c)) allows for a comprehensive discussion of hydrochar conversion and literature comparison. The atomic ratios of H/C and O/C for hydrochar exhibited a decreasing trend with increasing HTC severity, as expected [30], indicating a lesser dependency on temperature (β_1 of -0.166 and -0.123) and a greater dependency on H_2SO_4 concentration (β_2 of -0.399 and -0.243 in Table 5).

As expected, HTC treatments under milder conditions (run 17 (150 °C, 30 min, and water) and run 16 (150 °C, 90 min, and water)) exhibited lower dehydration and closer resemblance to the raw material. The most significant dehydration (0.21) occurred for the more severe hydrochar conditions (run 19 (220 °C, 30 min, and 0.2 mol L^{-1} of H_2SO_4)), however, this run showed only a small decrease in O/C ratio (0.77).

The positive coefficients for temperature and squared H_2SO_4 terms (A^2 with β_{11} of 0.1375 and C^2 with β_{33} of 0.2775) suggest increase O/C with the temperature and H_2SO_4 concentration increase. This can be explained by the fact that in the subcritical region, the dehydration process is dominant compared to other processes such as the carboxylation [42].

Kahn observed results with a similar trend. The atomic O/C atomic ratios of hydrochars from catalytic runs were higher than in non-catalytic runs at the temperatures of 225 and 250 °C [43].

It was reported that an increase in the carbon content of hydrochar at different processing parameters of HTC might be attributed to the removal of oxygen and hydrogen contents,

followed by dehydration and decarboxylation processes, consequently enhancing the fuel properties of hydrochar [14].

Furthermore, a decrease in atomic ratios of O/C and H/C, observed for hydrochars compared to the raw feedstock, indicates improved coalification. This process is primarily governed by decarboxylation and dehydration reactions, as previously suggested by Sharma et al. [44]. The removal of hydroxyl and carboxyl groups enhances hydrophobicity.

The O/C ratios of the hydrochar in runs 7 and 11 exhibited values that were in line with those found in other lignocellulosic biomasses subjected to HTC (Waste *Camellia oleifera* shells (0.24) [44], olive oil industry waste (0.23) [45], but in more severe conditions. In contrast to the H/C ratio, it was observed that the hydrothermal treatments that led to higher levels of dehydration did not correspond to those that promoted significant deoxygenation. It became evident that dehydration and decarboxylation reactions were the predominant pathways during the HTC of *Eucalyptus* residue, with the demethylation reaction having a relatively minor impact.

Higher carbon (C) and lower oxygen (O) levels were generally observed as the hydroprocessing temperature increased from 150 to 220 °C. This phenomenon likely occurred due to increased hydrolysis, dehydration of raw materials, potential volatilization, and compound dissolution, all of which increase with reaction temperature. Different concentrations of H_2SO_4 also contribute to this catalytic effect.

As anticipated and in line with the findings of previous research [46], lower atomic ratios of O/C and H/C were observed in hydrochars compared to the raw feedstock, signifying an enhancement in the coalification process. The removal of hydroxyl and carboxyl groups also contributes to increased hydrophobicity.

In general, hydrochar samples obtained following HTC at higher reaction temperatures (≥ 200 °C) may fall within the range between peat and hard lignite, as indicated by atomic ratios of H/C and O/C [47], as depicted in Fig. 3.

The observation of higher levels of carbon (C) and lower levels of oxygen (O) with increasing hydrothermal processing temperature, ranging from 150 to 220 °C, can be attributed to the enhanced extent of hydrolysis, dehydration of the raw material, the potential for volatilization, and the dissolution of compounds as the reaction temperature increases [48]. The catalytic influence of varying concentrations of H_2SO_4 also contributes to these findings.

Furthermore, the decrease in these atomic ratios indicates an increase in high-energy CC bonds and a decrease in low-energy HC and OC bonds, improving HHV [49]. In general, lower O/C and H/C ratios also specify a higher degree of carbonization and, hence, more potential for it to be exploited as solid fuel and higher stability in the soil when applied as a soil amendment [50].

3.6 Energetic Properties of Hydrochar

The HHV of hydrochar is a critical feature enabling its evaluation as a solid biofuel and the determination of crucial energy parameters, such as EF and EY, for comparative assessments with conventional fuels. Figure 6 presents response surface plots for HHV and EY.

An improvement in HHV was observed with the HTC process. In contrast to SY, HHV increased with greater process severity, reaching a peak value of 25.6 MJ kg^{-1} in run 20 (185 °C, 60 min, and 0.2 mol L^{-1} of H_2SO_4), representing a remarkable 33.4% enhancement compared to the raw material. Hydrochar from *Eucalyptus grandis* exhibited greater HHV values than low-grade fuels like peat (17.1 MJ kg^{-1}) and lignite (17.6–21.9 MJ kg^{-1}).

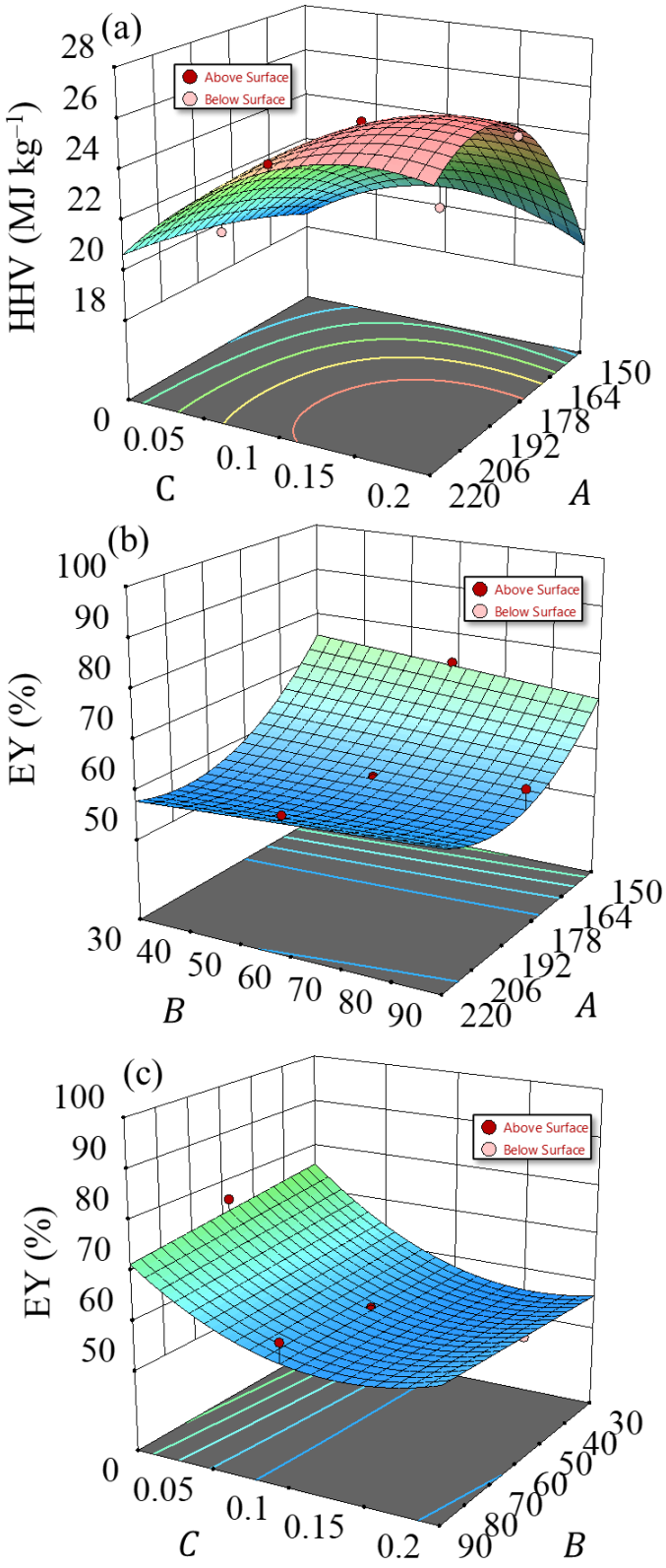

Figure 6. (a) HHV (MJ kg^{-1}); (b) and (c) EY (wt %) response surface for model responses considering the model's independent parameters *A* (temperature in °C) and *B* (time in min) and *A* (temperature in °C) and *C* (H_2SO_4 concentration in mol L^{-1}), respectively.

HHV improved with the treatment temperature (β_1 of 2.04 in Table 4), following an expected process of energy densification, and with the concentration of H_2SO_4 (β_2 of 2.98 in Table 4). Again, the acid concentration was the most critical parameter, followed by the reaction temperature, indicating a positive effect as shown by the positive coefficient in the coded equation. It means the HHV of hydrochar was increased at higher acid concentrations as HHV ranged from 19.65 to 25.60 MJ kg^{-1} when acid concentration changed from 0 to 0.2 mol L^{-1}.

One of the primary reasons could be the distribution of biomass constituents and their associated calorific values. The literature describes the HHV ranges of hemicellulose, cellulose, and lignin as 14.7–18.2, 16.1–19.0, and 22.3–26.6 MJ kg^{-1}, respectively [18]. Based on the degradation of these compounds with acid concentration and temperature, higher calorific values are expected at higher acid concentrations and temperatures. This behavior leads to the degradation of more significant proportions of hemicellulose and cellulose, resulting in higher lignin fractions, thus presenting hydrochar with a higher HHV [18].

Moreover, at elevated temperatures, decarboxylation occurs, reducing oxygen content and consequently increasing the HHV of the hydrochar [51]. This behavior supports the earlier discussed decrease in SY due to volatile release and carbon fixation (resulting in lower H/C and O/C ratios). Intrinsically linked to its final composition, hydrochars with lower O/C ratios (ranging between 18.06 and 25.6 MJ kg^{-1}) demonstrated a 33% improvement (EF=1.33). These results are consistent with HHV values of hydrochars derived from other biomass sources [40,44,52].

Compared with other biomass and thermochemical processes, a previous study investigated hydrochar from forest residues, reporting an HHV of 22.15–24.57 MJ kg^{-1} (200–240 °C, 120 min) [52]; Oliveira et al. [53] obtained HHV values of 19.5–21.3 MJ kg^{-1} (EF=1.09) while working with torrefaction *Eucalyptus* species treated at 160–230 °C for 5–15 hours. These observed values surpassed those found in the literature, suggesting that the catalytic medium

promoted an increase in the HHV of the produced hydrochars. Moreover, HHV of hydrochars produced at higher temperatures can be compared to sub-bituminous coal (25.4–27.4 MJ kg^{-1}) reported in the literature [54] and lignin (23.3–25.6 MJ kg^{-1}) [55]. Consequently, it is feasible to conclude that the experimental conditions allow for substantial hydrochar energy density modulation.

The increase in HHV of biomass after hydrothermal carbonization is a peculiar phenomenon of the HTC process, as widely reported [16,27,40]. Hansen et al. [40] stated that the fuel's HHV can be increased by up to 60% depending on the process conditions. Although solid yields tend to increase at lower temperatures, the trend for higher heating values (HHV) shows a reverse pattern. Hence, striking a balance in both responses is imperative to maximize the energy yield.

However, the impact of reaction time on hydrochar HHV was not as pronounced as that of reaction temperature, aligning with findings from a prior study [29]. This trend could be attributed to the relatively rapid biomass decomposition rate, requiring short residence times to complete the HTC process efficiently. Furthermore, it was noted that the influence of residence time on HTC reactions, such as hydrolysis, persists within a specific time interval. Beyond this, no significant effect was identified [14].

While maximizing HHV remains crucial for hydrochar used as a fuel, practical applications need to consider energy consumption and other pertinent factors. Hence, the cost of enhancing HHV must be balanced against SY when selecting operational conditions. Therefore, optimizing operational parameters considering adequate energy consumption would prove beneficial in ensuring efficient and profitable hydrochar production for process expansion.

Elevated values of EY indicate low mass losses or/and enhanced HHV. Two factors were examined, revealing significant adverse effects on EY. The concentration of H_2SO_4 (C) exhibited the most profound impact (β_3 of -7.62, as seen in Table 4), followed by temperature (A) (β_1 of -6.87). Reaction time (B) showed a non-significant effect (p = 0.6735). Prior studies

on hydrochar have reported values for EY 80.55 for corn stalk (181.9 °C, reaction time 39.7 minutes and 3.8 biomass loading (g/50 m L H_2O)) [56] and 79.70 for *Eucalyptus* (temperature 200 °C, reaction time 30 minutes and solid-to-liquid ratio of 4g:50m L) [57].

As for EY, the highest value obtained was 95.3% in run 17 (150 °C, 30 min, and 0 mol L^{-1} of H_2SO_4 (water)). Table S2 presents the analysis of variance (ANOVA) results for the three responses, with statistical significance determined by a p-value less than 0.05. Based on the ANOVA results, there appears to be a strong correspondence between the experimental data and the model. The experimental design method is an effective means to explore the influence of variables. Thus, RSM can be employed to analyze the impact of factors on each response.

Higher temperatures increase hydrochar's aromaticity, enhancing its energy content and stability [58]. However, it should be noted that higher temperatures reduce hydrochar yield [59,60]. The pressure is typically not controlled, as it is influenced by water's saturation vapor, which is temperature-dependent. Thus, available literature generally employs an autogenous pressure. Nevertheless, the "temperature effect" combines temperature and pressure, as increasing the former parameter also elevates the latter. Altering pressure also changes the degradation temperature. Therefore, it remains uncertain whether the impact on carbonization arises from temperature, pressure, or a combination of both [61]. Depending on the conditions, HTC typically yields 50 to 80% hydrochar, 5 to 20% effluent, and 2 to 5% gases [39].

The hydrothermal carbonization results in organic solubilization due to cell rupture, increasing macromolecule concentration in the liquid phase. Three possible reasons for carbon reduction are (i) decarboxylation reactions, (ii) complete oxidation due to the presence of air in the reactor headspace, and (iii) volatilization. The likelihood of decarboxylation and oxidation reactions is higher, as a significant amount of residual pressure (after cooling) was observed in the reactor. Since the reactor was not purged with nitrogen before HTC runs, residual oxygen in the headspace can react with carbon in the biomass, leading to CO_2 generation. Consequently,

a more significant fraction of carbon was lost in the gaseous phase compared to previous studies.

3.7 Hydrotreatment optimization

Achieving an ideal HHV requires greater HTC severity, a common requirement across various feedstock types. From an industrial perspective, optimizing HTC's operational parameters is vital, especially in process development. An ideal HTC process should be characterized by the lowest feasible temperature and reaction time to mitigate energy costs within the HTC system while maximizing SY and EY. This need is increasingly significant, considering the costs and environmental impacts as operations scale up. The optimal solution is presented in Table 5.

Employing the RSM within the parameter space investigated in this study, the hydrochar produced under HTC conditions of 185 °C for 30 min and 0.038 mol L^{-1} of H_2SO_4 was selected as the ideal choice, with a desirability value of 0.505. This selection aimed to minimize reaction time while maximizing solid and energy yields.

The optimal solution acquired aligns with both the Ternary diagram illustrating proximate results (Fig. 4(b)) and the Van Krevelen diagram (Fig. 5(c)). In the Ternary diagram, E_1185_{30} (185 °C treatment for 30 minutes with 0.1 mol L^{-1}) is positioned near the top corner, while the Van Krevelen diagram places E_1185_{30} (within the hard lignite region). These placements affirm the quality of the produced hydrochar and the selection of the optimum condition by the RSM, indicating similarities in the elemental ratios (H/C and O/C) to those observed in fossil fuels.

Table 5. Experimental and predicted values of responses at optimal HTC conditions.

Parameters	Value	Goal
Operational conditions		
A: Temperature (°C)	185	in range
B: Time (min)	30	minimize
C: H_2SO_4 concentration (mol L^{-1})	0.038	in range
Predict properties		
Solid Yield (%)	60.89	maximize
HHV (MJ kg^{-1})	22.26	maximize
Energy yield (%)	67.57	maximize
FR	0.57	maximize
H/C	1.01	minimize
O/C	0.27	minimize
Desirability	0.505	

The optimized hydrochar exhibited an SY of 60.89 % and EY of 67.57 %, reducing energy consumption during production. The optimal condition reported in this study would represent substantial cost and energy savings in process development and economic feasibility compared to other operational ranges, such as torrefaction.

New HTC experiments under the optimal reaction condition were conducted for the validation stage. The mean values of the validation results were: SY of 67.62%, HHV of 19.89 MJ kg^{-1} and EY of 72.27%. Consequently, suitable outcomes were achieved in this study, with errors of 6.73% and 6.95% for SY and EY, respectively. These errors fall below ±10%, a range deemed an acceptable variance according to Kang et al. [49], and they align with the values reported by Mohit and Remya [56] for validating optimization models of SY and FC in producing biochar from microalgae using pyrolysis.

4. Conclusion

This study employed Response Surface Methodology (RSM) to analyze and optimize the hydrothermal carbonization (HTC) process of Eucalyptus grandis sawdust residues. Statistical analysis was conducted to determine the effects of temperature, reaction time, and sulfuric acid concentrations on the solid and energetic yields of hydrochar.

Process optimization poses challenges as yields and the HHV trend in opposite directions. It became evident that the most influential factors in the process, within the studied range, were the acid concentration and reaction temperature. The highest hydrochar SY obtained in this study was 95.3% at 150 °C and 30 min, using water as the reaction medium. Meanwhile, the highest HHV reached 25.6 MJ kg^{-1} at 185 °C, 30 min, with 0.02 mol L^{-1} of H_2SO_4. Based on both SY and EY, along with overall desirability, the hydro processing conducted at a temperature of 185 °C, a reaction time of 30 min, and 0.038 mol L^{-1} of H_2SO_4 was identified as the optimal processing condition, aiming to minimize production costs while maximizing these energetic characteristics.

The results unveiled that the HTC process can generate hydrochar with satisfactory properties as a direct solid fuel or auxiliary fuel. However, further studies, technical-economic evaluations, and life cycle assessments are essential to appraise its benefits, limitations, and sustainability regarding process efficiency, energy consumption, product quality, and carbon balance.

Acknowledgments

The research presented was supported by the Brazilian National Council for Scientific and Technological Development (CNPq), the Foundation for the Coordination and Improvement of Higher Level or Education Personnel (Capes), the Research Support Foundation of Minas Gerais state (FAPEMIG) and the Multi-User Biomaterials and Biomass Energy Laboratory of the Federal University of Lavras.

References

[1] IEA Bioenergy. Annual Report 2022. Annu Rep 2022 2023;11:135–9. https://doi.org/10.3934/energy.2023007.

[2] Welfle AJ, Almena A, Arshad MN, Banks SW, Butnar I, Chong KJ, et al. Sustainability of bioenergy – Mapping the risks & benefits to inform future bioenergy

systems. Biomass and Bioenergy 2023;177. https://doi.org/10.1016/j.biombioe.2023.106919.

[3] Lucian M, Volpe M, Gao L, Piro G, Goldfarb JL, Fiori L. Impact of hydrothermal carbonization conditions on the formation of hydrochars and secondary chars from the organic fraction of municipal solid waste. Fuel 2018;233:257–68. https://doi.org/10.1016/j.fuel.2018.06.060.

[4] A. Silveira E, Santanna Chaves B, Macedo L, Ghesti GF, Evaristo RBW, Cruz Lamas G, et al. A hybrid optimization approach towards energy recovery from torrefied waste blends. Renew Energy 2023;212:151–65. https://doi.org/10.1016/j.renene.2023.05.053.

[5] Rodrigues JP, Ghesti GF, Silveira EA, Lamas GC, Ferreira R, Costa M. Waste-to-hydrogen via CO2/Steam-enhanced gasification of spent coffee ground. Clean Chem Eng 2022;4:100082. https://doi.org/10.1016/j.clce.2022.100082.

[6] Ghesti GF, Silveira EA, Guimarães MG, Evaristo RBWW, Costa M. Towards a sustainable waste-to-energy pathway to pequi biomass residues: Biochar, syngas, and biodiesel analysis. Waste Manag 2022;143:144–56. https://doi.org/10.1016/j.wasman.2022.02.022.

[7] Evaristo RBW, Ferreira R, Petrocchi Rodrigues J, Sabino Rodrigues J, Ghesti GF, Silveira EA, et al. Multiparameter-analysis of CO2/Steam-enhanced gasification and pyrolysis for syngas and biochar production from low-cost feedstock. Energy Convers Manag X 2021;12:100138. https://doi.org/10.1016/j.ecmx.2021.100138.

[8] Braghiroli FL, Passarini L. Valorization of Biomass Residues from Forest Operations and Wood Manufacturing Presents a Wide Range of Sustainable and Innovative Possibilities. Curr For Reports 2020;6:172–83. https://doi.org/10.1007/s40725-020-00112-9.

[9] Wang Y, Qiu L, Zhu M, Sun G, Zhang T, Kang K. Comparative Evaluation of Hydrothermal Carbonization and Low Temperature Pyrolysis of Eucommia ulmoides Oliver for the Production of Solid Biofuel. Sci Rep 2019;9:1–11. https://doi.org/10.1038/s41598-019-38849-4.

[10] Mao G, Huang N, Chen L, Wang H. Science of the Total Environment Research on biomass energy and environment from the past to the future : A bibliometric analysis 2018;635:1081–90.

[11] Molino A, Larocca V, Chianese S, Musmarra D. Biofuels Production by Biomass Gasification : A Review 2018:1–31. https://doi.org/10.3390/en11040811.

[12] Zhao P, Shen Y, Ge S, Chen Z, Yoshikawa K. Clean solid biofuel production from high moisture content waste biomass employing hydrothermal treatment 2014;131:345–67.

[13] Ghanim BM, Kwapinski W, Leahy JJ. Hydrothermal carbonisation of poultry litter: Effects of initial pH on yields and chemical properties of hydrochars. Bioresour Technol 2017;238:78–85. https://doi.org/10.1016/j.biortech.2017.04.025.

[14] Nizamuddin S, Baloch HA, Griffin GJ, Mubarak NM, Bhutto AW, Abro R, et al. An overview of effect of process parameters on hydrothermal carbonization of biomass. Renew Sustain Energy Rev 2017;73:1289–99. https://doi.org/10.1016/j.rser.2016.12.122.

[15] Danso-Boateng E, Shama G, Wheatley AD, Martin SJ, Holdich RG. Hydrothermal carbonisation of sewage sludge: Effect of process conditions on product characteristics and methane production. Bioresour Technol 2015;177:318–27. https://doi.org/10.1016/J.BIORTECH.2014.11.096.

[16] Afolabi OOD, Sohail M, Cheng YL. Optimisation and characterisation of hydrochar production from spent coffee grounds by hydrothermal carbonisation. Renew Energy 2020;147:1380–91. https://doi.org/10.1016/j.renene.2019.09.098.

[17] Akbari H, Akbari H, Fanaei F, Adibzadeh A. Optimization of parameters affecting the hydrothermal carbonization of wastewater treatment plant sewage sludge. Biomass Convers Biorefinery 2022. https://doi.org/10.1007/s13399-022-03427-8.

[18] Heidari M, Dutta A, Acharya B, Mahmud S. A review of the current knowledge and challenges of hydrothermal carbonization for biomass conversion. J Energy Inst 2019;92.

[19] Blach T, Engelhart M. Optimizing the hydrothermal carbonization of sewage sludge—response surface methodology and the effect of volatile solids. Water (Switzerland) 2021;13. https://doi.org/10.3390/w13091225.

[20] Heidari M, Salaudeen S, Arku P, Acharya B. Development of a mathematical model for hydrothermal carbonization of biomass : Comparison of experimental measurements with model predictions 2021;214.

[21] Chen Cheng QG, Lu D, Raheem Abdul QH, Su SL, Yu. G. Upgradation of coconut waste shell to value-added hydrochar via hydrothermal carbonization : Parametric optimization using response. Appl Energy 2022;327:120136. https://doi.org/10.1016/j.apenergy.2022.120136.

[22] Carvalho NT da S, Silveira EA, de Paula Protásio T, Trugilho PF, Bianchi ML. Hydrotreatment of Eucalyptus sawdust: The influence of process temperature and H2SO4 catalyst on hydrochar quality, combustion behavior and related emissions. Fuel 2024;360:130643. https://doi.org/10.1016/J.FUEL.2023.130643.

[23] Silveira EA, Macedo LA, Candelier K, Rousset P, Commandré J-M. Assessment of catalytic torrefaction promoted by biomass potassium impregnation through performance indexes. Fuel 2021;304:121353. https://doi.org/10.1016/j.fuel.2021.121353.

[24] Silveira EA, Luz S, Candelier K, Macedo LA, Rousset P. An assessment of biomass torrefaction severity indexes. Fuel 2021;288. https://doi.org/10.1016/j.fuel.2020.119631.

[25] Macedo LA, Silveira EA, Rousset P, Valette J, Commandré J-M. Synergistic effect of biomass potassium content and oxidative atmosphere: Impact on torrefaction severity and released condensables. Energy 2022;254:124472. https://doi.org/10.1016/j.energy.2022.124472.

[26] Otaviano CA MC, Paz-Cedeno FR, Pereira JFB MF. Hydrothermal pretreatment of Eucalyptus by-product and refining of xylooligosaccharides from hemicellulosic hydrolysate. Sep Purif Technol 2023;306. https://doi.org/10.1016/j.seppur.2022.122520.

[27] Arauzo PJ, Atienza-Martínez M, Ábrego J, Olszewski MP, Cao Z, Kruse A.

Combustion characteristics of hydrochar and pyrochar derived from digested sewage sludge. Energies 2020;13. https://doi.org/10.3390/en13164164.

[28] Murillo HA. Bioresource Technology Valorization of oat husk by hydrothermal carbonization : Optimization of process parameters and anaerobic digestion of spent liquors 2022;343.

[29] Gao P, Zhou Y, Meng F, Zhang Y, Liu Z, Zhang W, et al. Preparation and characterization of hydrochar from waste eucalyptus bark by hydrothermal carbonization. Energy 2016;97:238–45. https://doi.org/10.1016/j.energy.2015.12.123.

[30] Ameen M, Zamri NM, May ST, Azizan MT, Aqsha A, Sabzoi N, et al. Effect of acid catalysts on hydrothermal carbonization of Malaysian oil palm residues (leaves, fronds, and shells) for hydrochar production. Biomass Convers Biorefinery 2022;12:103–14. https://doi.org/10.1007/s13399-020-01201-2.

[31] Zhang C, Ho SH, Chen WH, Fu Y, Chang JS, Bi X. Oxidative torrefaction of biomass nutshells: Evaluations of energy efficiency as well as biochar transportation and storage. Appl Energy 2019;235:428–41. https://doi.org/10.1016/j.apenergy.2018.10.090.

[32] González-Arias J, Baena-Moreno FM, Sánchez ME, Cara-Jiménez J. Optimizing hydrothermal carbonization of olive tree pruning: A techno-economic analysis based on experimental results. Sci Total Environ 2021;784. https://doi.org/10.1016/j.scitotenv.2021.147169.

[33] Wikberg H, Ohra-Aho T, Pileidis F, Titirici MM. Structural and Morphological Changes in Kraft Lignin during Hydrothermal Carbonization. ACS Sustain Chem Eng 2015;3:2737–45. https://doi.org/10.1021/acssuschemeng.5b00925.

[34] Lu X, Berge ND. Influence of feedstock chemical composition on product formation and characteristics derived from the hydrothermal carbonization of mixed feedstocks. Bioresour Technol 2014;166:120–31. https://doi.org/10.1016/j.biortech.2014.05.015.

[35] Gao Y, Wang X, Wang J, Li X, Cheng J, Yang H, et al. Effect of residence time on chemical and structural properties of hydrochar obtained by hydrothermal carbonization of water hyacinth. Energy 2013;58:376–83. https://doi.org/10.1016/j.energy.2013.06.023.

[36] Volpe M, Fiori L, Volpe R, Messineo A. Upgrading of olive tree trimmings residue as biofuel by hydrothermal carbonization and torrefaction: A comparative study. Chem Eng Trans 2016;50:13–8. https://doi.org/10.3303/CET1650003.

[37] Chen Z, Wang M, Jiang E, Wang D, Zhang K, Ren Y. Pyrolysis of Torre fi ed Biomass 2018:1287–98.

[38] Malhotra M, Garg A. Hydrothermal carbonization of sewage sludge: Optimization of operating conditions using design of experiment approach and evaluation of resource recovery potential. J Environ Chem Eng 2023;11. https://doi.org/10.1016/j.jece.2023.109507.

[39] Zhang Y, Jiang Q, Xie W, Wang Y, Kang J. Effects of temperature, time and acidity of hydrothermal carbonization on the hydrochar properties and nitrogen recovery from corn stover. Biomass and Bioenergy 2019;122:175–82. https://doi.org/10.1016/j.biombioe.2019.01.035.

[40] Hansen LJ, Fendt S, Spliethoff H. Impact of hydrothermal carbonization on combustion properties of residual biomass. Biomass Convers Biorefinery 2022;12:2541–52. https://doi.org/10.1007/s13399-020-00777-z.

[41] Protásio TP, Scatolino MV, Lima MDRA, Figueiredo ACC, Rodrigues C, Bufalino L, et al. Insights in quantitative indexes for better grouping and classification of Eucalyptus clones used in combustion and energy cogeneration processes in Brazil. Biomass and Bioenergy 2020;143. https://doi.org/10.1016/j.biombioe.2020.105835.

[42] Khan TA, Saud AS, Jamari SS, Rahim MHA, Park JW, Kim HJ. Hydrothermal carbonization of lignocellulosic biomass for carbon rich material preparation: A review. Biomass and Bioenergy 2019;130. https://doi.org/10.1016/j.biombioe.2019.105384.

[43] Evcil T, Simsir H, Ucar S, Tekin K, Karagoz S. Hydrothermal carbonization of lignocellulosic biomass and effects of combined Lewis and Brønsted acid catalysts. Fuel 2020;279. https://doi.org/10.1016/j.fuel.2020.118458.

[44] Chen C, Liang W, Fan F, Wang C. The Effect of Temperature on the Properties of Hydrochars Obtained by Hydrothermal Carbonization of Waste Camellia oleifera Shells. ACS Omega 2021. https://doi.org/10.1021/acsomega.1c01787.

[45] Balmuk G, Cay H, Duman G, Kantarli IC, Yanik J. Hydrothermal carbonization of olive oil industry waste into solid fuel: Fuel characteristics and combustion performance. Energy 2023;278. https://doi.org/10.1016/j.energy.2023.127803.

[46] Volpe M, Wüst D, Merzari F, Lucian M, Andreottola G, Kruse A, et al. One stage olive mill waste streams valorisation via hydrothermal carbonisation. Waste Manag 2018;80:224–34. https://doi.org/10.1016/j.wasman.2018.09.021.

[47] Wang T, Zhai Y, Zhu Y, Li C, Zeng G. A review of the hydrothermal carbonization of biomass waste for hydrochar formation: Process conditions, fundamentals, and physicochemical properties. Renew Sustain Energy Rev 2018;90:223–47. https://doi.org/10.1016/j.rser.2018.03.071.

[48] Lu X, Pellechia PJ, Flora JR V, Berge ND. Bioresource Technology Influence of reaction time and temperature on product formation and characteristics associated with the hydrothermal carbonization of cellulose. Bioresour Technol 2013;138:180–90. https://doi.org/10.1016/j.biortech.2013.03.163.

[49] Liu Z, Quek A, Hoekman SK, Balasubramanian R. Production of solid biochar fuel from waste biomass by hydrothermal carbonization 2013;103:943–9.

[50] Raheem A, Ding L, He Q, Hussain F, Hussain Z, Sajid M, et al. Effective pretreatment of corn straw biomass using hydrothermal carbonization for co-gasification with coal : Response surface Methodology – Box Behnken design 2022;324.

[51] Kannan S, Gariepy Y, Raghavan GSV. Optimization and Characterization of Hydrochar Derived from Shrimp Waste. Energy and Fuels 2017;31:4068–77. https://doi.org/10.1021/acs.energyfuels.7b00093.

[52] Liang W, Wang G, Xu R, Ning X, Zhang J, Guo X, et al. Hydrothermal carbonization of forest waste into solid fuel: Mechanism and combustion behavior. Energy 2022;246:123343. https://doi.org/10.1016/J.ENERGY.2022.123343.

[53] Oliveira S De, Neiva DM, De C, Esteves B. Potential of Mild Torrefaction for

Upgrading the Wood Energy Value of Different Eucalyptus Species 2018:1–8. https://doi.org/10.3390/f9090535.

[54] Saba A, Saha P, Reza MT. Co-Hydrothermal Carbonization of coal-biomass blend: Influence of temperature on solid fuel properties. Fuel Process Technol 2017;167:711–20. https://doi.org/10.1016/j.fuproc.2017.08.016.

[55] Hoekman SK, Broch A, Robbins C. Hydrothermal Carbonization (HTC) of Lignocellulosic Biomass. Energy and Fuels 2011:1802–10.

[56] Kang K, Nanda S, Sun G, Qiu L, Gu Y, Zhang T. Microwave-assisted hydrothermal carbonization of corn stalk for solid biofuel production : Optimization of process parameters and characterization of hydrochar 2019;186.

[57] Lin Y, Ge Y, He Q, Chen P, Xiao H. The redistribution and migration mechanism of chlorine during hydrothermal carbonization of waste biomass and fuel properties of hydrochars. Energy 2022;244. https://doi.org/10.1016/j.energy.2021.122578.

[58] Zhang Y, Gao X, Li B, Li H, Zhao W. Assessing the potential environmental impact of woody biomass using quantitative universal exergy. J Clean Prod 2018;176:693–703. https://doi.org/10.1016/j.jclepro.2017.12.159.

[59] Ferrentino R, Merzari F, Fiori L, Andreottola G. Coupling hydrothermal carbonization with anaerobic digestion for sewage sludge treatment: Influence of HTC liquor and hydrochar on biomethane production. Energies 2020;13. https://doi.org/10.3390/en13236262.

[60] Liu XV, Hoekman SK, Farthing W, Felix L. TC2015: Life cycle analysis of co-formed coal fines and hydrochar produced in twin-screw extruder (TSE). Environ Prog Sustain Energy 2017;36:668–76. https://doi.org/10.1002/ep.12552.

[61] Yu Y, Guo Y, Wang G, El-kassaby YA, Sokhansanj S. Hydrothermal carbonization of waste ginkgo leaf residues for solid biofuel production : Hydrochar characterization and its pelletization 2022;324.